Effect of shoreline subsidence and anthropogenic activity on Northwest Territories' lakes.

Adam Houben

A thesis submitted to
The Faculty of Graduate and Postdoctoral Studies
In partial fulfillment of the requirements for the degree of
Doctor of Philosophy

Department of Biology
Chemical and Environmental Toxicology Specialization
University of Ottawa
Ottawa, ON, Canada

Abstract

Thawing permafrost – in the form of shoreline retrogressive thaw slump events – influence adjacent arctic tundra lake systems near Inuvik, NT. Slump-affected lakes demonstrated lower organic matter and key nutrients such as phosphorus (P), as well as greater water clarity. Key terrestrial permafrost soil indicators such as U, Sr, and Li, were identified to be elevated in slump-affected lakes, while other more biologically important metals (e.g. Fe, Mn) were significantly lower in affected lakes. These physical-chemical changes led to increasing P-limitation for both phytoplankton and periphyton, resulting in lower phytoplankton biomass (Chl-*a*). Using P as covariate in ANCOVA analysis, slump-affected lakes were also lower in phytoplankton biomass (Chl-*a*) relative to other study landscapes across the Canadian low-Arctic.

Slump-affected lakes also exhibited lower organic matter leading to lower overall Hg concentrations within slump-affected lakes. However, this same reduction in dissolved organic carbon (DOC) has also led to an increase in bioavailable Hg, and increased bioaccumulation of Hg in both periphyton as well as macroinvertebrate species in our most disturbed lakes with DOC concentrations less than 6 and 9 mg DOC/L, respectively. A negative correlation between Hg bioaccumulation and DOC above these concentrations was also observed, and is the typical condition within reference lakes.

The legacy impacts of mining were also observed in lakes within 25 km of the Giant Mine roaster stack in the Yellowknife region. Increases in both arsenic (As) and methyl mercury were measured in lakes nearer to the mine, with As concentrations well above water quality guidelines in lakes within 17 km of the roaster stack. This research highlights the necessity of baseline environmental monitoring prior to resource development, as well as the potential for compounded influences of such development within sensitive permafrost regions exposed to thawing.

Résumé

La fonte du pergélisol – sous forme de glissements de dégel de rivage – influence les systèmes lacustres de la toundra arctique près d'Inuvik, NT. Les lacs affectés par des glissements de dégel ont démontré des niveaux plus bas de matières organiques et de nutriments clés, tel que le phosphore (P), ainsi qu'une clarté de l'eau plus élevée. Certains indicateurs clés de la fonte du pergélisol, incluant les éléments U, Sr et Li, ont été identifiés comme étant plus élevés dans les lacs affectés par des glissements de dégel que ceux non-affectés, tant dit que certains métaux biologiquement plus importants (ex. Fe et Mn) étaient significativement moins élevés dans les lacs affectés. Ces changements physiques et chimiques ont mené à l'augmentation de la limitation phosphorique des phytoplanctons et périphytons, et subséquemment à une diminution de la biomasse de phytoplanctons (Chl-*a*). En utilisant P comme covariable dans une analyse ANCOVA, il a été démontré que les lacs affectés par des glissements de dégel ont aussi des biomasses de phytoplanctons (Chl-*a*) plus basses que celles d'autres lacs étudiés dans le Bas-Arctique canadien.

Par ailleurs, les niveaux plus bas de matières organiques des lacs affectés par des glissements de dégel ont aussi eu comme résultat de diminuer les concentrations totales d'Hg dans ces lacs affectés. Cependant, cette baisse en carbone organique dissous (COD) a aussi mené à une augmentation en Hg biodisponible, ainsi qu'à une bioaccumulation d'Hg plus élevée dans les espèces de périphyton et de macroinvertébré de les lacs les plus perturbés, ceux avec des concentrations de COD moins de 6 et 9 mg COD/L, respectivement. De plus, une corrélation négative entre la bioaccumulation d'Hg et le COD a été observée au-delà de ces concentrations, comme il l'est typiquement observé dans les lacs de référence.

Des répercussions d'activités minières ont aussi été observées dans les lacs à l'intérieur de 25 km de la cheminée principale de Giant Mine dans la région de Yellowknife. À vrai dire, des augmentations importantes d'arsenic (As) et de méthylmercure ont été mesurées dans les lacs plus près de la mine, avec des concentrations d'As bien au-dessus des recommandations pour l'eau dans les lacs à l'intérieur de 17 km de la cheminée de Giant Mine. Cette recherche met en évidence l'importance de la surveillance environnementale de référence, antérieure au développement de ressources naturelles, ainsi que la possibilité d'influences multiples provenant de ces

développements lorsqu'ils se situent dans les régions sensibles de pergélisol, telles que celles exposées à la fonte de pergélisol.

Acknowledgements

I wish to acknowledge and thank Jules Blais, without whom this thesis would never have been possible. Thank you for your infinite patience and encouragement, as well as welcoming environment both in and out of the lab. I would also like to thank Linda Kimpe for her enduring guidance in the lab and in preparing for the challenges of remote Arctic field work. Thank you also to Steve Kokelj for the memorable internship in Yellowknife, and to John Smol and Mike Pisaric for your assistance and knowledge throughout this strategic project.

I would like to thank Alex Poulain and Danielle Fortin for providing feedback as members of my committee throughout, and to my defense committee for your input. To the members of the Blais lab, past and present, thank you for the levity in and out of the lab. In particular, thank you to my field partners, Todd French, Rebecca D'Onofrio, and David Eickmeyer, for allowing me to drag you through the taiga and across tundra for hours on end. Additional thanks goes to the excellent teams at the Aurora Research Centre in Inuvik and the Taiga Lab in Yellowknife.

To my parents, sister, friends and family, I thank you for your unwavering support for my continued education and for enabling me to carve my path. Most importantly, I thank my wife Ann Balasubramaniam, for whom countless hours of counsel will never be recouped! This opportunity to go through a PhD alongside of you will always be cherished. Your unending love, advice, and support, has been invaluable.

Dedications

In memory of

Melanie Houben

and

Ellen Maloney

Table of Contents

List of Tables

List of Figures

1. General Introduction

1.1. Introduction to Thesis

Across the Arctic, several studies have identified significant trends of increasing freshwater organic carbon, nutrients, and algal production in relation to thawing permafrost, while also demonstrating greater contaminant uptake in organisms of these systems. One study (Carrie et al., 2010) identified that warmer and longer growing seasons were associated with elevated mercury and PCB concentrations in burbot due to increased algal growth and contaminant scavenging. In contrast, within the upland tundra lakes situated in the continuous permafrost zone east of the Mackenzie River delta, shoreline retrogressive thaw slump (SRTS) events associated with warmer growing seasons caused adjacent lakes to have lower organic carbon and colour, and greater water clarity, ionic activity, and pH values (Kokelj et al., 2005). In these systems there is little available data about algal productivity and contaminant uptake. In this thesis, I aim to delineate the limnological changes and shifts in primary production in response to shoreline retrogressive thaw slumps.

The complex interactions between climate warming, catchment geology and vegetation and the resultant permafrost thaw, along with subsequent changes in lake chemistry, may lead to varied biological and ecotoxicological responses.

Additionally, in this thesis, a second study site within a sub-Arctic taiga shield region, underlain with discontinuous permafrost was surveyed and the legacy impacts of a mining development, were assessed. This secondary study will assist in predicting impacts of development on shallow northern lakes. Indeed, this is also a growing concern as northern regions are experiencing increased mining and development pressure and the potential risks of legacy contaminants in freshwater could pose significant threat to human health in remote northern communities that access these lakes for as part of their traditional subsistence livelihoods.

This thesis expands the knowledge of thawing permafrost influences on the vast freshwater resources within permafrost regions in Canada, while also delineating the localized overlapping influences of natural resource development. Each chapter of this thesis is written as a stand-alone manuscript to be published as a research article in a peer-reviewed journal.

1.2. Thesis rationale

In this thesis, I propose that the effects of shoreline retrogressive thaw slump events on adjacent lake systems in the upland tundra landscape east of the Mackenzie River Delta will have a negative impact on biota. In particular, the expected lower nutrient availability in slump-affected lakes will lead to lower primary production. Further, the changes in physical-chemical properties of slump-affected lakes will alter contaminant availability. More specifically, Hg bioavailability will be altered due to the dramatic changes in organic carbon and sulfur availability, two key Hg constituents. The second component of this thesis aimed to delineate shifts in limnology in thaw-affected Arctic lakes from local natural resource development impacts. For this second aspect, the focus is on the Giant Gold Mine in Yellowknife, NT, and the environmental legacy on the surrounding lakes.

1.3. Hypotheses & Objectives

1.3.1. Hypotheses

The primary purpose of this thesis research was to determine if thawing permafrost – in the form of shoreline retrogressive thaw slump events adjacent to tundra lakes – due to climate warming, altered aquatic productivity and contaminant cycling, and to compare and contrast this between an Arctic tundra landscape and a sub-Arctic taiga-shield landscape impacted by mining.

- Hypothesis 1 (H1): Shoreline retrogressive thaw slump events within the glaciolacustrine tills of the upland tundra lake system East of the Mackenzie River Delta, leads to lower concentrations of organic and particulate nutrients, and thus lower primary production of affected lakes, due to complexation and subsequent sedimentation with incoming permafrost soils.
- Hypothesis 2 (H2): Shoreline retrogressive thaw slump events lowers overall mercury concentrations due to sedimentation and reduced terrestrial transport of organic matter, while enhancing mercury bioavailability within affected lakes.
- Hypothesis 3 (H3): Mining emissions elevate local lake concentrations of key analytes (e.g. arsenic & sulfate) confounding or amplifying permafrost thaw impacts on lakes.

The objectives outlined in each chapter of this thesis allowed me to support or refute H1-H3.

1.3.2. Objectives

Objective 1: To delineate the extent of change in primary production in tundra lakes affected by shoreline retrogressive thaw slump events.

Slump-affected lakes in the tundra uplands east of the Mackenzie River delta have lower DOC and higher clarity and ionic activity (Kokelj et al., 2005). In Chapter 2, I provide data that further illustrates chemical changes in slump-affected lakes, and how this translates into lower primary production, along a size gradient of thaw slump disturbance. In disturbed lakes, thaw slumping is the dominant influence on nutrient availability and primary production. When compared to several other studies across Canada's low-Arctic, our active slump-affected lakes demonstrate significantly lower Chl-*a* concentrations suggesting lower phytoplankton growth. These findings support the hypothesis that thaw slumps negatively influence nutrient availability and primary production in tundra lakes (H1).

Objective 2: To determine how chemical and biological changes in slump-affected lakes relate to Hg cycling.

In Chapter 3, I demonstrate the extent of change in potential Hg supply to slump-affected lakes across a tundra landscape experiencing significant environmental gradients as well as thaw slump events. Potential Hg sources, such as atmospheric and terrestrial loadings are compared in slump-affected and reference lakes, as well as across large environmental gradients, highlighting the dominant influence of shoreline retrogressive thaw slump events on adjacent lakes.

Objective 3: To determine how related chemical and biological changes in slump-affected lakes relate to Hg bioavailability.

In both Chapter 3 and Appendix, I demonstrate a non-linear, nonequilibrium relationship between Hg bioaccumulation in periphyton (Ch.3) and invertebrates (Appendix) and DOC concentrations, in support of a related experimental study (Chiasson-Gould et al., 2014). A DOC threshold concentration for Hg bioaccumulation factors was measured in the 5-9 mg DOC/L range, indicating that lakes with DOC concentrations below the threshold had a positive correlation with Hg BAFs, which were all slump-affected lakes. The large changes in lake physical and chemical

properties following a slump event have led to an unexpected increase in Hg bioaccumulation at several trophic levels.

Objective 4: To determine the extent that the Giant Gold Mine is a significant influence on lake chemistry within the same Yellowknife, NT, region experiencing significant warming and shoreline subsidence.

In Chapter 4, an assessment of the local influence of decades of emissions from Giant Mine, highlighting the necessity to determine confounding and/or combined effects of diffuse climate change and direct pollution on aquatic systems.

1.4. Background & Literature Review

1.4.1. Climate Change and Contaminants in the Canadian Arctic

Major environmental changes are occurring across the globe on both regional and continental scales as a result of human industry over the past century. Atmospheric carbon dioxide concentrations have increased by 35% since 1750 as a result of fossil fuel burning and land clearing. Correspondingly, the average global temperature has increased by 0.74°C over the last century (IPCC, 2007). This temperature flux is not homogenous as certain zones, such as the western Canadian Arctic, have already experienced temperature increases of up to 4°C over this same period, meanwhile, model projections suggest a further 2-12°C increase by 2090 (ACIA, 2005). Recent IPCC reports have also indicated that we are now tracking the upper range of earlier modelling exercises (IPCC, 2013). Within both study regions, Inuvik and Yellowknife, NT, maximum ice thickness has also significantly decreased by 5-8 m per decade between 1959-2014 (Figure 1.1). Increasing temperatures will drive further ecosystem responses relating to thawing permafrost and declining albedo. Associated positive feedbacks will result in further declines in Arctic sea and lake ice coverage (Barber et al., 2008), drainage of freshwater lakes and new wetland development as permafrost thaws, northward progression of the tree line (Turunen et al., 2009), the release of methane formerly stored in frozen tundra (Bloom et al., 2010), and potentially the subsequent enhancement of contaminant delivery to Arctic food webs. Biotic responses will

also be driven by these changes in water quality, vegetation, and precipitation patterns (ACIA, 2005), which in turn may amplify feedback loops.

Climate change and industrial contaminants have been identified as two principal concerns for Arctic residents. Indigenous communities have had relatively high exposures to several organochlorines and metal contaminants. For example, PCB concentrations were measured in the early 1990s to be elevated in a Belcher Island Inuit community (Cameron and Weis, 1993).

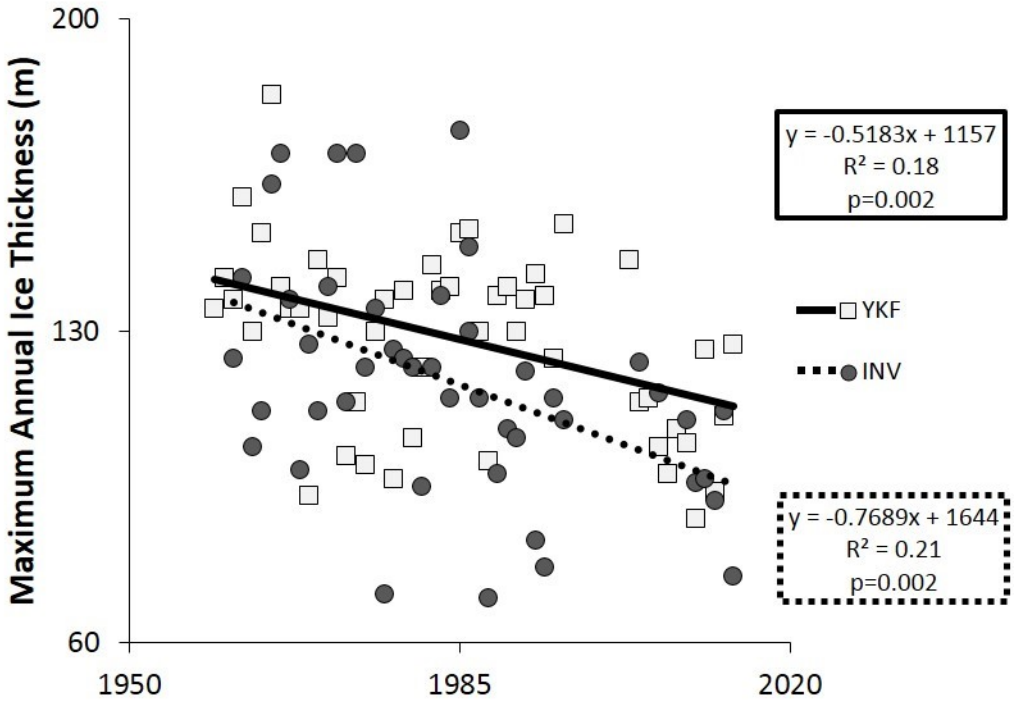

Figure 1.1: Maximum annual lake ice thickness in Yellowknife (YKF) and Inuvik (INV), from 1959-2014. Data was obtained from Environment Canada Ice Thickness Program.

Hg accumulation in Arctic communities was first observed in Alaskan mothers as early as 1976 (Galster, 1976) and in Greenland in 1983 (Hansen et al., 1983, 1990). Though regulations and bans on the use of toxic compounds has led to a decline in human concentrations in temperate latitude; in contrast, Arctic populations have been slow to experience a similar decline, and have either stabilized or increased in several regions. As well, the global decline of atmospheric organochlorines and mercury concentrations have not resulted in lower environmental concentrations within polar regions, such as the Mackenzie River watershed where fish (burbot) have higher concentrations (Carrie et al., 2010) of polychlorinated biphenyls (PCBs) and Hg. The authors proposed that drivers such as a warmer environment and related shortening in the ice-cover

period are driving greater primary production, algal scavenging of Hg and PCBs, enhanced MeHg production, and increased bioavailability to fish, rather than atmospheric concentrations. To compliment these proposed mechanisms, we hypothesize that the thermokarst activity that is rapidly accelerating due to environmental changes will alter biogeochemical cycles of lakes caused by loading of thaw slump material to lake systems. The warming of the Arctic is very likely to accelerate over the next century and our focus will be on thawing permafrost as a vector for net contaminant delivery into freshwater catchments as an early indicator for ecosystem health and adaptation to climate change. Mercury (Hg) is a non-degradable, high-density metal that has natural sources in the environment, but as has been noted (Macdonald et al., 2000) anthropogenic sources have accelerated their delivery to air sheds and watersheds over the last century. Mercury is of special concern for us as it is subject to long-range atmospheric transport with a long residence time and ultimately deposits onto the land and lakes to become integrated with soil and sediment cycling. Elemental forms are typically not as toxic as cationic forms or when incorporated into short hydrocarbons (e.g. methyl mercury). Anthropogenic emissions of Hg (e.g. coal combustion, waste incineration, metal production) exceeded natural sources by a factor of 4 by the mid-1980s. Mercury enters the atmosphere in its elemental form where atmospheric currents can direct global distribution from high industrial zones to remote areas. Atmospheric deposition occurs in particulate form (dry deposition) or as photochemically oxidized (Hg^{2+}) inorganic Hg (wet deposition). Once in aquatic and terrestrial environments inorganic mercury is either reduced back to its elemental form where volatilization to the atmosphere occurs, or it undergoes further biochemical transformation by methylation processes. Methyl mercury is a readily available form for bioaccumulation and is of greatest concern for biotic toxicity. In aquatic systems, both inorganic and organic mercury can further sediment out from the water column and be buried, or continue cycles of demethylation/methylation or redox reactions before being permanently buried, resuspended, or evaporated back into the atmosphere (Baird, 1999; Selin, 2009). In relation to permafrost thaw slumping, we aim to determine if the proportions and bioavailability of these Hg species are altered in the water, sediment, and biotic compartments of disturbed lakes, in comparison to undisturbed reference lakes.

1.4.2. Ground Ice & Thawing Permafrost

Permafrost is surficial geology that is annually or permanently frozen and is overlain by a seasonal active layer that repeatedly freezes and thaws; in the northern hemisphere, permafrost covers 25% of the terrestrial landscape (IPA 2010). Permafrost can be one of five types of ground ice, 1) pore ice typically found in deposited delta soils, 2) ice wedges, which occur in delta and tundra landscapes, 3) massive bodies of tubular ice, 4) basal glacier ice, and 5) accumulations of segregated ice (Burn and Kokelj, 2009). Segregated ice occurs at the interface between permafrost and the above active layer and can have a net accumulation of 10-30 cm in an ice-rich layer as water from the active layer migrates downward during summer thaw, with upward migration from permafrost in the winter (Cheng, 1983; MacKay, 1972). This ice-rich layer can also act as a zone of convective ion transport, a sink for soluble nutrients during static or aggrading ice conditions, or alternatively as a nutrient source during periods of active layer deepening (Kokelj and Burn, 2003). Dominant cations are commonly calcium (Ca^{2+}) and magnesium (Mg^{2+}) ions and can be up to 7.5 times higher in near-surface permafrost relative to the above active layer (Kokelj and Burn, 2005).

Both the active layer and permafrost layers vary in depth according to environmental factors such as latitude (Burn and Kokelj, 2009) and predominant air mass circulation, with the depth of permafrost being positively associated with cooler air temperatures, while the active layer is inversely related, adjusting seasonally. Other landscape-scale factors play a smaller role in permafrost aggradation, such as soil characteristics and water content (Burn and Kokelj, 2009), snow pack, direction of terrain slope and proximity to adjacent or overlying water bodies (Mackay 1974). Permafrost can range from several metres to several hundred metres deep while the active layer is commonly less than 1 m. On a continental scale, permafrost is categorized broadly into continuous (>90% frozen ground) and discontinuous (50-90% frozen) zones. Even within ubiquitous permafrost zones there are areas that do not freeze completely such as when talik formations occur under lakes or rivers. Taliks are unfrozen anomalies within permafrost and are associated with water bodies when the water column is deep enough to avoid freezing completely to the bottom, thus the ice insulates the underlying water and substrate from subsequent freezing. Increased warming triggers lateral expansion of these taliks, leading to shoreline collapse. Where there is a high enough excess ice content within the shoreline soils a retrogressive thaw slump can rapidly form and expand over several years (Aylsworth et al., 2000). Slumps can then quickly

ablate and grow, usually in a cyclical pattern, by even meters per year (Lantuit and Pollard, 2008; Lewkowicz, 1987) creating crater-like features adjacent to lakes that can be up to equivalent or even greater to the lake surface area, degrading a substantial proportion of the catchment (Lantz and Kokelj, 2008). Thaw slumps transfer large quantities of thawed ice and soil to the adjacent lakes.

Typically, the maximum depth of the terrestrial soil active layer expands to 0.35-0.65 m each summer (Burn and Kokelj, 2009). This relatively thin active layer is high in organic matter, providing much of the nutrients and minerals to tundra lake systems in our region, and is predominantly delivered via overland runoff in the relatively brief spring freshet. However, in a rapidly degrading shoreline retrogressive thaw slump event, the thawing front, or headwall, has been roughly estimated to be up to 10 m deep within our study region; and often deeper along larger lakes, rivers, or marine coasts, and landscapes (Kokelj et al., 2009a; Lantuit et al., 2005; Lewkowicz, 1987). The thawing permafrost is made-up of inorganic material diluted by massive beds of ice (Mackay, 1971), and greatly reduces the proportion of organic matter being delivered to lakes. Thereby, during and after a shoreline retrogressive thaw slump event, total and relative input of active layer components (e.g. organic matter) to adjacent lakes is reduced by, i) the relative dilution by inorganic material at the thaw front (headwall), and, ii) the resultant slump scar reducing the percent of catchment area overlain with organic matter to allow overland runoff to transport dissolved organic matter to lakes. Additionally, thaw slumps tend to be most active mid to late summer, as opposed to during the spring freshet, altering the seasonal timing in the delivery of certain compounds to the adjacent disturbed lakes. These geochemical distributions suggest that thawing permafrost enriches deeply sequestered mineral-associated chemicals into tundra lakes while causing the concentrations of surficially-sequestered organic-bound compounds to be reduced and/or diluted. Water penetrating deep into the ground erodes minerals, which, in turn, enriches pore water with major ions, transporting them by subsurface flow to adjacent lakes.

Within-lake processes, occurring after sediment particles are scoured from thaw slump scars to lake water, may also contribute to DOC losses from the water column. For example, Thompson et al. (2008) added thaw slump scar sediments to lake-water microcosms and found that DOC settled out, substantially reducing water colour. Additionally, Deison et al. (2012) observed that slump-affected lakes had greater sedimentation rates and they attributed lower algal derived carbon

and particulate organic carbon in surface sediments to dilution from the large volumes of inorganic tills arriving to lakes from adjacent thaw slumps.

1.4.3. Impacts on Lakes

Due to the great depth of permafrost surrounding lakes, ground water flow has very limited, if any, influence on lakes (Braddock and McCarthy, 1996). Catchment runoff occurs almost explicitly overland during the spring melt period, or can occur within the shallow organic active layer during the ice-free season after the active layer deepens. However, due to aridity in these remote regions these catchment inputs are often limited. As a result, chemical changes within lakes following retrogressive thaw slump events can be dramatic as large volumes of inorganic material are released from the permafrost. In a study of 22 lakes (11 disturbed by thaw slumping) it was observed that ionic strength, water clarity, and pH, all increased after thaw slump events (Kokelj et al., 2005). On average disturbed lakes had sulfate and calcium ion concentrations an order of magnitude greater than undisturbed reference lakes. Further, these same slump lakes had improved clarity and were almost a pH unit more alkaline on average. In subsequent studies, potentially competing environmental influences (e.g. surficial geology, proximity to both the tree line and Arctic coast) were tested for relationships with water chemistry flux, along with thaw slump activity, and found that permafrost degradation was the dominant driver, outside of a minor Na+ gradient in relation to the Arctic Ocean (Kokelj et al., 2009b; Kokelj and Burn, 2005). Further evidence of thaw slump effects on lake chemistry was the positive relationship of chemical change with the proportion of catchment disturbed, and the negative relationship to the age of the slump, suggesting larger and more recent thaw slumps have a greater impact on lake water chemistry. In undisturbed lakes, factors such as fire and soil type had a greater influence on lake chemistry. The proportion of lakes estimated to have thaw slumps is currently 8-12% in the upland tundra region east of the Mackenzie delta (Lantz and Kokelj, 2008) and are expected to increase in importance as warming continues.

Mining influences on lakes have been well documented in the past and have been related to significant pollution to downstream ecosystems. However, for the Giant Mine region in Yellowknife, few surveys have measured the effect of roaster emissions in nearby lakes outside of the mining property over its 50-year lifespan. Further, the potential for compounding influences from thawing permafrost in these areas affected by resource development are not well known.

Outside of the Giant Mine property, several studies of the landscape have noted elevated concentrations of As and other related mining combustion by-products, such as higher sulfate and other trace metal concentrations in lake sediments (Andrade et al., 2010; Galloway et al., 2015) and soils and vegetation (Hutchinson et al., 1982; Koch et al., 2000a, 2000b; St-Onge, 2007), as well as bird species (Koch et al., 2005). However, to date, very little data are available for lake chemistry. This information is key as aquatic organisms are important food sources to both wildlife and human diets. It is important to assess ecosystem responses to resource development, and in particular within a region that is concurrently experiencing rapid environmental change.

1.5. References

ACIA (2005) *Arctic Climate Impact Assessment*. Cambridge, United Kingdom: Cambridge University Press.

Andrade CF, Jamieson HE, Kyser TK, Praharaj T and Fortin D (2010) Biogeochemical redox cycling of arsenic in mine-impacted lake sediments and co-existing pore waters near Giant Mine, Yellowknife Bay, Canada. *Applied Geochemistry*. 25(2): 199–211. doi:10.1016/j.apgeochem.2009.11.005.

Aylsworth JM, Duk-Rodkin A, Robertson T and Traynor JA (2000) Landslides of the Mackenzie valley and adjacent mountainous and coastal regions. In: Dyke LD and Brooks GR (eds) *The physical environment of the Mackenzie valley, Northwest Territories: A base line for the assessment of environmental change*. Ottawa: Geological Survey of Canada, Natural Resources Canada, 167–176.

Baird C (1999) *Environmental Chemistry*. New York, USA: Freeman.

Barber D, Lukovich J, Keogak J, Baryluk S, Fortier L and Henry GHR (2008) The changing climate of the Arctic. *Arctic* 61(Suppl 1): 7–26.

Bloom AA, Palmer PI, Fraser A, Reay DS and Frankenberg C (2010) Large-scale controls of methanogenesis inferred from methane and gravity spaceborne data. *Science* 327: 322–325. doi:10.1038/nchem.467.

Braddock JF and McCarthy KA (1996) Hydrologic and microbiological factors affecting persistence and migration of petroleum hydrocarbons spilled in a continuous-permafrost region. *Environmental Science & Technology* 30(8): 2626–2633.

Burn CR and Kokelj S V (2009) The environment and permafrost of the Mackenzie Delta Area. *Permafrost and Periglacial Processes* 20: 83–105: doi:10.1002/ppp.

Cameron M and Weis IM (1993) Organochlorine contaminants in the country food diet of the

Belcher Island Inuit, Northwest Territories, Canada. *Arctic* 46(1): 42–48.

Carrie J, Wang F, Sanei H, Macdonald RW, Outridge PM and Stern GA (2010) Increasing contaminant burdens in an Arctic fish, burbot (*Lota lota*), in a warming climate. *Environmental Science & Technology* 44(1): 316–322.

Cheng G (1983) The mechanism of repeated-segregation for the formation of thick layered ground ice. *Cold Regions Science and Technology* 8: 57–66.

Chiasson-Gould SA, Blais JM and Poulain AJ (2014) Dissolved organic matter kinetically controls mercury bioavailability. *Environmental Science & Technology* 48(6): 3153–3161.

Deison R, Smol JP, Kokelj S V, Pisaric MFJ, Kimpe LE, Poulain AJ, et al. (2012) Spatial and temporal assessment of mercury and organic matter in thermokarst affected lakes of the Mackenzie Delta Uplands, NT, Canada. *Environmental Science & Technology* 46(16): 8748–55. doi:10.1021/es300798w.

Galloway JM, Palmer M, Jamieson HE, Patterson RT, Nasser N, Falck H, et al. (2015) Geochemistry of lakes across ecozones in the Northwest Territories and implications for the distribution of arsenic in the Yellowknife region. Part 1: Sediments. doi:10.4095/296954.

Galster WA (1976) Mercury in Alaskan Eskimo mothers and infants. *Environmental Health Perspectives* 15: 135–40.

Hansen JC, Ulrk T and Boh J (1990) Prenatal exposure to methyl mercury among Greenlandic polar Inuits. *Archives of Environmental Health* 45(6): 355–358.

Hansen JC, Wulf HC, Kromann N and Albøge K (1983) Human exposure to heavy metals in East Greenland. 1. Mercury. *Science of the Total Environment* 26(3): 233–43.

Hutchinson TC, Aufreiter S and Hancock RG V (1982) Arsenic pollution in the Yellowknife area from gold smelter activities. *Journal of Radioanalytical Chemistry* 71(1–2): 59–73. doi:10.1007/BF02516141.

IPCC (2007) Climate Change 2007: The Physical Science Basis. Contribution of Working Group I to the Fourth Assessment Report of the Intergovernmental Panel on Climate Change. Cambridge, United Kingdom: Cambridge University Press.

IPCC (2013) Climate Change 2013: The Physical Science Basis. Contribution of Working Group I to the Fifth Assessment Report (AR5). Final Draft Underlying Scientific-Technical Assessment. Cambridge, United Kingdom: Cambridge University Press.

Koch I, Mace J V and Reimer KJ (2005) Arsenic speciation in terrestrial birds from Yellowknife, Northwest Territories, Canada: the unexpected finding of arsenobetaine. *Environmental Toxicology and Chemistry* 24(6): 1468–1474: doi:10.1897/04-155R.1.

Koch I, Wang L, Ollson C a., Cullen WR and Reimer KJ (2000a) The predominance of inorganic arsenic species in plants from Yellowknife, Northwest Territories, Canada. *Environmental*

Science & Technology 34(1): 22–26. doi:10.1021/es9906756.

Koch I, Wang L, Reimer KJ and Cullen WR (2000b) Arsenic species in terrestrial fungi and lichens from Yellowknife, NWT, Canada. *Applied Organometallic Chemistry* 14(5): 245–252.

Kokelj S V and Burn CR (2003) Ground ice and soluble cations in near-surface permafrost, Inuvik, Northwest Territories, Canada. *Permafrost and Periglacial Processes* 14(3): 275–289. doi:10.1002/ppp.458.

Kokelj S V and Burn CR (2005) Geochemistry of the active layer and near-surface permafrost, Mackenzie Delta region, Northwest Territories, Canada. *Canadian Journal of Earth Sciences* 42: 37–48. doi:10.1139/E04-089.

Kokelj S V, Jenkins RE, Milburn D, Burn CR and Snow NB (2005) The influence of thermokarst disturbance on the water quality of small upland lakes, Mackenzie Delta region, Northwest Territories, Canada. *Permafrost and Periglacial Processes* 16(4): 343–353. doi:10.1002/ppp.536.

Kokelj S V, Lantz TC, Smith SL, Kanigan JCN and Coutts R (2009a) Origin and polycyclic behaviour of tundra thaw slumps, Mackenzie Delta region, Northwest Territories, Canada. *Permafrost and Periglacial Processes* 20: 173–184: doi:10.1002/ppp.

Kokelj S V, Zajdlik B and Thompson MS (2009b) The impacts of thawing permafrost on the chemistry of lakes across the subarctic boreal-tundra transition, Mackenzie Delta region, Canada. *Permafrost and Periglacial Processes* 20: 185–199: doi:10.1002/ppp.

Lantuit H, Couture N, Pollard WH, Haltigin T and De Pascale, G Budkewitsch P (2005) Short-term evolution of coastal polycyclic retrogressive thaw slumps on Herschel Island, Yukon Territory. *Berichte zur Polar- und Meeresforschung (Reports on Polar and Marine Research)* 506: 72–75.

Lantuit H and Pollard WH (2008) Fifty years of coastal erosion and retrogressive thaw slump activity on Herschel Island, southern Beaufort Sea, Yukon Territory, Canada. *Geomorphology* 95(1–2): 84–102. doi:10.1016/j.geomorph.2006.07.040.

Lantz TC and Kokelj S V (2008) Increasing rates of retrogressive thaw slump activity in the Mackenzie Delta region, N.W.T., Canada. *Geophysical Research Letters* 35(6): 1–5. doi:10.1029/2007GL032433.

Lewkowicz AG (1987) Headwall retreat of ground-ice slumps, Banks Island, Northwest Territories. *Canadian Journal of Earth Sciences*. 24(6): 1077–1085.

Macdonald RW, Barrie LA, Bidleman TF, Diamond ML, Semkin RG, Gregor DJ, et al. (2000) Contaminants in the Canadian Arctic: 5 years of progress in understanding sources, occurrence and pathways. *Science of the Total Environment* 254(2–3): 93–234.

Mackay JR (1971) The origin of massive icy beds in permafrost, western Arctic Coast, Canada.

Canadian Journal of Earth Sciences 8(4): 397–422.

MacKay JR (1972) The world of underground ice. *Annals of the Association of American Geographers* 62(1): 1–22.

Selin NE (2009) Global biogeochemical cycling of mercury: a review. *Annual Review of Environment and Resources* 34(1): 43–63. doi:10.1146/annurev.environ.051308.084314.

St-Onge SM (2007) Impacts of arsenic and sulphur dioxide contamination from mining activities on forest health near Yellowknife, NWT. MSc Thesis, Carleton University. 139 pp.

Thompson MS, Prowse TD, Kokelj S V and Wrona FJ (2008) The impact of sediments derived from thawing permafrost on tundra lake water chemistry: an experimental approach. *Ninth International Conference on Permafrost*, Fairbanks, AK, USA, 5 pp.

Turunen M, Soppela P, Kinnunen H, Sutinen M-L and Martz F (2009) Does climate change influence the availability and quality of reindeer forage plants? *Polar Biology* 32(6): 813–832. doi:10.1007/s00300-009-0609-2.

2. The Impacts of Permafrost Thaw Slump Events on Limnological Variables in Upland Tundra Lakes, Mackenzie Delta region

Adam J Houben,*[†] Todd D French,[†] Steven V Kokelj,[‡] Xiaowa Wang,[‖] John P Smol,[§] Jules M Blais,[†]

[†] University of Ottawa - Program for Chemical and Environmental Toxicology, Department of Biology, University of Ottawa, Ottawa, ON, Canada K1N 6N5,

[‡] NWT Geoscience Office, Government of the Northwest Territories, Yellowknife, NT, Canada X1A 2R3,

[‖] Environment Canada, 867 Lakeshore Road, Burlington, Ontario, L7R 4A6, Canada

[§] Queen's University - Paleoecological Environmental Assessment and Research Laboratory (PEARL), Department of Biology, Queen's University, Kingston, ON, Canada K7L 3N6

This article has been published as *Houben et al. 2016. Fundamental and Applied Limnology. DOI: 10.1127/fal/2016/0921.* with minor modifications for this thesis.

Statement of author contributions:

AJH, TDF, SVK, XW, JPS, JMB

Authors' Contributions: Adam J Houben – lead researcher and author; Todd D French – field research and editorial review of manuscript; Steven V Kokelj – guidance in permafrost research and editorial review of manuscript; Xiaowa Wang – laboratory analyses of water chemistry; John P Smol –review of manuscript; Jules M Blais – research director and editorial review of manuscript.

2.1. Abstract

Thawing permafrost is widespread in Canada's western Arctic. In upland tundra situated north of Inuvik (NWT), ice-rich permafrost is thawing to form retrogressive thaw slumps, a process that transports large volumes of previously frozen inorganic material to adjacent lakes. Prior studies have indicated base water chemistry changes in slump-affected lakes, including lower dissolved organic carbon (DOC) and increased major ion concentrations. Here we demonstrate significant reductions in DOC and colour, and increases in water clarity as a function of the percent of catchment area disturbed by slumping. The influx of thawed sediments and solutes leads to ionic enrichment, and direct loading of several trace metals, including uranium, strontium, and lithium. The influx of ion-rich sediments from thaw slumps is associated with higher pH, and lower concentrations of several biologically important metals, including Fe, Mn, and Al, in the water column. The sedimentation of organics and particulates from the water column is a probable driver for the removal of major nutrients (N and P) leading to significantly lower planktonic chlorophyll *a* (Chl-*a*) concentrations in thaw slump affected lakes by as much as two thirds when comparing the most thaw slump affected lakes to reference lakes. Both phytoplanktonic and periphytic algal measurements indicate greater reductions in primary production in active slump-affected lakes as opposed to stabilized slump-affected lakes. We also highlight the slump-driven reduction in Chl-*a* concentrations relative to 11 other studies across Canada`s low Arctic as well as other ecotypes. In these already nutrient-poor systems, future warming-accelerated thaw slumping will likely reduce overall primary production and alter the limnological characteristics in similar tundra systems.

Key Words: Shoreline retrogressive thaw slump, Primary production, phosphorus, nitrogen, chlorophyll-*a*, Arctic, Tundra Lakes, Climate Change, Permafrost, Thermokarst, dissolved organic carbon, pH, major Ions, trace metals

2.2. Introduction

Arctic lakes are being affected by exceptional climate warming. In particular, annual air temperatures in Canada's western Arctic have increased 3-4 °C over the last century (Lantz and Kokelj, 2008; Prowse et al., 2009). Temperatures across the Arctic are expected to increase by an additional 5–7 °C by the end of the 21st Century, twice that of the expected global rate (Kattsov and Källén, 2005). With increased warming, Arctic terrestrial landscapes underlain by permafrost are thawing,

liberating previously frozen sediments and organic and soluble materials. The implications on aquatic ecosystems are greatly understudied.

Climate warming increases permafrost temperatures leading to thermokarst, such as shoreline retrogressive thaw slumps (SRTS) (Kokelj and Jorgenson, 2013). SRTS events occur along ice-rich shorelines and have been increasing in both size and number throughout the western Canadian Arctic (Segal et al., 2016) and, in particular to this study, to the east of the Mackenzie River delta (Lantz and Kokelj, 2008). Landscapes across the northern hemisphere have large proportions of their surface covered with thermokarst lakes many of which are vulnerable to further thaw slumping.

Arctic lakes provide important habitat for wildlife during the summer months and changes to surface water chemistry may have a critical effect on these typically oligotrophic systems. However, studies on basic limnological conditions in northern lakes from these regions are limited. Studies of the direct impacts of thermokarst features on aquatic biota are even fewer. Dugan et al. (2012) found elevated loading of total dissolved solids, including major ion content, following a large active layer detachment. Hydrological systems in the western Arctic are characterized by runoff over a shallow frost table. Permafrost in the region is hundreds of metres thick and ice-rich in the near-surface, so thermokarst-driven surface disturbances are likely to have the most significant impacts on aquatic systems(Kokelj et al., 2013; Kokelj and Jorgenson, 2013). The impacts that permafrost thaw will have on groundwater contributions and surface water chemistry will contrast by region dependent on factors such as bedrock and surficial geology. Several studies have described thermokarst-driven increases in major ions and lower DOC (Kokelj et al. 2005; Kokelj et al. 2009b; Malone et al. 2013) within the Mackenzie Delta Region, while in contrast several different studies indicate that thawing permafrost under the context of a warming Arctic will increase the allochthonous contribution of nutrients and dissolved organic carbon (DOC) to lakes (Carrie et al., 2010; Wrona et al., 2006). Increased nutrients (N, P) will typically enhance primary production, while the increased DOC influx may attenuate light and limit photosynthetically active radiation (PAR) (Wetzel, 2001). However, within our study region of small upland tundra lakes east of the Mackenzie Delta disturbed by SRTS events, prior studies have shown significant changes in water chemistry as one study comparing 11 lake-pairs found that DOC was lower in disturbed lakes on average, while pH, specific conductivity, and water clarity were all elevated (Kokelj et al., 2005). These few available studies highlight the variable and already fragile state of Arctic tundra lake systems, and indicate that any further stressors such as the intensification of thaw slumping could affect biological productivity (Thompson et al., 2012).

Our objective in this study was to further determine the relationships between the scale of thaw slump activity (size and age) and key limnological parameters, and in particular biologically relevant indicators such as N, P, and Chl-*a* concentrations in water, phytoplankton, and periphyton. We also included measurements of trace metal concentrations in water, sediments, and permafrost soils from the headwall and slump scars, as well as from catchment soils. We employed a paired-lake design to assess freshwater biogeochemical changes along a gradient of shoreline retrogressive thaw slumping, ranging from 0% of total catchment area slumped in reference lakes, up to 34% slumped in the most disturbed slump-affected lakes. Additionally, the relative age of thaw slumping was also considered by comparing actively degrading slump-affected lakes with lakes that had stabilized thaw slumps. In addition, we then compared our Chl-*a* concentrations with other lake studies from across Canada and the northern USA, after using total phosphorus as a covariate, and with particular focus on similar low Arctic landscapes, in order to assess if thaw slump events are major drivers for ecological change relative to greater continent-wide ranges in these two variables.

2.3. Methods

2.3.1. Study Area

This study was undertaken in the tundra uplands located to the east of the Mackenzie River delta, between Inuvik (68°21'54.60" N, 133°42'27.37" W) and the Beaufort Sea (Figure 2.1). The lake elevations of our study sites ranged from 18-225 m asl (mean, median of 73, 50 m asl) and are not affected by spring flooding or alluvial sedimentation regimes of the Mackenzie River Delta. The uplands are characterized by thousands of lakes, and rolling, hummocky terrain underlain by ice-rich permafrost (Mackay, 1966) that is susceptible to thaw slumping (Lantz and Kokelj, 2008). Soils are dominated by Wisconsinian tills derived from carbonate and shale bedrock, within a near-treeless landscape (Burn and Kokelj, 2009).

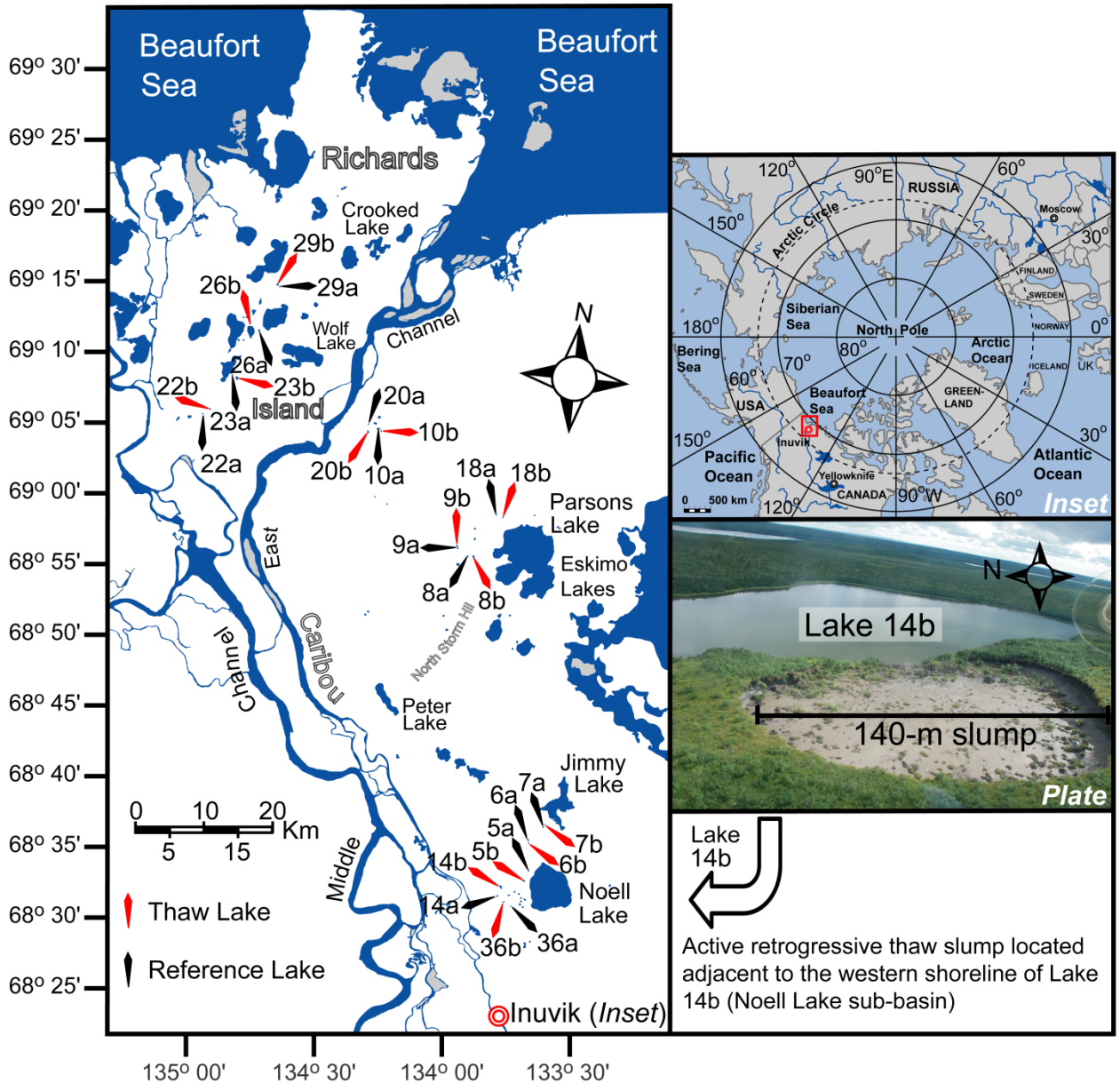

Figure 2.1: Map of the study region in the upland tundra zone northeast of Inuvik, Northwest Territories, Canada. The paired-lake study design is delineated by thaw and reference lakes. The upper right enlarged map indicates our location (red box) within the Arctic polar region. In the lower right, a representative active shoreline retrogressive thaw slump is shown.

There is a steep climate gradient between Inuvik and the Beaufort Sea. Mean annual air temperatures at Inuvik are -9.2°C and -10.8°C at Tuktoyaktuk (Burn and Kokelj, 2009). The persistence of sea ice in summer increases the strength of this gradient in early summer. The region is characterized by the transition from boreal forest near Inuvik to low-shrub tundra near the coast (Lantz et al., 2010). The area is underlain by continuous permafrost several hundreds of meters thick, overlain by a seasonally thawed active-layer approximately 35–85 cm thickness (Burn and Kokelj, 2009;

Kokelj et al., 2009a). Ground temperatures have increased in parallel with warming air temperatures (Burn and Kokelj, 2009), likely contributing to the increasing frequency and size of retrogressive thaw slumps (Figure 2.1). Slumps up to several hectares in areaoccur along shorelines of up to 15% of the upland lakes between Inuvik and the Beaufort Sea (Kokelj et al., 2009b; Lantz and Kokelj, 2008).

2.3.2. Field Sampling

Over three years (2009-2011) upland tundra lakes were sampled along a south-north gradient between Inuvik and Richards Island (Figure 2.1). In 2009, we selected lakes located across the full 100+ km range of this region to assess environmental effects, such as marine coast influences, proximity to the treeline, and recent fire history. In 2010, lakes were selected along a reduced latitudinal gradient, and we increased the range of the SRTS size (as a proportion of total catchment area). In 2011, in addition to our regular sampling, we also examined the water quality of input and output streams, and water column vertical structure. Lake surface area ranged from 0.8–116.5 ha with catchment area and maximum depth ranging from 4.7–254.4 ha and 1.5–10.9 m, respectively; mean and median values for each of these physical characteristics skewed to the lower limits of these ranges, (Table 2.1). Two lake types were sampled: i) Reference lakes — or lakes not having shoreline thaw slumps (denoted "a"); and ii) Slump-affected lakes — or lakes having shoreline thaw slumps (denoted "b"). For slump-affected lakes, the size of retrogressive thaw slumps ranged from 3% to 35% of total catchment area (Table 2.1), as determined from air photo analysis and ground surveys (Kokelj et al., 2005). The geomorphology, initiation, and development of thaw slumps are described by Kokelj et al. (2009).

Additionally, the relative age of a SRTS was broadly categorized into Active and Stable thaw slump groups based on whether or not exposed ground ice and an actively ablating headwall were present. The active slumps had steep, degrading headwalls, with very little to no vegetation growing on the thaw slump scar. In active disturbances, materials may flow downslope from the slump scar zone into the adjacent water body. The category of stable slump-affected lakes typically had > 50% vegetation cover on the thaw slump scar with shallow to non-existent headwalls.

Surface water samples were collected during relatively short sampling windows in June 20 – July 8, 2009; July 6, 2010; and June 30 – July 6, 2011. Water grab samples (0.5 m depth) for the analysis of nutrients, phytoplankton, major ions, $total_T$ and $total\text{-}dissolved_D$ metals (e.g. Fe, Al and Mn), pH, DOC, and dissolved inorganic carbon (DIC) were collected from the littoral zone (2009) and

Table 2.1: Physical characteristics of 38 tundra study lakes east of the Mackenzie River Delta, NT, Canada. Lakes were sampled June-July, 2009-2011. Lake pairs are denoted by similar number, while reference ("a") and slump-affected ("b") are differentiated by the following letter. D to Coast: distance to Arctic marine coast; %CD: percent of catchment area disturbed by thaw slumping; LA: lake area; CA: catchment area; Zmax: maximum lake depth; Burn Status: catchments with fire occurrence in last 50 years. Lakes are sorted by Slump Activity and %CD.

Lake	N	W	D to Coast (km)	Slump Activity	%CD	LA (ha)	CA (ha)	Z_{max} (m)	Surficial Geology	Burn Status
02a	68°30'09	133°39'55	108	Reference	0	2	17.2	6.1	Moraine	Recent
03a	68°31'14	133°40'18	106	Reference	0	1.3	13.1	10.3	Moraine	Recent
04a	68°30'57	133°39'39	106	Reference	0	1.2	15.5	2.5	Moraine	Recent
05a	68°33'04	133°38'23	103	Reference	0	2.9	20.9	10.9	Moraine	Unburned
06a	68°35'25	133°38'33	99	Reference	0	3.6	19.7	2.3	Moraine	Unburned
07a	68°36'18	133°35'27	100	Reference	0	1.4	18.1	2.7	Moraine	Unburned
09a	68°58'05	133°53'53	67	Reference	0	3.1	29.3	2.7	Moraine	Unburned
10a	69°07'05	134°10'05	49	Reference	0	2.3	26.3	3.4	Moraine	Unburned
12a	68°31'06	133°22'27	114	Reference	0	2.8	25	6.8	Moraine	Unburned
14a	68°31'02	133°44'55	106	Reference	0	3.4	33.5	7.5	Moraine	Recent
18a	69°00'26	133°45'28	65	Reference	0	2.1	18.4	5	Moraine	Unburned
19a	68°52'44	134°13'29	67	Reference	0	2.8	24.6	4.2	Glaciofluvial	Unburned
22a	69°08'28	134°49'06	40	Reference	0	1.9	8.3	2.8	Moraine	Unburned
26a	69°14'50	134°36'37	30	Reference	0	6.5	58.2	2.8	Moraine	Unburned
29a	69°18'13	134°31'56	25	Reference	0	3	14.5	3.8	Glaciofluvial	Unburned
36a	68°30'10	133°42'02	108	Reference	0	0.8	6.6	9.5	Moraine	Recent
23b	69°11'08	134°41'18	36	Stable	4	17.7	74.3	5.9	Moraine	Unburned
02b	68°30'26	133°40'08	107	Stable	6	4.9	15.9	3.4	Moraine	Recent
19b	68°52'58	134°12'56	67	Stable	6	6.1	28.1	7	Glaciofluvial	Unburned
12b	68°31'55	133°21'13	112	Stable	8	8.7	14.2	6.5	Moraine	Unburned
20b	69°07'01	134°12'53	49	Stable	8	4.8	17.9	3	Moraine	Unburned
06b	68°35'17	133°38'16	99	Stable	11	1.2	7.5	2	Moraine	Unburned
18b	69°00'13	133°43'55	64	Stable	12	2.7	4.7	5.2	Moraine	Unburned
04b	68°30'49	133°39'08	107	Stable	14	5	17.8	9.9	Moraine	Recent
36b	68°30'37	133°43'34	108	Stable	20	3.9	24.4	7.4	Moraine	Recent
29b	69°18'23	134°32'30	25	Stable	21	5.7	14.3	4.5	Moraine	Unburned
03b	68°30'40	133°39'51	107	Stable	24	4	15.3	11.3	Moraine	Recent
15b	68°51'39	133°56'06	74	Active	2	10.4	229.9	7	Moraine	Unburned
07b	68°36'32	133°35'12	99	Active	3	3.1	34.7	5	Moraine	Unburned
14b	68°31'45	133°44'14	104	Active	5	9.2	45.1	10.5	Moraine	Recent
11b	69°08'09	134°10'25	48	Active	6	10.5	39.4	5.2	Moraine	Unburned
16b	68°56'48	133°53'48	69	Active	6	14.1	63	6.6	Colluvial	Unburned
26b	69°14'45	134°38'21	30	Active	6	116.5	254.4	3.5	Moraine	Unburned
05b	68°32'14	133°39'27	104	Active	7	2.8	27.7	9	Moraine	Unburned
08b	68°57'24	133°50'27	69	Active	12	6.5	32.7	4.1	Moraine	Unburned
22b	69°08'44	134°47'02	41	Active	29	3.5	11.7	6.9	Moraine	Unburned
10b	69°07'14	134°10'52	49	Active	31	11.4	23.3	10.4	Moraine	Unburned
09b	68°58'14	133°53'59	67	Active	34	3.6	7.2	3	Moraine	Unburned

pelagic zone (2010-2011) of each lake. Prior to sampling, bottles (polyethylene) and caps were cleaned with dilute HCl (3-d soak), followed by thorough triple rinsing with distilled deionized water, (10% HNO_3 was used for trace metal collection bottles). Bottles were triple rinsed with lake water and filled to the rim to void the sample of air. Samples for metal analyses were preserved with concentrated HNO_3 to 2% of sample volume (dissolved fractions preserved after filtration). Samples for DOC, DIC, and total dissolved metal determinations were filtered within hours of collection, (47-mm diam.; 0.45-µm Sartorius filters, supported AcetatePlus, plain) and the filtrate analyzed. Water samples were kept cool (4 °C) and in the dark until analysis. Field temperature and specific (@ 25 °C) conductivity (SpC) were determined with a Y.S.I. Model 85 multimeter. Stream water surface grabs (2011) were collected in a similar manner. The timing of our sampling was consistent across the three years as ice-out timing and lake temperatures were comparable. Hydrological balances in this region are dominated by a spring freshet dilution event as the major input, followed by a summer-long evaporation and concentration period (230 mm drawdown of lakes) that far exceeds average precipitation in this same period (Pienitz et al., 1997a). Indeed, the results reported here are representative of mid-summer conditions and not annual averages, as sampling was post-spring freshet and before the summer-long evaporation and concentration period.

2.3.3. Water Analyses

All chemical analyses were performed at either Environment Canada's (EC) National Laboratory for Environmental Testing (NLET), Burlington, ON, or Taiga Environmental Laboratory, Yellowknife, NT, which both maintain Canadian Association for Laboratory Accreditation. At NLET, pH was determined with a Thermo Orion Model 106 meter. The remaining analyses at NLET were performed following EC's standard operating procedures (SOP): *i*) Cl^- and SO_4^{2-} (major anions SOP #1080); *ii*) Ca^{2+}, Mg^{2+}, Na^+ and K^+ (major cations #1061); *iii*) DOC and DIC (#1021); *iv*) Fe, Al and Mn (# 2003); *v*) apparent (Col_A) and true (Col_T) colour (#1501); *vi*) nitrogen species (TN: #1150; TKN: #1170; NH3: #1161; NO3: #1181; NO2: #1182); and *vii*) phosphorus species (TP: #1190; SRP: #1200).

2.3.4. Periphyton collections

Periphyton samples were collected from artificial substrates after 3-4 weeks *in situ* growing period. At each lake, three clean, white polyethylene shields (60 x 12 cm) with a total combined surface area of 6443 cm^2 (Figure S1), were deployed at 0.5 m under the water surface and left for periphytic algae to colonize for 3-4 weeks. Shields were then collected and stored in bags at -20°C until they were

processed. Using 250 mL of deionized water, periphyton were scraped and rinsed from the shields into an algal slurry. For chlorophyll analysis, a 10 mL aliquot was then filtered onto a 45 mm GFF filter and then stored at -20°C before assaying (Desrosiers et al., 2006). Chlorophyll concentrations were then measured using a dimethyl sulfoxide extraction with subsequent absorbance measured on a spectrophotometer at wavelengths of 664, 647, and 630 nm for Chl-*a*, *b*, and *c*, respectively (Sartory and Grobbelaar, 1984).

2.3.5. Statistical Treatment

The study design involved the pairing of each slump-affected lake with a nearby reference lake. Pairings were based primarily on geographical proximity (Figure 2.1), but other factors such as morphometric similarity were also considered (Table 2.1). Data were Ln-transformed prior to statistical analyses to satisfy assumptions of normality. To initially determine important biogeochemical factors influenced by SRTS events, a general linear modal (GLM) assessing SRTS activity status (reference, stable, active) and inter-annual variation (2009, 2010, 2011) was performed. Overall, inter-annual variation was only observed in a few relevant parameters as determined via GLM, such as pH and Secchi depth. For these parameters, individual years were tested separately, while most other parameters were pooled in subsequent linear regression analysis. For the significantly affected limnological parameters, linear regression was then used to determine water chemistry variation in relation to the scale of SRTS disturbance, measured as the percent of catchment area degraded by SRTS events, ranging from 0–34% of catchment area. We also compared limnological parameters to other potentially competing influences, such as lake to catchment area ratios, proximity to the marine coast and northern extent of treeline, as well as fire history within individual catchments; though in-general or otherwise stated, thaw slump disturbance was the dominant influence on lake chemistry. All statistical analyses were completed using SPSS 16.0 (2007).

Finally, as our primary focus was on thaw slump influences on biological indices, to test if TP and Chl-*a* results from our slump affected lakes were distinguishable drivers of ecological change relative to other systems from across Canada and northern USA, we compiled data (TP and Chl-*a*) from 11 studies that we categorized by geography (e.g. high versus low Arctic) and ecotype (e.g. tundra versus boreal forest), as already defined in the studies. Data was log-transformed to meet assumptions of normality. Two ANCOVA tests of Chl-*a* concentrations with TP as a covariate were performed: first, all 13 lake categories across Canada and northern USA that were reported were compared;

second, only low Arctic lake categories, of which our study lakes are located, were tested in a similar ANCOVA.

2.4. Results

2.4.1. Surface Water Chemistry

We observed dramatic differences in water chemistry between lakes affected by the presence or absence of thaw slumps. In addition, we also modeled the scale of thaw slump disturbance on water chemistry as a function of the percent of catchment area disturbed by SRTS events. A significant increase in specific conductivity (SpC) was observed in relation to the percent of the catchment area disturbed by thaw slumping (Figure 2). This parameter is a sum of ions (SO_4^{2-}, Cl^-, Ca^{2+}, Mg^{2+}, Na^+, and K^+), where sulfate and calcium were the major anion and cation, respectively, dominating both our reference and slump-affected lakes (Table 2.2), and all demonstrated a similar positive relationship with the percent of catchment area disturbed by thaw slump activity. However, Cl^- concentrations did not demonstrate a significant response to (%CD), and noting that chloride concentrations in reference lakes did exhibit a significant negative relationship with distance to the marine Arctic Ocean coast.

The pH values in slump-affected lakes (Table 2.2) were neutral to alkaline and nearly a pH unit greater than those in reference lakes, on average. When comparing pH against the percent catchment area slumped (Figure 2.2), significant inter-annual variation was taken into account, and each year was plotted separately. In each year (2009-11), pH increased in direct relation to the proportion of catchment area slumped (r^2 = 0.61, 0.35, 0.66; F = 37, 10, 43; p = 2.8×10^{-6}, 0.006, 1.4×10^{-6}, df_{total} = 25, 19, 23; for 2009, 2010, 2011, respectively). The higher pH also corresponds with significantly greater DIC concentrations in slump-affected lakes (Table 2.2) and with increasing percent of catchment disturbed (Figure 2.2).

Thaw slumping also affected lake water DOC, such that the average DOC concentrations for slump-affected lakes was less than half that of reference lakes (Table 2.2). DOC concentration was negatively related to percent catchment area slumped (r^2 = 0.48, F = 63.6, $p < 0.001$; Figure 2.2). Not surprisingly, the measurement of true colour (Figure 2.2) was also inversely related to percent catchment area slumped (r^2 = 0.66, F = 135.3, $p < 0.001$), while Secchi depth was positively correlated (r^2 = 0.34-0.51, F = 15.8-18.9, $p < 0.001$, for 2010 and 2011, respectively; Figure 2.2).

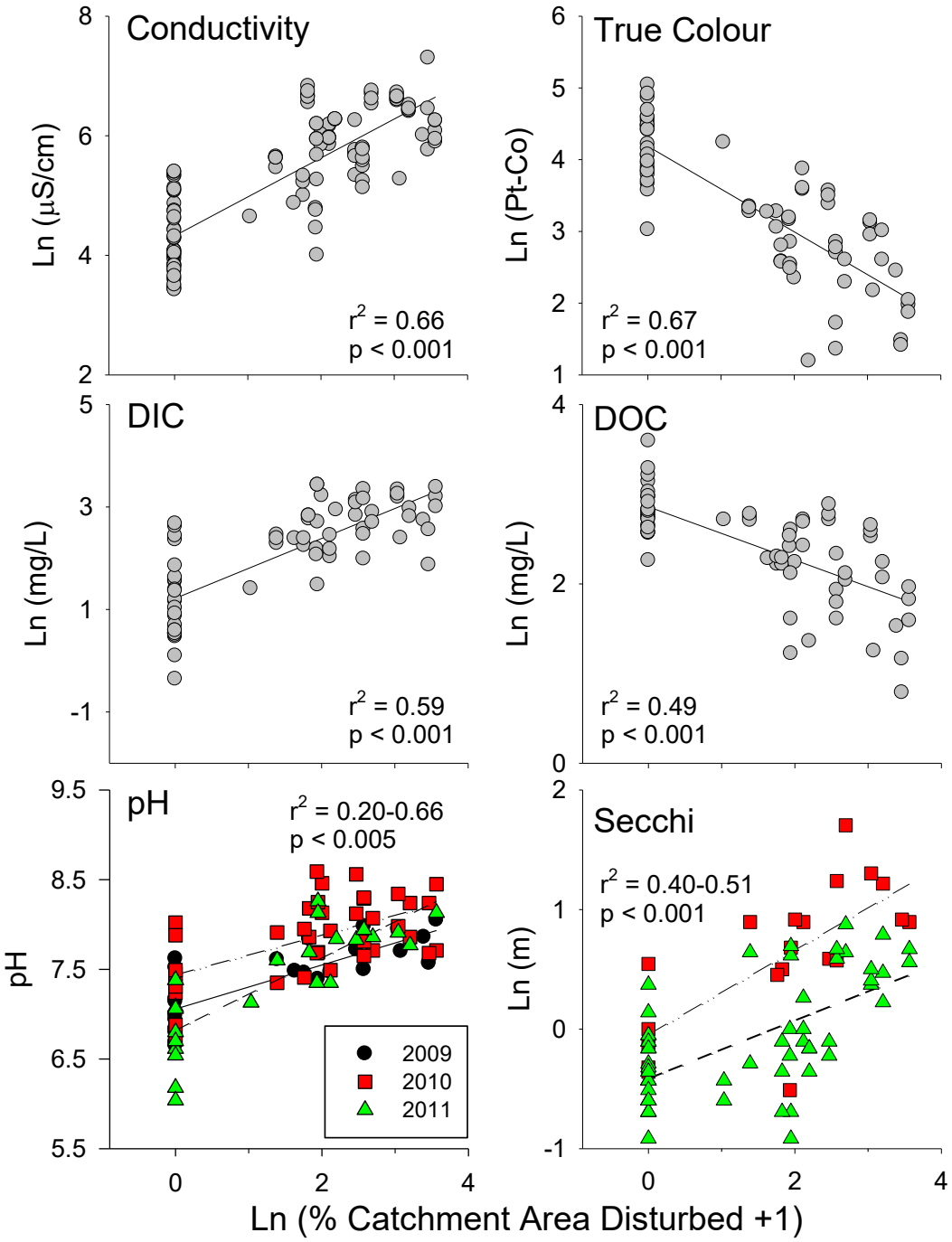

Figure 2.2: Water chemistry as a response to the percentage of catchment area disturbed by thaw slumping (Ln %CD+1). Samples pooled from the summers of 2009-2011; n = 69. A: specific conductivity, r^2=0.66, p<0.001. B: True Colour, r^2=0.67, p<0.001. C: Dissolved Inorganic Carbon (DIC), r^2=0.59, p,0.001. D: Dissolved Organic Carbon (DOC), r^2=0.49, p<0.001. E: pH, 2009 (circles, n=24), 2010 (squares, n=39), 2011 (triangles, n=24), r^2=0.20-0.66, p<0.005. F: Secchi depth, 2010 (squares, n=20), 2011 (triangles, n=57), r^2=0.34-0.51, F=15.8-18.9, p<0.0004, df=19-31. For pH and Secchi, all years are shown separately, as a prior two-way ANOVA highlighted inter-annual variation; annual results were still significant as indicated by the statistical ranges.

Table 2.2: Descriptive statistics for water chemistry variables categorized by slump-affected lakes and reference lakes. Independent t-Test results comparing between these two categories are included. Sampled lakes were from the tundra uplands, East of the Mackenzie Delta, 2009-2011.

Statistic	Category	Units	N	Mean	Min	Max	SD	t	df	P
Secchi	Slump	m	33	1.85	0.40	5.50	1.08	-3.9	50	<0.001
	Reference		19	0.85	0.50	1.73	0.32			
True Colour	Slump	mg L^{-1}	44	19.51	3.30	69.50	12.89	9.5	69	<0.001
	Reference		27	72.89	20.60	155.00	33.53			
DOC	Slump	mg L^{-1}	43	9.86	2.20	17.90	4.27	6.3	46	<0.001
	Reference		27	17.53	9.60	36.40	5.38			
DIC	Slump	mg L^{-1}	44	16.24	4.10	30.90	7.46	-7.7	69	<0.001
	Reference		27	4.23	0.70	14.50	3.85			
pH	Slump	-	44	7.73	7.13	8.26	0.25	-9.0	68	<0.001
	Reference		26	6.99	6.04	8.02	0.44			
SpC	Slump	µS cm^{-1}	47	421.79	54.80	925.00	236.90	-7.6	75	<0.001
	Reference		30	87.10	31.00	220.80	58.33			
SO4	Slump	mg L^{-1}	44	125.73	3.85	347.00	111.75	-5.2	68	<0.001
	Reference		26	10.90	0.30	47.50	12.53			
Cl	Slump	mg L^{-1}	44	4.08	1.25	9.03	1.83	-2.7	46	0.010
	Reference		26	2.73	0.62	7.75	2.14			
Ca	Slump	mg L^{-1}	44	47.58	5.75	113.00	29.10	-6.7	68	<0.001
	Reference		26	8.66	2.68	26.70	6.48			
Mg	Slump	mg L^{-1}	44	16.53	2.08	40.40	10.65	-6.4	68	<0.001
	Reference		26	2.97	1.16	7.86	1.93			
Na	Slump	mg L^{-1}	44	10.69	2.01	31.10	7.79	-5.1	68	<0.001
	Reference		26	2.84	1.48	6.68	1.55			
K	Slump	mg L^{-1}	44	2.39	0.48	4.40	1.09	-5.4	68	<0.001
	Reference		26	1.10	0.40	2.70	0.68			
SiO2	Slump	mg L^{-1}	28	0.98	0.06	2.36	0.64	2.9	37	0.006
	Reference		20	1.59	0.24	3.44	0.74			
TN	Slump	µg L^{-1}	44	381.94	131.00	678.00	131.05	4.5	59	<0.001
	Reference		27	519.31	353.00	734.00	120.92			
TP	Slump	µg L^{-1}	44	17.71	6.40	50.70	11.30	3.7	68	<0.001
	Reference		26	29.93	10.60	67.90	16.25			
TDP	Slump	µg L^{-1}	44	7.55	2.80	60.90	8.71	2.6	57	0.014
	Reference		27	12.81	5.40	45.70	8.27			
SRP	Slump	µg L^{-1}	44	1.31	0.20	5.70	1.06	3.9	69	<0.001
	Reference		27	2.96	0.70	11.20	2.45			
Chl-*a*	Slump	µg L^{-1}	44	3.48	0.20	19.30	4.34	2.8	68	0.007
	Reference		27	4.53	0.60	19.60	3.64			

Additionally, we measured vertical profiles at 1 m resolution in five lake pairs (Figure S3), on June 30, 2011, only several weeks following ice-out. The datademonstrated consistent thermocline structure between 2-4 m for all lakes, with or without thaw slump disturbance.

2.4.2. Nutrients & Primary Production

Slump-affected lakes had lower nutrient (N, P) concentrations (Table 2.2) of up to half of that measured on average in reference lakes. In addition, phosphorus and nitrogen concentrations in our lake systems both demonstrated significant negative slopes when regressed against the percent catchment area slumped (Figure 2.3A: total P (TP), total dissolved P (TDP), and soluble reactive P (SRP); Figure 2.3B: total nitrogen (TN)). Phytoplankton chlorophyll-*a* concentrations in slump-affected lakes were also significantly lower than reference lakes (Table 2.2) as well as inversely related to percent catchment area slumped (Figure 2.3C: phytoplankton chlorophyll-*a* concentrations (Chl-*a*), r^2=0.18, p=3.3x10^{-4}). Periphyton growth rate measurements (Chl-*a*, -*b*, -*c*) were likewise inversely related to the percent catchment area slumped, and were consistent for periphyton Chl-*a*, -*b*, and -*c* concentrations for each year (2009-11, Figure 2.3D). However, only periphyton Chl-*a* concentrations were significantly related to percent of catchment area disturbed (Chl-*a*, r^2=0.12, p=0.050; Chl-*b*, r^2=0.11, p=0.054; Chl-*c*, r^2=0.07, p=0.128). Indeed, both phytoplanktonic biomass (µg Chl-*a* L^{-1}) and periphytic growth rates (µg Chl-*a* m^{-2} day^{-1}) were positively correlated with TP concentrations (Figure 2.3E: Phytoplankton Chl-*a* vs TP, r^2=0.44, p<0.001 and periphyton growth rates vs TP, r^2=0.18, p=0.001). Due to significant inter-annual variation, both stable isotopes ^{15}N and ^{13}C were assessed separately by individual years. Regardless, in either 2009 or 2010, no significant difference in carbon source ($\delta^{13}C$) or food web baseline ($\delta^{15}N$), when comparing between reference and slump-affected periphyton tissue samples (Figure 2.3F), was observed.

When comparing lake effects by disturbance status (i.e. active, stable, and reference), we observed lower biological activity and nutrient (N, P) concentrations in lakes with more active slumps (Figure 2.4). Both total phosphorus (TP) and soluble reactive phosphorus (SRP) were significantly lower in lakes adjacent to active thaw slumps versus both reference lakes and lakes with stable thaw slumps along the shorelines (Figure 2.4a). Average TP concentrations were 29.9, 23.2, and 13.2 µg L^{-1}, while SRP was 2.96, 1.76, and 0.94 µg L^{-1} for reference, stable, and active thaw slump lakes, respectively. Likewise, total nitrogen (TN) concentrations in lakes decreased from 519, 429, to 343 µg L^{-1} in reference, stable, and active lakes, respectively. Both active and stable slump affected lakes were significantly lower than reference lakes for TN (Figure 2.4b). As a result, lakes adjacent to active thaw slumps had significantly lower Chl-*a* concentrations with respect to reference lakes and lakes with stable thaw slumps (Figure 2.4c). Concentrations for phytoplankton Chl-*a* were 4.53, 5.48, and 1.81 µg L^{-1}, for reference, stable, active, respectively; with stable lakes demonstrating large variation and active lakes the least variation. Additionally, the molar total nitrogen to total phosphorus ratios are also

displayed (Figure 2.4d), illustrating significantly higher N:P ratios in lakes disturbed by active thaw slumps.

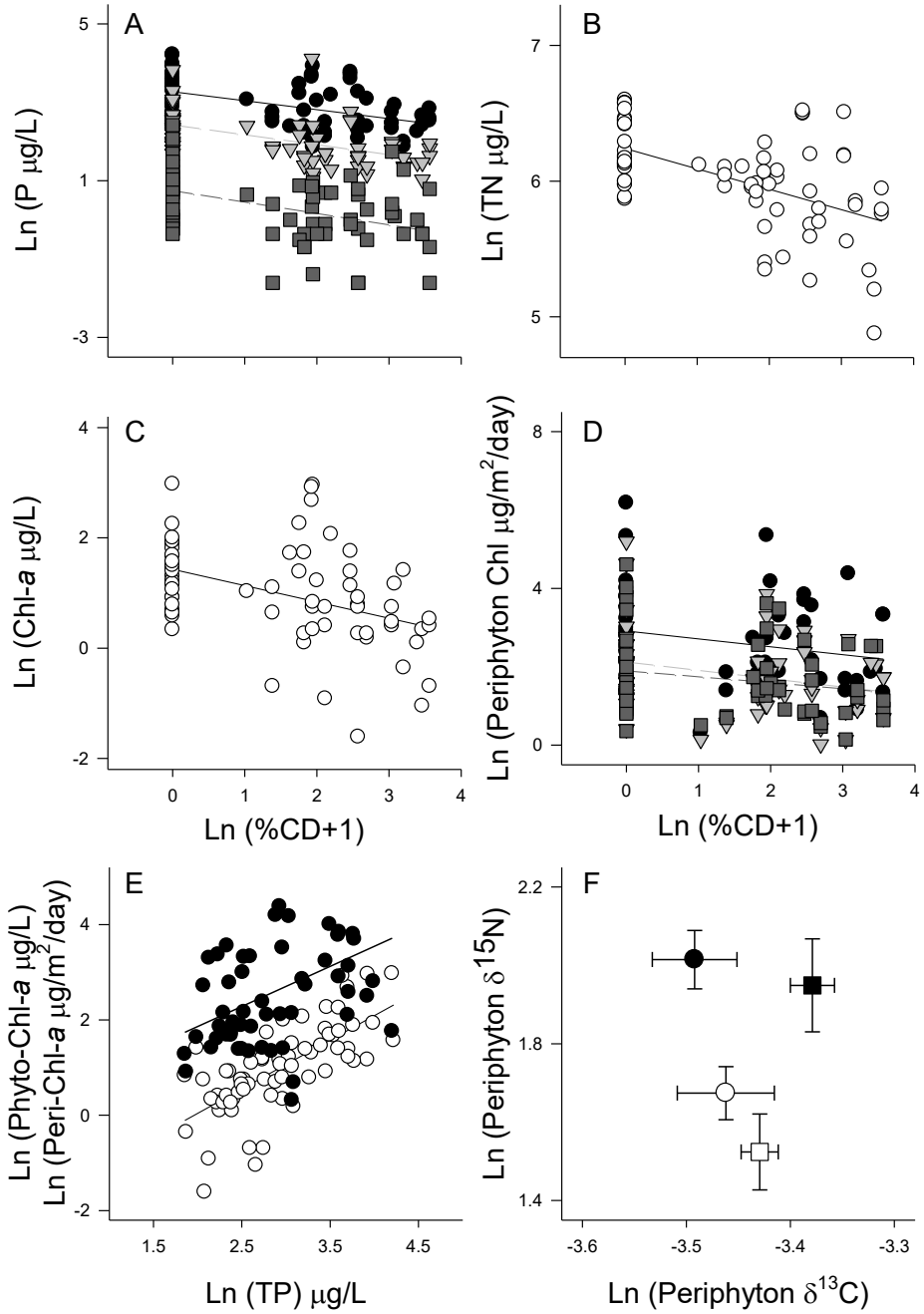

Figure 2.3: Aquatic nutrients and nutrient indicators of primary production in tundra lakes. %CD is the percent of catchment area disturbed by thaw slumping. A: phosphorus (Total Phosphorus (TP), circles; Total Dissolved Phosphorus, triangles; and Soluble Reactive Phosphorus, squares) exhibited r^2 values of 0.18-0.23, $p<0.0005$. B: Total Nitrogen (TN) with $r^2 = 0.28$, $p<0.001$. C: phytoplankton chlorophyll-*a* concentrations (Chl-*a*), $r^2=0.18$, $p<0.001$. D: periphyton chlorophyll growth rates; Chl-*a* (circles) $r^2=0.12$, $p=0.050$; Chl-*b* (triangles) $r^2=0.11$, $p=0.054$; Chl-c (squares) $r^2=0.07$, $p=0.131$. E: Phytoplankton Chl-*a* vs TP, $r^2=0.44$, $p<0.001$ and periphyton growth rates vs TP, $r^2=0.18$, $p=0.001$; F: periphyton tissue stable isotopes ^{15}N and ^{13}C plotted by individual year (2009 – solid fill; 2010 – open symbols) and thaw status (reference – circles; slump-affected lakes – squares); one standard error represented.

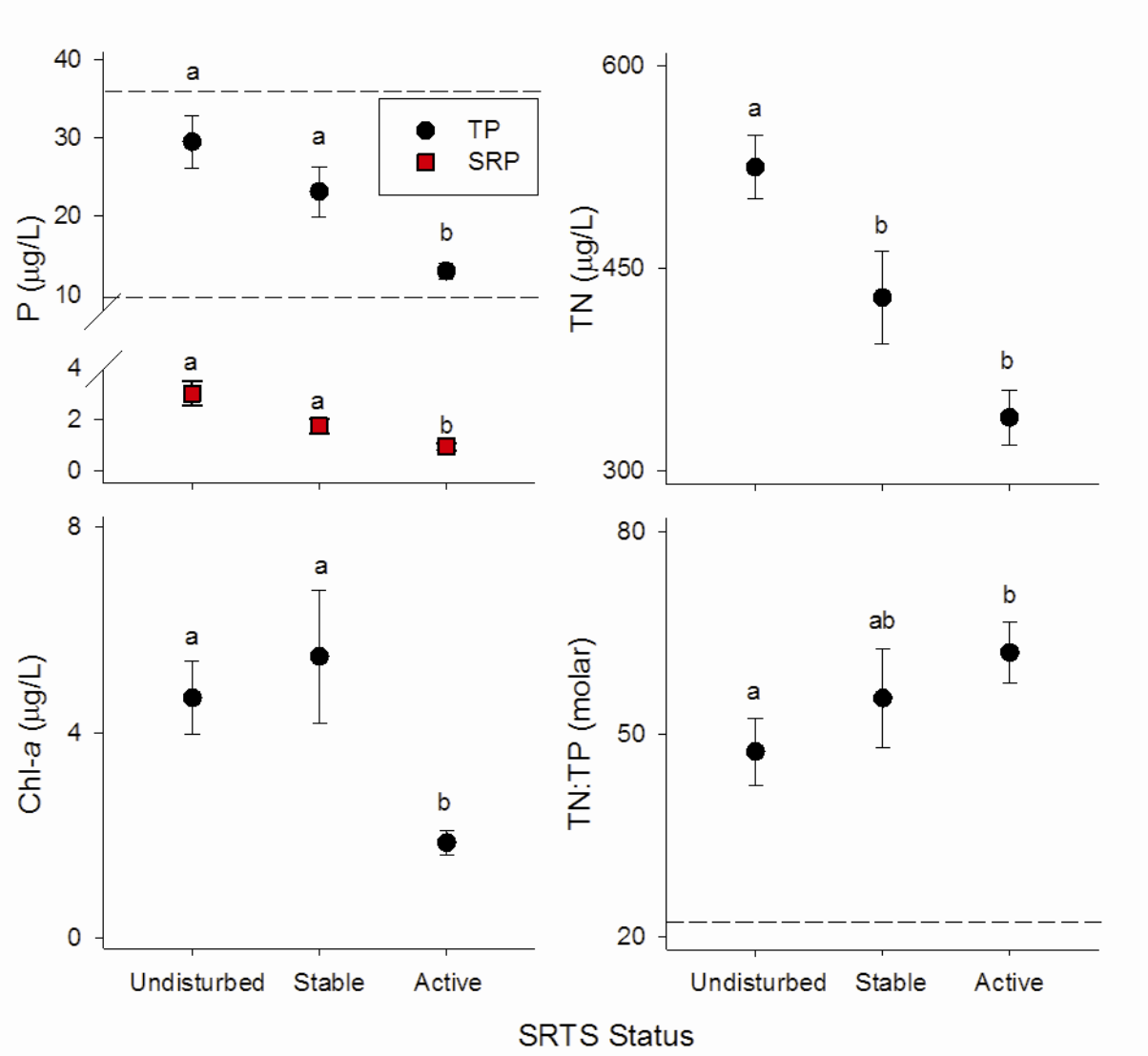

Figure 2.4: Nutritional indicators in tundra lakes grouped by disturbance status: 0) Reference lakes; 1) Lakes with stable thaw slumps with more than 50% of thaw slump scar having vegetation growing; 2) Lakes with active thaw slumps occurring, i.e. <50% re-vegetation of thaw slump scar. Data are pooled across 2009-2011; n=69; error bars represent one standard deviation; letters indicate significance (1-way ANOVA, $p<0.05$). Dashed lines in the phosphorus figure indicate eutrophication (TP>35 µg L^{-1}) and oligotrophy (TP<10 µg L^{-1}). The molar N:P ratio also indicates a threshold for the onset P-deficiency (N:P > 22) (Guildford et al., 1994), and none were below the established TN:TP < 14 for N-deficiency.

We then compared Chl-*a* concentrations in our slump-affected lakes with other studies (as cited in Figure 2.5) across Canada using ANCOVA to standardize for TP. In general, lakes were categorized by vegetation distribution in all studies included in this analysis. The lowest Chl-*a* concentrations were in the High Arctic (estimated marginal mean (MM) = 0.6 µg L^{-1}), while the highest Chl-*a* measurements were from Northern Boreal Lakes in Northern British Columbia (MM = 15.1 µg L^{-1}), the Alberta Shield (MM = 7.3 µg L^{-1}), and temperate New England (MM = 9.0 µg L^{-1}) (Figure 2.5a). A significant grouping of all Low Arctic lake categories and the temperate southern Ontario lake group

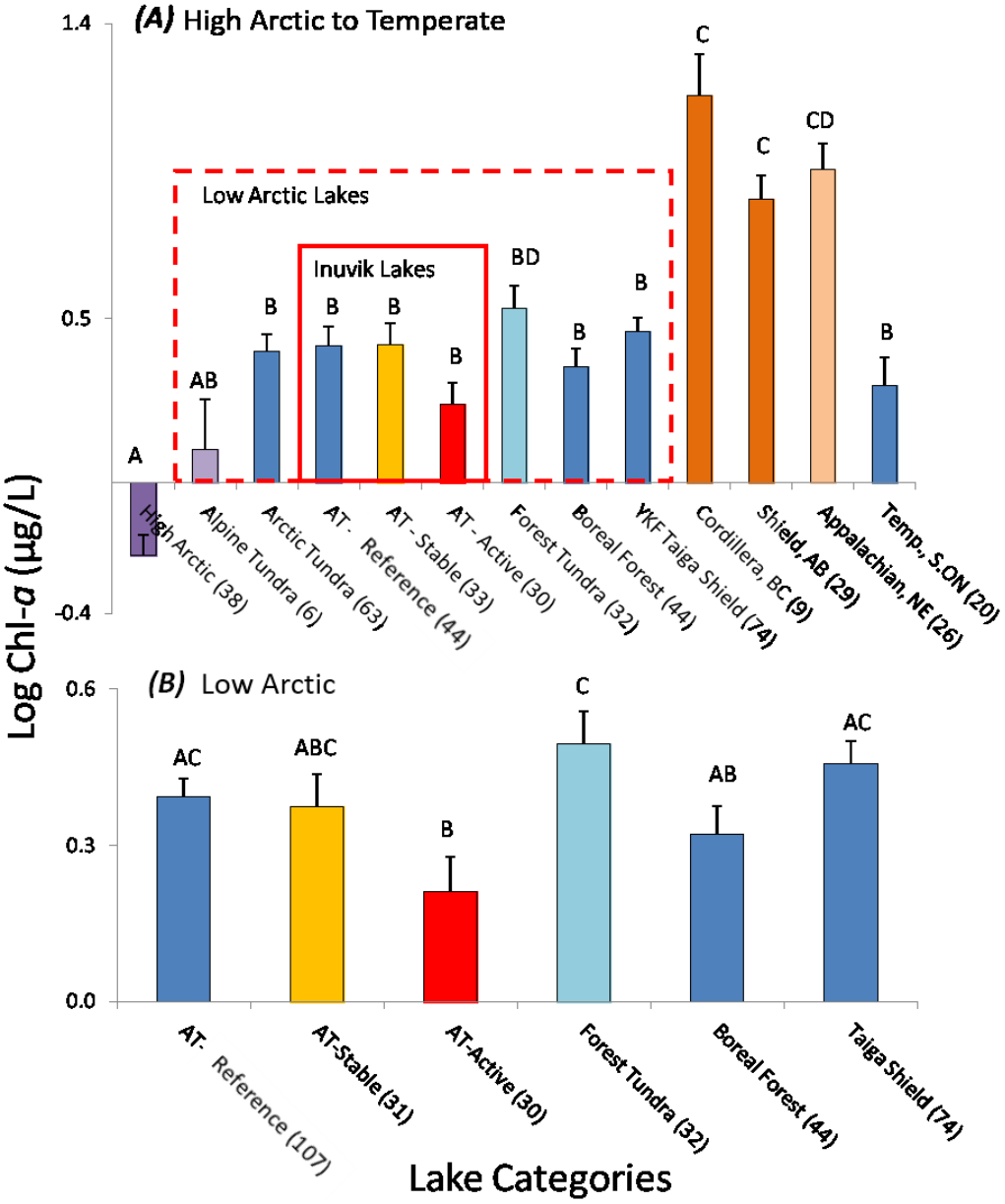

Figure 2.5: ANCOVA marginal mean estimates of Chl-*a*, using TP as a covariate, in lakes categorized by ecotype, from (A) 11 studies across Canada and northern USA, and (B) 6 studies located in low Arctic ecotypes of Canada similar to our survey. In (A), our study lakes include AT- Reference, AT-Stable, and AT-Active lake categories. In (B) AT-Reference combines reference lakes from our study and other studies' reference Arctic tundra lakes. Chl-*a* evaluated at Log(TP) = 1.2 µg L^{-1}. Parentheses indicate sample size (n), letters above bars indicate statistical significance. AT = Arctic Tundra. Dashed box indicates lakes considered low Arctic, while solid box indicates Inuvik study lakes, i.e. reference, stable, and active slump activity. High Arctic = High Arctic lake category (Lim et al., 2001); Low Arctic = Alpine Tundra (Pienitz et al., 1997a), Arctic Tundra (AT) (Ogbebo et al., 2009; Pienitz et al., 1997a, 1997b; Rühland et al., 2003; Rühland and Smol, 1998), AT-Reference, AT-Stable, and AT-Active (this study), Forest Tundra (Ogbebo et al., 2009; Pienitz et al., 1997a, 1997b; Rühland et al., 2003), Boreal Forest (Pienitz et al., 1997a, 1997b; Rühland et al., 2003; Rühland and Smol, 1998), Yellowknife (YKF) region Taiga Shield (Ostrofsky and Rigler 1987, Houben Unpublished); Sub-Arctic & Temperate = Cordillera, BC (French and Petticrew, 2006), Shield, AB (Prepas and Trew, 1983), Appalachian, NE (Dillon and Rigler, 1974), Temp., S.ON (Dillon and Rigler, 1974).

had intermediate estimated marginal means for Chl-*a* concentrations ranging from 1.3 µg L^{-1} to 3.4 µg L^{-1}. Within the Low Arctic lake categories, our active slump-affected lakes had the lowest Chl-*a* MM (1.73 µg L^{-1}), except for the Alpine Tundra lake category, which was significantly similar to the High Arctic lake category. We then compared Chl-*a* in only the Arctic Tundra lake categories, of which our slump-affected lakes were also categorized, in a similar ANCOVA where TP was again the covariate (Figure 2.5b). ANCOVA results indicated that our Active slump-affected lakes were significantly lower than all Reference Arctic Tundra, Forest Tundra, and Taiga Shield lakes ($F=3.3$, $p=0.04$, $df=2$). Stable slump-affected lakes were intermediary and not significantly different from either reference or active slump lake categories, nor other Low-Arctic Tundra lake categories.

2.4.3. Trace Metals

Several important trace metal concentrations were related significantly (both positively and negatively), to the percent catchment area slumped (Figure 2.6). Uranium, strontium, and lithium were related positively to percent catchment area slumped, and were present almost entirely in the dissolved phase. Uranium in reference lakes ranged from 0.01-0.26 ng L^{-1} (mean = 0.06 ng L^{-1}), while disturbed lakes ranged from 0.03-1.55 µg L^{-1} (mean = 0.49 µg L^{-1}), with an average 8-fold higher concentration in slump-affected lakes compared to reference lakes. Strontium was also higher in slump-affected lakes by 6-fold, on average, from 24.5 µg L^{-1} (reference) to 143.9 µg L^{-1} (slump-affected), while lithium was 3-fold higher in slump-affected lakes, with the mean concentration increasing from 2.58 µg L^{-1} in reference lakes to 9.04 µg L^{-1} in slump-affected lakes. To note, our most active slump-affected lake, INV-14b, had concentrations for the above three metals greater than the 95% upper confidence interval (CI). More generally, lakes with metal concentrations (U, Sr, Li), greater than the 95% CI were all slump-affected lakes.

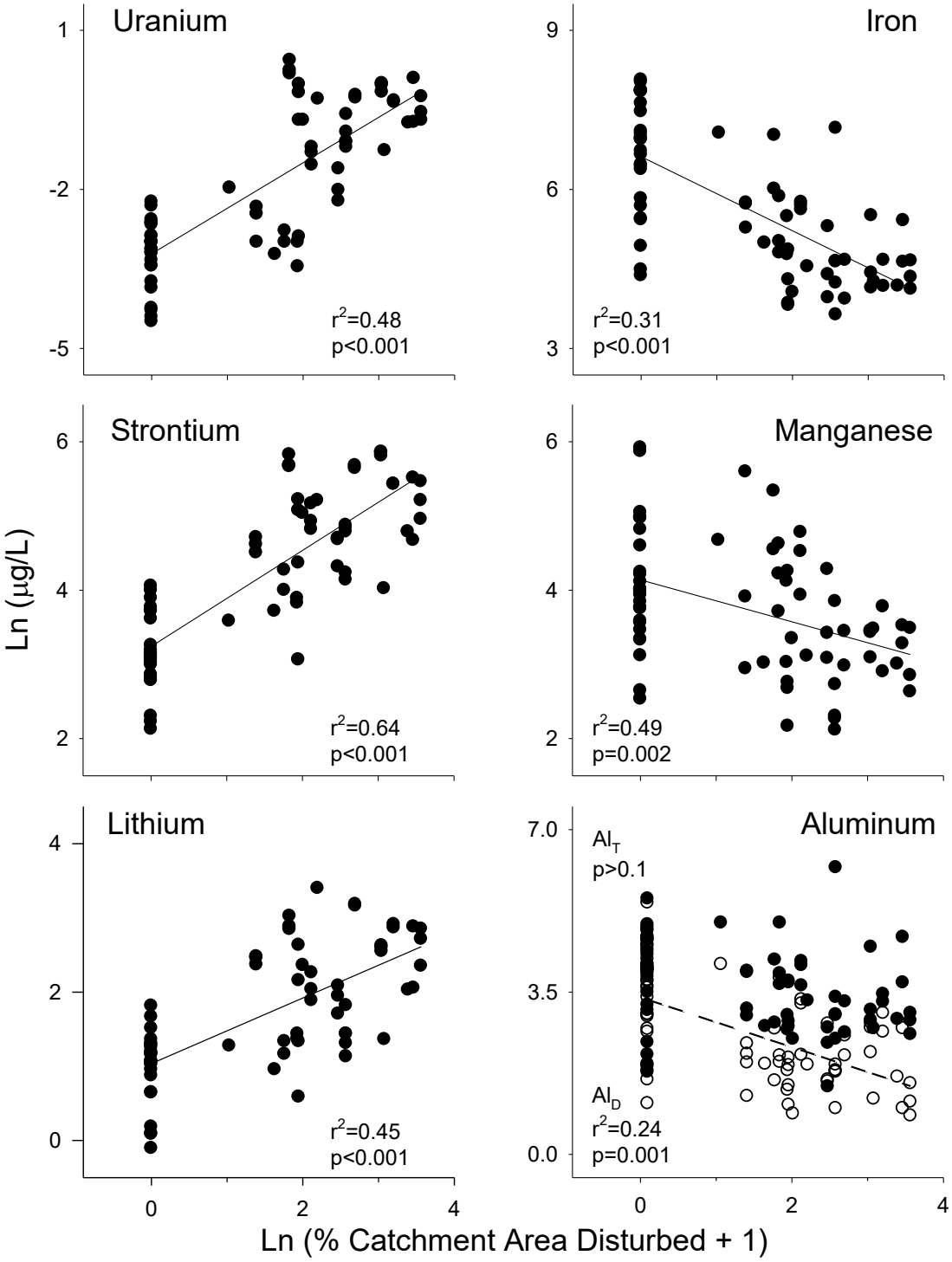

Figure 2.6: Aquatic total metal concentrations (black circles) measured in tundra lakes as a function of the percent area of catchment disturbed by thaw slumping (Ln %CD+1). Dissolved fractions (open circles) were only included when concentrations were less than 90% of total metal concentration on average or indicated a shift in the proportion of dissolved to total metal concentration.

In contrast, several abundant trace metals had lower total concentrations as well as lower proportions in the dissolved phase as a function of percent of catchment disturbed by thaw slumping (Figure 2.6). Concentrations of iron (Fe), manganese (Mn), and aluminum (Al) all exhibited significant inverse relationships with the percent of catchment area disturbed. In our reference lakes, both the total and dissolved Fe concentrations (1253 and 648 μg L^{-1}, respectively) were greater than slump-affected lakes (73 and 254 μg L^{-1}, dissolved and total Fe concentrations, respectively). Total Mn concentrations averaged 197 and 129 μg L^{-1} in reference and slump-affected lakes, respectively. Average dissolved Mn concentrations were 126 μg L^{-1} in reference lakes and 60 μg L^{-1} in slump-affected lakes. For Al, only the dissolved concentration demonstrated a significant inverse relationship with the percent of catchment area disturbed by thaw slumping. Average concentrations for total Al in our lakes were 75 and 50 μg L^{-1} in reference and slump-affected lakes, respectively; though greater variation was measured in slump-affected lakes as the maximum concentration measured was 485 μg L^{-1}, while only 247 μg L^{-1} in reference lakes.

2.5. Discussion

2.5.1. Primary Production in Slump-affected Lakes

In a study analyzing sediment cores from a subset of these study lakes, Thienpont et al. (2013) found that slump-affected lakes had greater diatom-based biological changes, and algae typical of clearer water were more abundant in slump-affected lakes. Their results suggested a downward shift in production from the euphotic zone to the benthos, which may be expected as water transparency increases following the settlement of suspended sediment resulting from slump disturbance and stabilization. A mesocosm experiment (Moquin and Wrona, 2015) also demonstrated increased benthic bacterial production in slump-affected chambers, while increased benthic macroinvertebrates in slump-affected lakes was also observed (Moquin et al., 2014). However, it was also observed in these same sediment cores that slump affected lakes had similar fluxes of algal-derived (S2) carbon and Chl-*a* (Deison et al., 2012), indicating that overall lake production had not changed. To contrast, when examining our lake nutrient chemistry and primary production variables (N, P, and Chl-*a*) from the water column, significant negative relationships with the percent of catchment area disturbed (Figure 2.3A-C) were apparent, with a significant relationship between P and Chl-*a* (Figure 2.3E) suggesting that P was the key limiting nutrient. Thus, a shift to clear-water algae typical of benthic habitats is likely occurring, however this vertical shift in primary production to the benthos is apparently not

compensating for the loss in phytoplankton production within the euphotic zone. These results suggest that nutrients are potentially buried by sedimentation more rapidly than benthic algae can utilize them due to thaw slump influences. Further, the increased water clarity has also led to an increase in rooted macrophyte biomass in slump-affected lakes (Mesquita et al., 2010), which are able to exploit buried nutrients that are potentially unavailable to benthic algae. Figure 2.7 provides a summary diagram depicting these processes. Additionally, we measured TP in lake-bottom sediments, permafrost soils, and active-layer soils from organic-rich tundra and thaw slump scar areas (Figure S4). Of the potential terrestrial P-sources, the 0-0.5 cm interval sections from the organic-rich active layer of the upland catchment soil sections had the highest P-concentrations, as opposed to soil samples from thaw slump head walls and slump scars (Figure S4). This suggests that reference lakes may have greater catchment P-loading due to the higher proportion of intact organic-rich active layer, whereas catchments with thaw slumps may be lower. However, lake sediment samples from our slump-affected lakes have as high or even higher P-concentrations than lake sediments in reference lakes, suggesting that additional internal lake processes in slump-affected lakes are causing greater P-sedimentation.

Using our regression analysis (Figure 2.3C), we estimate a 65% reduction in Chl-*a* concentrations when comparing reference lakes to lakes with the largest proportion of catchment area slumped (34%). This result highlights the impact that thaw slumps have on the primary production in adjacent lakes, which is all the more significant when we consider that up to 15% of lakes locally in the Mackenzie upland tundra region have shoreline thaw slumps, and the proportion of lakes and intensity of impacts is likely to increase with projected warming (Lantz and Kokelj, 2008). When comparing the nutritional status of reference lakes with those adjacent to active and stable slumps (Figure 2.4A), we note that reference lakes tend to be mesotrophic to eutrophic (TP = 10.6-67.9 µg L^{-1}, median = 28.4 µg L^{-1}; eutrophic threshold of TP > 35 µg L^{-1}; Wetzel 2001). Meanwhile, the lakes with stable slumps range from oligotrophic to eutrophic (TP = 6.5-50.7 µg L^{-1}, median TP = 20.3 µg L^{-1}). Active slump-affected lakes are generally oligotrophic to mesotrophic (TP = 6.4-26.2 µg L^{-1}, median = 12.4 µg L^{-1}; oligotrophy at TP < 10 µg L^{-1}). It is also noteworthy that molar N:P ratios indicate that all lakes, regardless of activity, are likely P-limited (Figure 2.4D) as average ratios, including ± one standard error, are all above a reported threshold of N:P > 22 (Downing and McCauley, 1992; Guildford et al., 1994). Phosphorus is currently the key limiting nutrient in our tundra lakes and, as our data and analysis suggest, shoreline retrogressive thaw slump events would further decrease P levels. Further acceleration of climate driven slumping would likely increase P-limitation in impacted lakes. Indeed, when comparing between thaw slump status categories, our active slump-affected lakes

have, on average, half the total phosphorus concentration recorded in reference lakes. Similar comparisons between reference and slump-affected lakes corroborate these N, P, and Chl-*a* trends (Thompson et al., 2012).

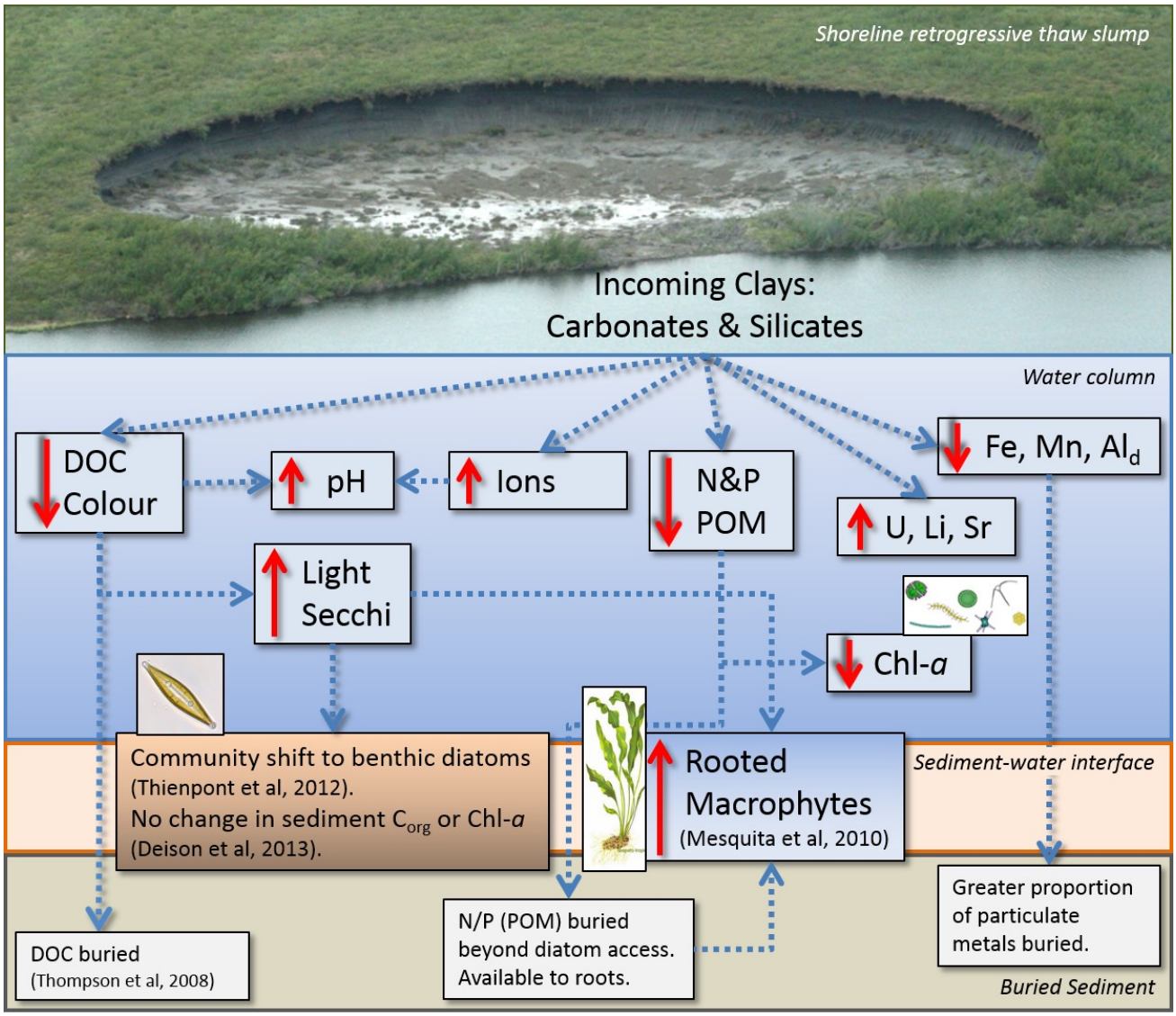

Figure 2.7: Summary diagram illustrating the change in concentrations of several parameters following thump slump events in tundra lakes in the Canadian western Arctic, 2009-2011.

We also compared Chl-*a* concentrations between lake categories from selected studies from across Canada and the northeast USA with ANCOVA using TP as a covariate. We observed that lake categories within the low Arctic, where our study lakes were located, were a statistically significant intermediary group between high Arctic and most sub-Arctic and temperate regions across Canada in

the production of Chl-*a* (Figure 2.5a). Within the low Arctic lake categories, we observed that alpine tundra lakes are also not significantly distinct from high Arctic lakes. Alpine tundra lakes often have limnological parallels to high Arctic environments, as the cooler temperatures with altitude can be analogous to cooler temperatures at higher latitudes. The unique nature of lower Chl-*a* production in alpine tundra lakes distinguished this grouping from the other low Arctic lake categories. From this we observe that our active slump-affected lakes had the lowest marginal mean (MM) Chl-*a* estimates from all other lake categories, with the noted exceptions of alpine tundra and high Arctic lake categories. However, this result was not significantly different from other low Arctic lake categories. This lack of significance within the low Arctic lake categories may be due to the much lower Chl-*a* estimates for High Arctic lakes and the higher Chl-*a* estimates for Sub-Arctic and Temperate lake categories.We then focused only on Low Arctic lake categories to determine if thaw slumps were significant influences on Chl-*a* production (Figure 2.5b). Our ANCOVA results for Low Arctic lake categories demonstrated that active slump-affected lakes had the lowest Chl-*a* marginal mean estimates of all lake categories and were significantly lower than similar reference Arctic Tundra (AT) lakes across several studies, as well as other ecotypes, such as Forest Tundra and Taiga Shield lake categories (Figure 2.5b). These ANCOVA results suggest that, as TP is used as a covariate, our active slump-affected lakes produce significantly lower phytoplankton Chl-*a* per unit of TP relative to most lake categories across Canada's lower Arctic regions. Given the vast area of Canada's Low Arctic region and continued warming, slump-affected lakes will be hot spots for significantly lower phytoplankton production in an increasing number of lakes.

2.5.2. Surface Water Chemistry and Light Penetration

As demonstrated in prior studies that contrasted slump-affected and reference lake categories (Kokelj et al., 2005, 2009b), we further corroborate water chemistry results by using a gradient of thaw slump disturbance. Large increases in major ion concentrations with respect to the percent of catchment area disturbed were recorded; predominantly SO_4^{2-}, Ca^{2+}, and Mg^{2+}, represented as specific conductivity in Figure 2.2. The large increase in ionic content is associated with the thawing of ion-rich till horizons that characterize near-surface permafrost (Hammerschmidt et al., 2006; Kokelj et al., 2005; Kokelj and Burn, 2003). Leaching of previously frozen tills in slump-affected catchments is a possible explanation for our observation that major ions were enriched in slump-affected lakes (Kokelj et al., 2005; Malone et al., 2013; Semkin et al., 2005). Tills derived from carbonate and shale bedrock

account for the enrichment of base cations and SO_4^{2-} enrichment in slump-affected lakes(Kokelj et al., 2009b; Lacelle et al., 2007).

Lakewater pH was also higher in slump-affected lakes, increasing by 0.47-0.99 pH units on an annual average, with respect to reference lakes over the years 2009-2011. The reduction in DOC and related acidic subcomponents (humic and fulvic acids) likely contributed to higher pH levels. Additionally, via piecewise regression we observed a pH breakpoint centered at a DOC concentration of 8-9 mg L^{-1} (Figure S2), where pH increased or remained constant with DOC below a threshold DOC concentration of 8-9 mg L^{-1}, and decreased rapidly with DOC above the 8-9 mg L^{-1} threshold.

The bulk of the organic contribution to lakes originates from the shallow organic-rich active layer and is mainly transported by overland runoff. Our observation of significantly lower DOC in slump-affected lakes is similar to other studies (Kokelj et al., 2005; Mesquita et al., 2010). Additionally, light extinction in lakes is highly correlated with DOC concentrations (Guildford et al., 1994) and that high extinction rates can lead to light deficiency limiting autotrophic production over nutrient deficiency (Hecky and Guildford, 1984). In our study lakes, a negative relationship between Secchi depth and DOC was observed (r^2=0.30, F=17.26, $p<0.001$). As DOC is lower in slump-affected lakes, the resultant increase in light penetration within these lakes might, independently from other processes, further depress DOC concentrations by enhancing *in situ* DOC photodegradation affecting the remineralisation of organic C to DIC (Ma and Green, 2004; Porcal et al., 2010). Since our slump-affected lakes catchments have disturbances that impact 3% to 35% of the catchment area, a significant portion of the terrestrial contributory area may be stripped of the overlying organic-rich active layer. Both the active degradation of the slump headwall diluting the organic matter input to the lake with thawing mineral-rich permafrost soils, plus the subsequent reduction in catchment surface area containing an organic-rich active layer, contribute to lower organic inputs to the adjacent lakes.

If light limitation were occurring in reference lakes, as is often the case in Arctic systems, the observed increase in light penetration in slump-affected lakes (measured via increased Secchi and reduced DOC and colour) may enhance primary production. However, competing reduction in nutrients from these processes appears to have instead reduced growth. Further, characterization of water clarity demonstrated a significant positive relationship between Secchi depth and percent area of catchment disturbed. This, however, did not translate into an observable change in temperature-driven primary production or a change in lake temperature itself in slump-affected lakes. Additionally, our vertical profiles of five lake pairs (Figure S3), demonstrated consistent thermocline structure between 2-4 m for all lakes, with or without thaw slump disturbance. Thus, in our narrow time-frame

for sampling, no positive feedback on further temperature change was observed in our 10 thaw slump lakes, which were 6-13 m deep. Prior reports indicated that lakes in early September of 2004 were isothermal in the top 3-5 m, but that lakes shallower than 5 m tended to be isothermal (Kokelj et al., 2005). Thermocline development in general may continue throughout the summer, migrating to depths as deep as 8.4 m in certain lakes later into the summer, as reported by Thompson (2009).

The likely dominance of thaw slump events on abiotic lake chemistry over other environmental variables, such as temperature, allochthonous inputs, and recent fire history, has already been discussed (Kokelj et al., 2005). However, our data show that chloride concentrations were highest in reference lakes near the ocean coast, which was noted in Pienitz *et al.* (1997) and Kokelj et al. (2009). This is likely due to marine aerosols drifting inland, as has been shown in many Arctic limnological surveys near coastal regions (Liao et al., 2014; Poulain et al., 2007). However, we did not observe any further relationships between coastal proximity and nutrients nor primary production.

2.5.3. Trace Metals

The presence of thaw slumps has a strong influence on metal geochemistry (Figure 2.6). Concentrations of U, Sr, and Li were highly correlated with the percent of catchment area slumped, and were mostly in dissolved forms for all lakes. The proportion of dissolved to total metal concentrations for U, Sr, and Li did not change with respect to slump-affects ($p > 0.05$). Total uranium concentrations increased 9-fold on average compared to reference lakes, though are still at least an order of magnitude below Canadian Water Quality Guidelines (1987) of 15 and 33 $\mu g\ L^{-1}$ for long and short term exposure, respectively. The maximum Li concentration measured in slump-affected lakes was 24.1 $\mu g\ L^{-1}$, however there are no Canadian water quality limits for lithium and most freshwater systems are below 200 $\mu g\ L^{-1}$. Lithium is predominantly found in several aluminum silicate minerals (petalite, lepidolite and spodumene) and an aluminum fluorophosphate mineral, amblygonite, suggesting that the mechanism for increased lithium in our slump-affected lakes is due to the direct introduction of the thawing inorganic permafrost soils, largely composed of aluminum silicate glacial tills.

Material transported from thaw slumps to adjacent lakes is a likely source for Sr and Li, as headwall and slump scar soil samples indicated significantly higher concentrations for both metals in comparisons with active layer catchment soils (Figure S4). As well, sediments from slump-affected lakes had significantly greater Sr and Li levels than in reference lake sediments, indicating the greater input and sedimentation of these permafrost-derived materials. Uranium demonstrated a very similar

pattern (Figure 2.6) as Sr and Li, and though lake sediments in slump-affected lakes were not significantly dissimilar from reference lake sediments (Figure S4), uranium is also a likely component of the incoming permafrost soils.

The reduction in solubility for biologically important metals, such as Fe, Mn, and Al in slump-affected lakes, may be due to the related increase in pH by almost one full pH unit in slump-affected lakes (Figure 2.2). Higher pH may lead to precipitation of certain metals out of the water column, as observed in the steeper regression slope for the dissolved measurements of Fe and Al (Figure 2.6). For Fe, this specific shift in pH leads to the formation of insoluble ferric hydroxide, which precipitates out of the water column reducing biological availability of Fe to phytoplankton (Drever, 1997). For Mn_T, the reduction in relation to percent of catchment area disturbed is significant; however, we do not record a significant result for Mn_D, though we would expect a similar reduction in solubility as pH increases above 7.0 (Wetzel, 2001). However, based on the near ubiquity of this metal in all of our reference and slump-related soil and sediment measurements (Figure S4), thaw slump influences may not demonstrate a significant influence on Mn concentrations. In contrast, no relationship between Al_T and percent of catchment area slumped was observed ($p>0.05$), suggesting that incoming Al from $AlSiO_4$-rich clays maintains suspended Al_T, but Al_D is still negatively related to SRTS disturbance due to subsequent pH increases reducing Al-solubility. Water quality guidelines state a concentration limit of 100 µg Al L^{-1} when pH ≥ 6.5, and only 5 µg Al L^{-1} for pH < 6.5 (CCME, 1987). Thus, a combined effect of reduced Al-solubility due to more alkaline conditions in slump-affected lakes, with an overall reduction in Al concentrations, indicates that slump-affected lakes reduce the concerns for Al toxicity to aquatic organisms. Soil and sediment measurements of Fe and Al (Figure S4) both suggest permafrost sources, along with significantly high Si concentrations in permafrost soils, further indicative of incoming silicates. Also, direct effects of thaw slumps on metal concentrations and solubility may occur as incoming inorganic slump material, loaded with negatively charged sulfates and carbonates, binding directly to metals, and subsequently sediment out of the water column once larger complexes are formed.

Prior studies have similarly shown that watershed acidification increases the leaching of Fe, Al, and Mn, from both allochthonous and autochthonous sources, to lake water, sometimes to the extent that, for example, monomeric-Al becomes toxic to biota (Bowlby et al. 1988; Scheider et al. 1979; Johnson et al. 1981; Urban et al. 1990; Demers et al. 2010). The apparent increase in metal precipitation (Figure 2.6) for Fe, Mn, and Al, due to increased alkalinity, suggests reduced solubility

with respect to increasing percent area of catchment disturbed by thaw slumping, and these metals are likely sedimenting out of the water column, and thus reducing toxicity of certain labile metals.

Iron, manganese, and aluminum demonstrated the largest negative relationships to percent of catchment area disturbed we observed in our trace metals analyses and were on average less than 50% dissolved. Additionally, the proportion of dissolved Fe, Al, and Mn also decreased when compared to increasing percent of catchment area disturbed by thaw slumping. For iron, using the estimated linear regression model, the proportion dissolved in reference lakes was 45% on average, whereas at our greatest measured slump disturbance (34% of catchment area), dissolved iron was only 18% of the total concentration. Similarly, the proportion of dissolved aluminum in reference lakes was 56% on average and decreased to 21% for the most disturbed lakes. The same trend was observed for manganese where on average the dissolved fraction was 12% in the reference lakes and 7% in the highly disturbed lakes.

Of the other metals screened in lake water, none were found to be over Canadian Water Quality Guidelines (CWQG), although several had substantial decreases from being within an order of magnitude of the maximum acceptable concentration (MAC) in reference lakes, to being several orders of magnitude lower than the guidelines in slump-affected lakes. Arsenic (As) had maximum concentration of 0.7 to 1.3 $\mu g\ L^{-1}$ in reference lakes, and was 0.1 to 0.8 $\mu g\ L^{-1}$ in slump affected lakes, well below the CWQG for arsenic at 10 $\mu g\ L^{-1}$. Cr and Pb had similar trends, with maximum concentrations of 1.5 and 5.0 $\mu g\ L^{-1}$, respectively, in reference lakes, while in slump-affected lakes Cr and Pb concentrations were as low as 0.04 and 0.01 $\mu g\ L^{-1}$, respectively. However, after measuring lake surface sediment concentrations, As was the only trace metal with significant thaw slump influences to have concentrations above both Interim Sediment Quality Guidelines (ISQG) (5,900 $\mu g\ kg^{-1}$ dw) and Probable Effect Level (PEL) (17,000 $\mu g\ kg^{-1}$ dw) (CCME, 1998). Notably, all thaw slump sediments, as well as slump headwall soils and slump scar soils, were above the arsenic ISQG, while only two reference lake sediment samples were just above this threshold. With shifts to benthic communities and rooted macrophytes in slump-affected lakes, as discussed above, arsenic toxicity in slump-affected lakes should be an area of future study.

2.6. Conclusions

We summarize the effects of shoreline retrogressive thaw slumps on mid-summer water quality in 39 lakes of the Mackenzie Delta uplands. In our tundra system, which is overlain with ice-rich, glacial tills, we observed significant changes in water chemistry across a large gradient of thaw slump

disturbance. We measured significant negative relationships between major nutrients (N and P) and both the proportion of catchment disturbed by thaw slumping and the relative age (activity) of slump events. Our lakes are P-limited, and even though an increase in light penetration was measured, thaw slumps have led to a reduction in primary productivity in phytoplankton and periphyton, by up to an estimated 65% in phytoplankton in our most disturbed (34% of catchment area disturbed) slump-affected lakes.

Additionally, we measured several trace metals (Li, Sr, U) to be highly associated with thaw slumps, likely due to the influx of thawed soils. In contrast, several micronutrients (Al, Fe, Mn) demonstrated a negative relationship to thaw slumping, especially a decrease in solubility, suggesting greater sedimentation and removal from the water column following slump events. Metal toxicity may be of increasing importance as climate warming accelerates shoreline thaw slump activity, with uranium concentrations increasing substantially in the water column (but remaining well below CCME limitsset at 15 µg/L) and arsenic sedimentation elevated in slump-affected lakes. While As concentrations in the water column are within CCME limits, concentrations in lake bottom sediments were well above environmental sediment quality guidelines. With the increased sedimentation of nutrients and certain trace metals, and a shift to benthic algae and rooted macrophytes, toxicity may be amplified in the altered food webs of slump-affected lakes. Future work on the potential for bioconcentration and biomagnification of these trace metals, as well as other persistent pollutants such as mercury and organic contaminants, is clearly needed.

Generally, lakes in the Canadian Arctic are strongly influenced by climate-related factors (e.g. permafrost, vegetation, weathering, and duration of snow and ice cover). We demonstrate that, not only within our study site of the upland tundra region east of the Mackenzie River Delta, but also when compared to other studies across Canada's low Arctic region, retrogressive thaw slump events are an important influence on limiting nutrient availability and primary production in affected lakes. With future warming predicted (ACIA, 2005), thaw slumps are expected to increase in frequency and size, as will associated changes in limnological variables we described here.

2.7. Acknowledgements

We thank Michael Pisaric (Carleton University), Joshua Thienpont (Queen's University), and Peter deMontigny (Carleton University) for field, project-design, and technical support. We are especially grateful to William Hurst and Donald Ross of Aurora Research Institute (Aurora College, Inuvik) for logistical support. Laboratory analyses for nutrient and trace metal water chemistry were

provided by the National Laboratory for Environmental Testing, Burlington, ON, and Taiga Environmental Laboratory, Yellowknife, NT. NWT Geological Survey Contribution #0101. Financial and logistical support for this research was provided by NSERC Discovery and Strategic grants to J.M.B. and J.P.S. Additional support was provided by the Northern Contaminants Program, Polar Continental Shelf Program, Northern Scientific Training Program, Indian and Northern Affairs Canada, Environment Canada, and Aurora College, Government of Northwest Territories.

2.8. References

ACIA (2005) *Arctic Climate Impact Assessment*. Cambridge, United Kingdom: Cambridge University Press.

Burn CR and Kokelj S V (2009) The environment and permafrost of the Mackenzie Delta Area. *Permafrost and Periglacial Processes* 20(April): 83–105: doi:10.1002/ppp.

Canadian Council of Ministers of the Environment (1987) Canadian water quality guidelines for the protection of aquatic life. In: Canadian Council of Ministers of the Environment (ed) *Canadian Environmental Quality Guidelines*. Winnipeg, Manitoba, 1–13.

Carrie J, Wang F, Sanei H, Macdonald RW, Outridge PM and Stern GA (2010) Increasing contaminant burdens in an Arctic fish, burbot (Lota lota), in a warming climate. *Environmental Science & Technology* 44(1): 316–322.

Deison R, Smol JP, Kokelj S V, Pisaric MFJ, Kimpe LE, Poulain AJ, et al. (2012) Spatial and temporal assessment of mercury and organic matter in thermokarst affected lakes of the Mackenzie Delta Uplands, NT, Canada. *Environmental Science & Technology* 46(16): 8748–55. doi:10.1021/es300798w.

Desrosiers M, Planas D and Mucci A (2006) Total mercury and methylmercury accumulation in periphyton of Boreal Shield lakes: influence of watershed physiographic characteristics. *Science of the Total Environment* 355(1–3): 247–58. doi:10.1016/j.scitotenv.2005.02.036.

Dillon PJ and Rigler FH (1974) The phosphorus-chlorophyll relationship in lakes. *Limnology and Oceanography* 19(5): 767–773.

Downing JA and McCauley E (1992) The nitrogen:phosphorus relationship in lakes. *Limnology and Oceanography* 37(5): 936–945.

Drever JI (1997) *The Geochemistry of Natural Waters*. Upper Saddle River, New Jersey, USA, 07548: Prentice-Hall, Inc.

Dugan HA, Lamoureux SF, Lewis T and Lafrenière MJ (2012) The impact of permafrost disturbances and sediment loading on the limnological characteristics of two high Arctic lakes. *Permafrost and Periglacial Processes* 23(2): 119–126. doi:10.1002/ppp.1735.

French TD and Petticrew EL (2006) Chlorophyll a seasonality in four shallow eutrophic lakes (northern British Columbia, Canada) and the critical roles of internal phosphorus loading and temperature. *Hydrobiologia* 575(1): 285–299. doi:10.1007/s10750-006-0377-8.

Guildford SJ, Hendzel LL, Kling HJ, Fee EJ, Robinson GGC, Hecky RE, et al. (1994) Effects of lake size on phytoplankton nutrient status. *Canadian Journal of Fisheries and Aquatic Sciences* 51(12): 2769–2783. doi:10.1139/f94-277.

Hammerschmidt CR, Fitzgerald WF, Lamborg CH, Balcom PH and Tseng CM (2006) Biogeochemical cycling of methylmercury in lakes and tundra watersheds of Arctic Alaska. *Environmental Science & Technology* 40(4): 1204–11.

Hecky RE and Guildford SJ (1984) Primary productivity of Southern Indian Lake before, during, and after impoundment and Churchill River diversion. *Canadian Journal of Fisheries and Aquatic Sciences* 41(4): 591–604. doi:10.1139/f84-072.

Kattsov VM and Källén E (2005) Future climate change: modeling and scenarios for the Arctic. In: Symon C, Arris L and Heal B (eds) *Arctic Climate Impact Assessment*. Cambridge, United Kingdom: Cambridge University Press, 99–150.

Kokelj S V and Burn CR (2003) Ground ice and soluble cations in near-surface permafrost, Inuvik, Northwest Territories, Canada. *Permafrost and Periglacial Processes* 14(3): 275–289. doi:10.1002/ppp.458.

Kokelj S V, Jenkins RE, Milburn D, Burn CR and Snow NB (2005) The influence of thermokarst disturbance on the water quality of small upland lakes, Mackenzie Delta region, Northwest Territories, Canada. *Permafrost and Periglacial Processes* 16(4): 343–353. doi:10.1002/ppp.536.

Kokelj S V and Jorgenson MT (2013) Advances in thermokarst research. *Permafrost and Periglacial Processes* 24(2): 108–119. doi:10.1002/ppp.1779.

Kokelj S V, Lacelle D, Lantz TC, Tunnicliffe J, Malone L, Clark ID, et al. (2013) Thawing of massive ground ice in mega slumps drives increases in stream sediment and solute flux across a range of watershed scales. *Journal of Geophysical Research: Earth Surface* 118(2): 681–692. doi:10.1002/jgrf.20063.

Kokelj S V, Lantz TC, Smith SL, Kanigan JCN and Coutts R (2009a) Origin and Polycyclic Behaviour of Tundra Thaw Slumps, Mackenzie Delta region, Northwest Territories, Canada. *Permafrost and Periglacial Processes* 20: 173–184: doi:10.1002/ppp.

Kokelj S V, Zajdlik B and Thompson MS (2009b) The impacts of thawing permafrost on the chemistry of lakes across the subarctic boreal-tundra transition, Mackenzie Delta region, Canada. *Permafrost and Periglacial Processes* 20: 185–199: doi:10.1002/ppp.

Lacelle D, Doucet a, Clark ID and Lauriol B (2007) Acid drainage generation and seasonal recycling in disturbed permafrost near Eagle Plains, northern Yukon Territory, Canada. *Chemical Geology* 243(1–2): 157–177. doi:10.1016/j.chemgeo.2007.05.021.

Lantz TC, Gergel SE and Kokelj S V (2010) Spatial heterogeneity in the shrub tundra ecotone in the Mackenzie Delta Region, Northwest Territories: implications for Arctic environmental change. *Ecosystems* 13(2): 194–204: doi:10.1007/s10021-009-9310-0.

Lantz TC and Kokelj S V (2008) Increasing rates of retrogressive thaw slump activity in the Mackenzie Delta region, N.W.T., Canada. *Geophysical Research Letters* 35(6): 1–5. doi:10.1029/2007GL032433.

Liao J, Huey LG, Liu Z, Tanner DJ, Cantrell CA, Orlando JJ, et al. (2014) High levels of molecular chlorine in the Arctic atmosphere. *Nature Geoscience*. Nature Publishing Group 7(12): 1–4. doi:10.1038/ngeo2046.

Lim DSS, Douglas MS V, Smol JP and Lean DRS (2001) Physical and chemical limnological characteristics of 38 lakes and ponds on Bathurst Island , Nunavut , Canadian High Arctic. *International Review of Hydrobiology* 86(1): 1–22.

Ma X and Green SA (2004) Photochemical transformation of dissolved organic carbon in Lake Superior: an in-situ experiment. *Journal of Great Lakes Research*. Elsevier 30(Supplement 1): 97–112. doi:10.1016/S0380-1330(04)70380-9.

Mackay JR (1966) Segregated epigenetic ice and slumps in permafrost Mackenzie Delta area, NWT. *Geographical Bulletin* 8(1): 59–80.

Malone L, Lacelle D, Kokelj S V and Clark ID (2013) Impacts of hillslope thaw slumps on the geochemistry of permafrost catchments (Stony Creek watershed, NWT, Canada). *Chemical Geology*. doi:10.1016/j.chemgeo.2013.07.010.

Mesquita PS, Wrona FJ and Prowse TD (2010) Effects of retrogressive permafrost thaw slumping on sediment chemistry and submerged macrophytes in Arctic tundra lakes. *Freshwater Biology* 55(11): 2347–2358: doi:10.1111/j.1365-2427.2010.02450.x.

Moquin PA, Mesquita PS, Wrona FJ and Prowse TD (2014) Responses of benthic invertebrate communities to shoreline retrogressive thaw slumps in Arctic upland lakes. *Freshwater Science* 33(4): 1108–1118. doi:10.1086/678700.

Moquin PA and Wrona FJ (2015) Effects of permafrost degradation on water and sediment quality and heterotrophic bacterial production of Arctic tundra lakes: an experimental approach. *Limnology and Oceanography* 60(5): 1484–1497: doi:10.1002/lno.10110.

Ogbebo FE, Evans MS, Brua RB and Keating JJ (2009) Limnological features and models of chlorophyll-a in 30 lakes located in the lower Mackenzie River basin , Northwest Territories (Canada). *Journal of Limnology* 68(2): 336–351: doi:10.3274/JL09-68-2-16.

Ostrofsky M and Rigler F (1987) Chlorophyll-phosphorus relationships for subarctic lakes in western Canada. *Canadian Journal of Fisheries and Aquatic Sciences* 44: 775–781. doi:10.1139/f87-094.

Pienitz R, Smol JP and Lean DRS (1997a) Physical and chemical limnology of 59 lakes located between the southern Yukon and the Tuktoyaktuk Peninsula, Northwest Territories (Canada). *Canadian Journal of Fisheries and Aquatic Sciences* 54(2): 330–346. doi:10.1139/cjfas-54-2-330.

Pienitz R, Smol JP and Lean DRS (1997b) Physical and chemical limnology of 24 lakes located between Yellowknife and Contwoyto Lake, Northwest Territories (Canada). *Canadian Journal of Fisheries and Aquatic Sciences* 54(2): 347–358. doi:10.1139/cjfas-54-2-347.

Porcal P, Amirbahman A, Kopáček J and Norton SA (2010) Experimental photochemical release of organically bound aluminum and iron in three streams in Maine, USA. *Environmental monitoring and assessment* 171(1–4): 71–81. doi:10.1007/s10661-010-1529-x.

Poulain AJ, Garcia E, Amyot M, Campbell PGC, Raofie F and Ariya PA (2007) Biological and chemical redox transformations of mercury in fresh and salt waters of the high arctic during spring and summer. *Environmental Science & Technology* 41(6): 1883–8.

Prepas EE and Trew DO (1983) Evaluation of the phosphorus-chlorophyll relationship for lakes off the Precambrian Shield in Western Canada. *Canadian Journal of Fisheries and Aquatic Sciences* 40: 27–35.

Prowse TD, Furgal C, Wrona FJ and Reist JD (2009) Implications of climate change for Northern Canada: freshwater, marine, and terrestrial ecosystems. *Ambio* 38(5): 282–289.

Rühland KM and Smol JP (1998) Limnological characteristics of 70 lakes spanning Arctic treeline from Coronation Gulf to Great Slave Lake in the central Northwest Territories, Canada. *International Review of Hydrobiology* 83(3): 183–203.

Rühland KM, Smol JP, Wang X and Muir DCG (2003) Limnological characteristics of 56 lakes in the central Canadian Arctic treeline region. *Journal of Limnology* 62(1): 9–27. doi:10.4081/jlimnol.2003.9.

Sartory DP and Grobbelaar JU (1984) Extraction of chlorophyll a from freshwater phytoplankton for spectrophotometric analysis. *Hydrobiologia* 114: 177–187.

Segal RA, Lantz TC and Kokelj S V (2016) Acceleration of thaw slump activity in glaciated landscapes of the western Canadian Arctic. *Environmental Research Letters*. IOP Publishing 11(3): 0. doi:10.1088/1748-9326/11/3/034025.

Semkin RG, Mierle G and Neureuther RJ (2005) Hydrochemistry and mercury cycling in a High Arctic watershed. *Science of the Total Environment* 342(1–3): 199–221. doi:10.1016/j.scitotenv.2004.12.047.

Thienpont JR, Rühland KM, Pisaric MFJ, Kokelj S V, Kimpe LE, Blais JM, et al. (2013) Biological responses to permafrost thaw slumping in Canadian Arctic lakes. *Freshwater Biology* 58(2): 337–353. doi:10.1111/fwb.12061.

Thompson MS (2009) The impact of permafrost degradation on the pelagic water chemistry and biota of small tundra lakes. University of Victoria. PhD Thesis.

Thompson MS, Wrona FJ and Prowse TD (2012) Shifts in plankton, nutrient and light relationships in small tundra lakes caused by localized permafrost thaw. *Arctic* 65(4): 367–376.

Wetzel RG (2001) *Limnology: Lake and River Ecosystems*. San Diego, CA, USA: Elsevier.

Wrona FJ, Prowse TD, Reist JD, Hobbie JE, Lévesque LMJ and Vincent WF (2006) Climatechange effects on aquatic biota, ecosystem structure and function. *Ambio*. Royal Swedish Academy of Sciences 35(7): 359–369. doi=10.1579/0044-7447(2006)35[359:CCEOAB]2.0.CO;2.

2.9. Supplementary Information

2.9.1. S-Methods:

Artificial substrate construction for periphyton collection

Periphyton was collected in our lakes by using artificial substrates *in situ* over an exposure period of 3-4 weeks in surface waters at 0.5 m depth.

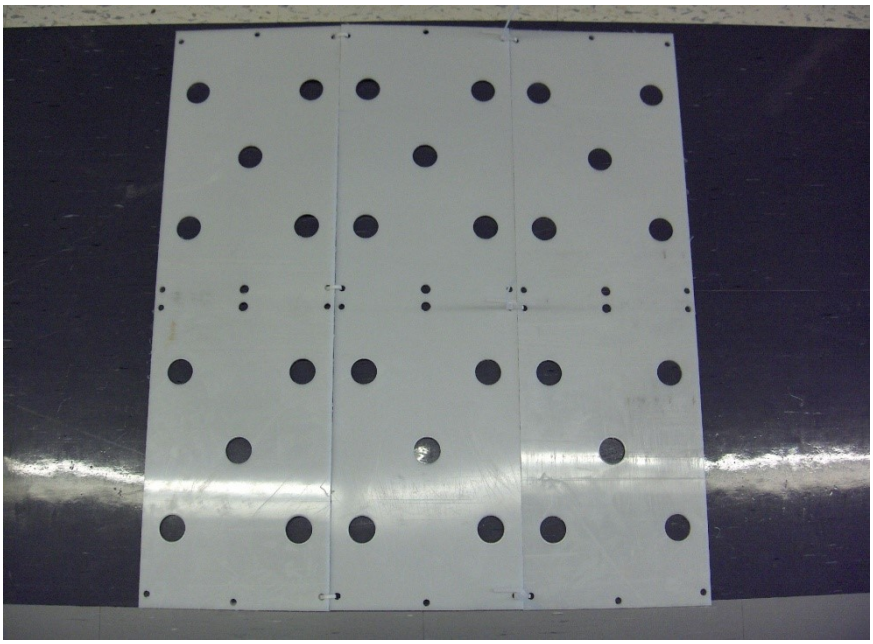

Figure 2.S1: Polyethylene shields used as artificial substrates for collecting periphyton in surface waters of our study lakes. Each shield measures 18 x 60 cm. Three shields were used for a total combined surface area of 6480 cm^2.

Vertical Lake Structure - Hypolimnetic Water Chemistry, Light, and Thermal Regimes

We also investigated the potential for physical-chemical changes within hypolimnetic waters of slump-affected lakes. We suspected that potential shifts in thermal structure, compounded with increased light clarity, may lead to greater photodegradation and redox potential that may then both lead to remineralization of nutrients to the water column. The large introductions of inorganic compounds may alter redox and re-mineralization processes, thus affecting internal loading of nutrients. Vertical profiles of temperature, oxygen, and conductivity were measured from June 30 to July 4, 2011, in 5 lake-pairs (Fig S3) all located in the Noel Lake region (Fig 2.1) to reduce environmental and geographical variation. Additionally, in all 10 of these lakes, we sampled basic water chemistry variables, trace metals, and nutrients from the mid-hypolimnion, to compare with

epilimnetic measurements, and found that results were very similar between the two water layers. The comparison provided a top (epilimnion) versus bottom (hypolimnion) approach to further compare potential changes in the physical-chemical structure of thaw slump-affected lakes.

Trace Metals Analyses

Trace metals were measured in the surface sediments of our tundra lakes from the top 0-2.0 cm of an Ekman grab taken from the middle of the study lakes on July 4, 2011. Headwall soil samples were collected from active thaw slump headwalls from 0.3-3.5 m depth in March, 2010, while soils were frozen. Thaw slump scar surface soil samples (0-2.0 cm) were collected from 5 sites on June 30, 2011. Additionally, 7 catchment soil samples from the organic-rich active layer, adjacent to disturbed lakes, were collected along a transect spanning much of our study site. Soil plugs were sectioned into 0.5 cm sub-samples down to the permafrost, ranging from 4.0-14.5 cm. All soil and sediment samples were freeze dried and sent to SGS Mineral Services, Lakefield, ON, for aqua regia digestion and ICP-MS analysis (protocol IMS12B). Metal concentrations in soil and sediment samples were then compared by 1-way ANOVA across soil and sediment categories with Tukey post-hoc analysis.

2.9.2. S-Results:

Surface water chemistry

When comparing pH measurements to DOC concentrations in our study lakes, a threshold relationship is observed, centred from DOC concentrations of 8-9 mg L^{-1}. Figure S1 labels data points by either slump-affected (red circle) or reference (blue square) lakes, while the breakpoint regression lines show each individual year (2009-2011). The breakpoints centred ranged from DOC concentrations of 6.9-9.2, 9.2-9.4, and 8.3-8.4 mg L^{-1} for the years 2009-11, respectively. By labelling each data point as a slump or reference site, it is evident that, at the lower range of DOC concentrations, all lakes are slump-affected, while the majority of lakes above the 8-9 mg L^{-1} threshold are reference lakes.

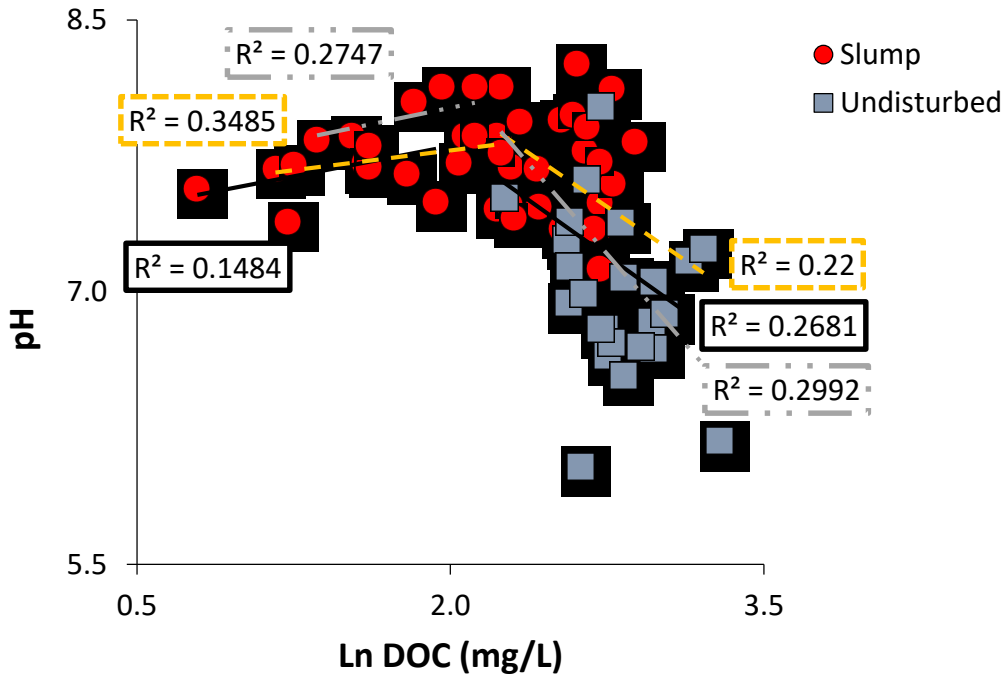

Figure 2.S2: pH as a function of DOC in tundra lakes north of Inuvik, NT, 2009-2011. Breakpoint regression lines for each year 2009-2011. Data points are labelled by slump-affected or reference lake, not by year. Solid line is 2009; dash is 2010; and dash-dot is 2011. The number of samples for the first inclining half of each breakpoint regression included 4-8 samples, while the declining half ranged from 12-19 samples. With all years combined, the first inclining regression has r^2=0.28, p=0.028, n=17; while the declining regression has r^2=0.26, p<0.0001, n=51.

Vertical Lake Structure - Hypolimnetic Water Chemistry, Light, and Thermal Regimes

Lakes ranged from 6-12 m in maximum depth and water chemistry measurements were taken every half-metre. Temperature profiles of slump-affected lakes were compared with reference lakes to determine if the increased clarity and reduced colour enhanced greater light penetration, increased warming, and extended the euphotic zone to deeper depths. Though water clarity measurements, such as increased Secchi depth and reduced colour (Fig 2.2) with increased %CD, would suggest deeper solar radiative penetration in slump-affected lakes, at the time of vertical profiling we found no significant decreases in epilimnetic temperature as a function of thaw slump activity. Further, the mean depth and thickness of the thermocline itself was not found to be significantly different between reference lakes and slump-affected lakes (Fig S3). Dissolved oxygen was similar between reference and slump-affected lakes and followed a similar vertical structure with near saturation (90% saturation on average) in surface waters (0-2 m), decreasing down to less than 50% oxygen saturation just below the thermocline (4 m depth on average), to almost anoxic conditions at the greatest depths in our deeper lakes. Conductivity measurements documented higher hypolimnetic concentrations relative to the

epilimnion, in both reference and slump-affected lakes. This is not surprising, given the low oxygen conditions in these lakes that often leads to mineral resolubilization.

When comparing epilimnetic and hypolimnetic water chemistry in a simple paired t-Test, the important significant results reported in surface waters were replicated in the hypolimnion. The few water chemistry parameters, notably N and P, that were not significant, still exhibited a similar relationship in the hypolimnion as observed in the euphotic zone, i.e. N and P concentrations were lower in slump-affected lakes. The lack of significance in the hypolimnion may be due to the lower number of samples. DOC concentrations demonstrated low variation in reference lakes (DOC range: 13.2-15.6 mg L^{-1}), while slump-affected lakes had a much greater range (3.7-16.1 mg L^{-1}). No explanation due to slump activity or relative size of the thaw slump was apparent. We also measured phytoplankton production to determine if increased water clarity led to increased Chl-*a* concentrations. However, results were not significantly different between reference and slump-affected lakes. The average Chl-*a* concentration in hypolimnetic samples was 4.7 µg L^{-1}, ranging from 2.4-8.4 µg L^{-1}, for both reference and slump-affected lakes combined. When compared with surface water samples, the average Chl-*a* is 4.0 µg L^{-1}, ranging from 0.2-19.6 µg L^{-1}, demonstrating the overall low productivity in these lakes.

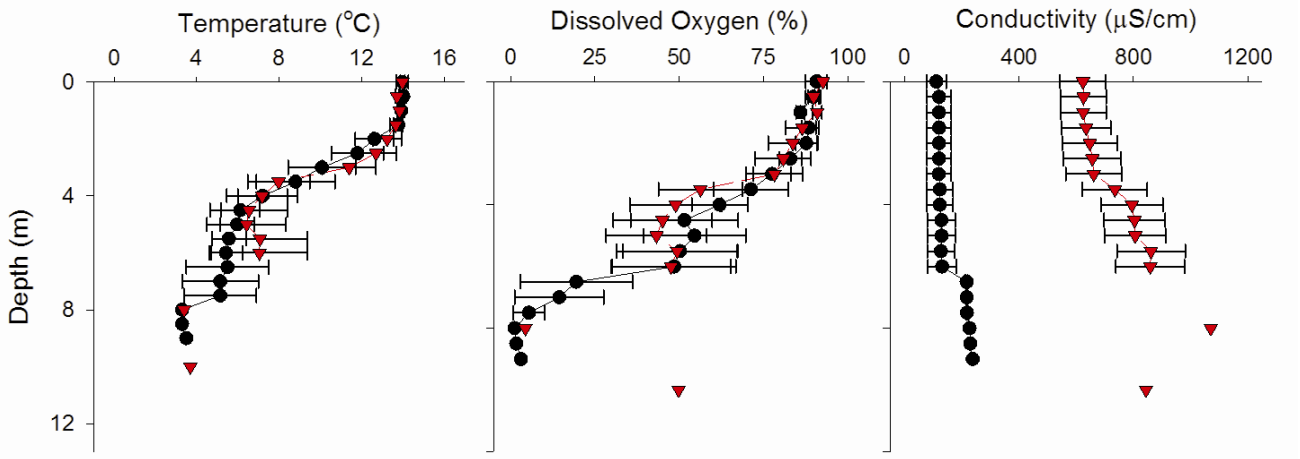

Figure 2.S3: Average water column structure for both slump-affected and reference lakes in the upland tundra lake region north of Inuvik, NT, collected Jun. 30/11. Closed circles are reference lake averages at each depth, triangles are thaw slump lakes; one standard error included. Data averaged from 5 lakes for both plots, with decreasing n at depth, as lakes varied in maximum depth starting at approximately 6.0 m.

Stream Water Chemistry

Streams flowing into and out of our study lakes were also surveyed to further show that thaw slumps were the primary influence on physicochemical changes in disturbed lakes. From a subset of catchments, 4 headwater streams receiving only catchment run-off inputs were contrasted with outlet streams from both our reference lakes (n=4) and slump-affected lakes (n=7) (Table S1). Samples were collected 5-10 m up-stream or down-stream from adjacent lakes. Measurements of specific conductivity, one of the strongest indicators of thaw slumping in lake waters, were significantly different between all three stream categories ($F=12.8$, $p=0.002$). As expected, inlet streams had the lowest average conductivity (32 µS cm^{-1}), whereas reference lakes and their outlet streams were identical to each other (both averaged 55 µs cm^{-1}), and only slightly higher than the inlet streams. To contrast, our slump-affected lakes and their connected outlet streams were both an order of magnitude higher (408 and 338 µS cm^{-1}, respectively), than all reference lakes and streams.

Measurements of biological production in streams indicated that Chl-*a* concentrations from catchment inlets (1.85 µg L^{-1}) were significantly lower ($F=4.44$, $p=0.042$) than outlet streams from both reference lakes (8.23 µg L^{-1}) and slump-affected lakes (7.53 µg L^{-1}) (Table S1). No significant difference between outlet streams for both reference and slump-affected lakes was observed.

Table 2.S1: Water quality variables contrasting streams flowing into (Inlet) and out of (Outlet) reference or slump-affected lakes in the tundra upland region east of the Mackenzie River delta, Northwest Territories, Canada. Stream chemistry was measured 20-June-2011 and lake chemistry 06-July-2011. DO: Dissolved Oxygen; SpC: Specific Conductivity; POC: Particulate Organic Carbon; PON: Particulate Organic Nitrogen; Chl-*a*: Chlorophyll-a. Mean values are shown with Standard Deviations in parentheses below.

Water Body Category	Disturbance Level	Temperature (°C)	DO (%)	SpC (µS cm^{-1})	POC (mg L^{-1})	PON (mg L^{-1})	Chl-*a* (µg L^{-1})
Inlet	Reference	11.0	76	32	0.73	0.06	1.85
	(n=4)	-3.0	-16	-18	-0.24	-0.02	-0.07
Lake	Reference	17.8	93	55	0.74	0.07	4.10
	(n=4)	-0.6	-5	-14	-0.22	-0.02	-2.36
Lake	Slump-Affected	16.6	104	408	1.03	0.14	5.44
	(n=7)	-0.8	-11	-209	-1.02	-0.17	-6.48
Outlet	Reference	13.7	92	55	1.11	0.11	8.23
	(n=3)	-1.6	-13	-15	-0.22	-0.01	-1.18
Outlet	Slump-Affected	13.2	96	338	1.04	0.14	7.53
	(n=7)	-2.4	-4	-149	-0.64	-0.11	-2.51

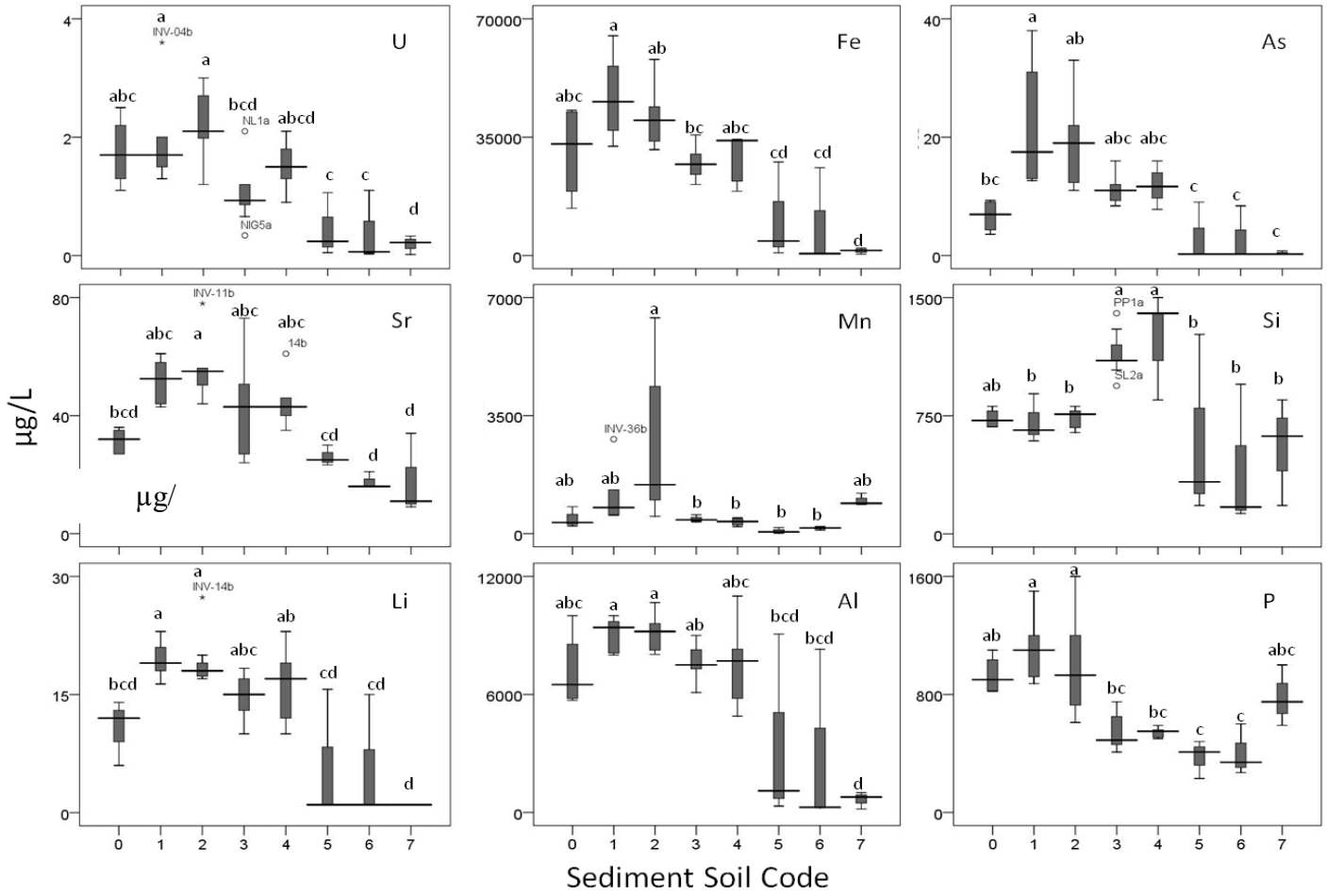

Figure 2.S4: Trace metal measurements collected from soil and lake sediments in the Mackenzie Delta upland region, June 20-July 6, 2011. (0: reference lakes, n=5; 1: stable slump lakes, n=6; 2: active slump lakes, n=7; all 0-2.0 cm), thaw slump headwall soils (3: 0.3-3.5 m, n=9), thaw slump scar soils (4: 0-2 cm, n=5), and active layer catchment soil sections (5: 6-15 cm, n=3; 6: 4-4.5 cm, n=3; 7: 0-0.5 cm, n=3).

2.9.3. S-Discussion: Vertical Structure

In a past study of shield lakes, Fee et al (1996) observed water transparency to be a significant influence on the euphotic depth in lakes smaller than 500 ha. The same study attributed the amount of transparency to be controlled by DOC concentrations in oligotrophic lakes. In our slump-affected lakes, the increased Secchi depths combined with reduced colour and DOC measurements suggests the euphotic zone could decrease in depth. However, our one-time vertical profiles from June 30, 2011 does not support such a phenomenon (Fig S3). It is likely that maximum stratification had not been achieved this early in the cold Arctic tundra environment and that a significant difference between reference and slump-affected lakes was not recorded this early in the open-water season. However, past thermocline estimates of 3-5 m were measured in lakes from the same region later in the year (early September, 2004) and no mention of slump-related differences in thermal structure were discussed (Kokelj et al., 2005). The patterns of thermal structure over a full growing season represent an important research area to delineate influences on available photosynthetically active radiation (PAR), the vertical distribution of biota, and habitat availability for warm or cold water dwelling organisms.

Further, when comparing hypolimnetic waters with the overlying epilimnetic waters in the "top vs bottom" analysis, we did not observe any new relationships that were not already described in the above epilimnetic water samples. As discussed above, two processes are likely acting in concert to alter the biogeochemical dynamics in slump-affected lakes, namely: 1) the introduction of ion-rich, inorganic clays, silicates, and carbonates from the degrading thaw slump headwalls and runoff from the bare scar slopes (Carey, 2003; Kokelj et al., 2005; Thompson et al., 2008) are acting in concert as a scrubber of the water column as mineral ions adsorb to aquatic organic material and inorganic nutrients leading to sedimentation (Wetzel, 2001) (e.g. negatively charged phosphates binding to incoming Ca^{2+} and Mg^{2+} cations); and 2) over time, the loss of up to one third the surface area of the catchment's organic-rich active layer results in less nutrients and organic matter being introduced to these lake systems from direct overland runoff. The former scenario could lead to removal of nutrients from the water column to the benthos, leading to benthic nutrient enrichment. However, the lack of evidence to support any enhanced nutrient concentrations in hypolimnetic waters does not support this mechanism. With the large input of both inorganic permafrost and active-layer soils, there is a possibility of organic material to be diluted, and thus reducing the impact of any benthic eutrophication from enhanced sedimentation.

In our stream analysis, the slightly lower conductivity in catchment inlet streams with respect to the downstream reference lakes and related outlet streams is likely due to melt water related dilution in the catchment streams, in contrast to summer-long evaporative enrichment (Burn and Kokelj, 2009) in the downstream reference lakes and streams. Regardless, these effects on conductivity are negligible to the major amplification of ionic activity in slump-affected lakes that leads to downstream transport of the dissolved and suspended inorganic material composed of clays, sulfates, (aluminum) silicates, and (calcium) carbonates, from incoming slump material. Indeed, we show that incoming catchment water, in the form of input streams to our lakes, is significantly altered when transiting through a slump-affected lake, as demonstrated by the six-fold increase in conductivity in slump-affected outlet streams. These results further confirm that internal lake processes from thaw slump events are the dominant drivers of water chemistry, and that non-thermokarst catchment processes are secondary influences in disturbed lakes. It is clear that thaw slump events may be affecting algal growth, as reflected by declining Chl-*a* production.

3. Mercury in tundra lakes disturbed by shoreline retrogressive thaw slumps in the western Canadian Arctic

Adam J Houben,*[†] Todd D French,[†] Alex J. Poulain, [†] Steven V Kokelj,[‡] John P Smol,[§] Jules M Blais,[†]

[†] University of Ottawa - Program for Chemical and Environmental Toxicology, Department of Biology, University of Ottawa, Ottawa, ON, Canada K1N 6N5,

[‡] NWT Geoscience Office, Government of the Northwest Territories, Yellowknife, NT, Canada X1A 2R3,

[§] Queen's University - Paleoecological Environmental Assessment and Research Laboratory (PEARL), Department of Biology, Queen's University, Kingston, ON, Canada K7L 3N6

This article is completed and will be submitted for publication.

Statement of author contributions:

AJH, TDF, AJP, SVK, JPS, JMB

Authors' Contributions: Adam J Houben – lead researcher and author; Todd D French – field research and editorial review of manuscript; Steven V Kokelj – guidance in permafrost research and editorial review of manuscript; John P Smol –review of manuscript; Jules M Blais – research director and editorial review of manuscript.

3.1. Abstract

In the Inuvik area (68°21'54.60" N, 133°42'27.37" W) of Canada's western Arctic, recent warming has resulted in increased rates of shoreline retrogressive thaw slump disturbances. Within upland tundra lakes we compared Hg among slump-affected lakes and nearby reference lakes. With disturbed catchments experiencing up to a third of land area slumping, we hypothesized significantly lower Hg-delivery to adjacent slump-affected lakes. The related changes in water chemistry led to lower aquatic total and methyl mercury concentrations as a function of the percent of catchment area disturbed by thaw slumping (%CD). However, even with the lower overall aquatic Hg availability in slump-affected lakes, periphyton Hg bioconcentration factors (BCF) were also positively correlated with %CD. We also identified a threshold response relationship between Hg BCFs and DOC centred at 5.8 mg DOC/L. Thus in lakes below the threshold, which were only achieved in slump-affected lakes, periphyton had a positive relationship between Hg BCF and DOC concentrations. This supports the potential for non-equilibrium dynamics to drive Hg bioconcentration. These results highlight the significance of underlying geology driving chemical cycles following permafrost thaw, and specifically, that within highly inorganic glaciolacustrine landscapes, further climate warming may lead to enhanced Hg bioavailibilty in aquatic systems.

Key Words: Mercury, Primary production, bioaccumulation, Mackenzie River Delta, Shoreline Retrogressive Thaw Slump

3.2. Introduction

Mercury toxicity remains a major concern in certain Arctic species, as concentrations have continued to rise despite reduction in emissions from anthropogenic activities in some parts of the world over recent decades (AMAP, 2011; Hylander and Goodsite, 2006). Factors affecting the recent trend in Hg deposition are still being debated (Kirk et al., 2011; Muir et al., 2009; Outridge et al., 2005, 2007; Stern et al., 2009), but it can be reasonably inferred that increasing Hg transport to the Arctic from upwind industrial locales is a contributing factor (Cole and Steffen, 2010;

Hammerschmidt et al., 2006) as well as increasing concentrations of reactive gaseous mercury (RGM) following atmospheric mercury depletion events (AMDE) depositing across polar coastal landscapes (Cole et al., 2014; Steffen et al., 2014). A major summary of temporal trends for Hg and POPs (Braune et al., 2005) concluded that there are significant Hg increases in marine biota across Canada's Arctic, however, regional differences add complexity in assigning Hg sources, and whether or not climate change is a major driver in all cases.

In addition to the stresses caused by Hg and other pollutants, Arctic ecosystems are being affected by climate warming. Annual air temperatures in Canada's western Arctic increased at a mean rate of 0.7 ºC decade^{-1} from 1966–1995 (ACIA, 2005; Serreze et al., 2000). Temperatures across the Arctic are expected to increase by an additional 5–7 ºC by the end of the 21st Century, with this warming rate being twice that of the expected global rate (Kattsov and Källén, 2005). Changes in thermal regimes also appear to be causing AMDEs to occur earlier in the year (Cole and Steffen, 2010) with less of the deposited Hg being returned to the atmosphere (Steffen et al., 2005). The resultant net increase in Hg deposition has likely contributed to the recent increases in bottom-sediment Hg observed in some Arctic lakes. Increased Hg deposition during AMDEs is related to changes in the periodicity of sea-ice coverage, which have in turn affected the emission of seawater halogens that regulate AMDEs (Steffen et al., 2008). Freshwater discharge to the Arctic Ocean increased by 7% over the period 1936–1999, and this change was positively correlated with seasonal temperatures (Peterson et al. 2001). Dissolved organic carbon (DOC) concentrations, to which Hg binds (Barkay et al., 1997), in Arctic rivers are positively correlated with discharge; thus, as river discharge has increased, Hg exports to the Arctic Ocean have increased with climate warming (Carey, 2003; Friedlingstein et al., 2006; Leitch et al., 2007; Semkin et al., 2005). Thawing permafrost and general warming have also led to elevated fish Hg burdens due to algal scavenging (Carrie et al., 2010). Further, these authors hypothesized that the recently observed melting of permafrost inland may be a major source of organically bound Hg being transported to marine environments. Another study (MacMillan et al., 2015) found that in thawing ponds and ice wedge formations, high inputs of organic matter, nutrients, and microbial activity led to elevated MeHg.

Within the upland tundra lake region East of the Mackenzie River delta, it has been observed that shoreline retrogressive thaw slump (SRTS) events are increasing in both size and frequency over the last half century due to warming temperatures and shifting precipitation patterns (Lacelle

et al., 2010; Lantz and Kokelj, 2008). SRTS events (Figure 3.1), up to several hectares, have been increasing in size and frequency over recent decades and are now present on the shorelines of 6–17% of lakes between Inuvik and the Beaufort Sea (Burn and Kokelj, 2009; Kokelj et al., 2005, 2009b; Lantz and Kokelj, 2008). SRTS events within the upland tundra lake region of the Mackenzie Delta, have also led to significant reductions in DOC and colour alongside increasing clarity, pH, and major ions – including sulfate and calcium (Kokelj et al., 2009b). Notably, the reductions in DOC and nutrients are in steep contrast to other thermokarst studies (Carrie et al., 2010; MacMillan et al., 2015; Vonk et al., 2015), and suggest an alternative Hg cycling in response to warming-induced permafrost thaw.

Within the tundra upland lakes of the Mackenzie Delta region, our study aims to utilize a paired-lake design to understand how slump-affected lakes alter aquatic Hg dynamics in contrast to geomorphologically similar reference lakes. More specifically, we aim to quantify aquatic Hg concentrations in slump-affected lakes and reference lakes, and to determine the bioavailability of Hg to aquatic primary producers in relation to increases in base cations and decreases in pH and DOC following a thaw slump event. Our paired-lake design assessed a gradient of SRTS events by using a measure of the percent of catchment area disturbed by thaw slumping (%CD) that ranged between 3-34% of total catchment area slumped in our disturbed lakes, and contrasted this with the paired reference lakes that had 0% of the catchment area slumped.

This study was undertaken in the tundra uplands located to the east of the Mackenzie River delta, between Inuvik (68°21'54.60" N, 133°42'27.37" W) and the Beaufort Sea (Figure 3.1). Elevations (16-225 m a.s.l) prevent lakes in the study area from being inundated by the Mackenzie River, even during spring (May–August) floods. The uplands are characterized by having thousands of lakes affected by thermokarst, rolling and hummocky terrain with embedded ground ice, soils dominated by Wisconsinan tills derived from carbonate and shale bedrock (10–14 km thick), and a near-treeless landscape (Burn and Kokelj, 2009; Kokelj and Burn, 2005). The area is within a continuous-permafrost zone. Permafrost thickness can be up to several hundred meters thick, and active-layer thickness is about 35–65 cm (Burn and Kokelj, 2009; Kokelj et al., 2009b). Ground temperatures in the area have increased in parallel with warming air temperatures.

3.3. Materials and Methods

3.3.1. Study Lakes & Sampling

From 2009-2011, 38 lakes along a North-South gradient between Richards Island and Inuvik NT, (Figure 3.1) were sampled as described in Houben et al (2016). Lake surface area ranged from 0.8–116.5 ha with catchment area and maximum depth ranging from 4.7–254.4 ha and 1.5–10.9 m, respectively (Table 3.1). Lakes >5 m deep can be thermally stratified during the open-water season, but shallower lakes in the area tend to be isothermal (Kokelj and Burn, 2005). Two lake types were sampled: *i*) reference lakes: lakes not having shoreline thaw slumps (denoted "a"); and *ii*) slump-affected lakes: lakes having shoreline thaw slumps (denoted "b"), (Table 3.1). The geomorphology, formation, and progression of thaw slumps are described by (Kokelj et al., 2009a).

The lakes were sampled 2009-2011, from June 20 to July 8 each year. Water grab samples (0.5-m depth) for the analysis of major ions, total Hg (Hg_T) and total CH_3Hg ($MeHg_T$), pH, DOC, and dissolved inorganic carbon (DIC, $\Sigma CO_2 + H_2CO_3 + HCO_3^{1-} + CO_3^{2-}$) were collected from the littoral zone of each lake. Prior to sampling, bottles (polyethylene) and caps were cleaned with dilute HCl (3-d soak), followed by thorough rinsing with distilled deionized water. Bottles were triple rinsed with lake water; they were filled to the rim to void the sample of air. Samples for Hg analysis were preserved with 12N HCl. Samples for DOC and DIC determinations were hand pumped, within hours of collection, through 47-mm diam./0.45-µm Sartorius filters (supported AcetatePlus, plain) and the filtrate analyzed. Water samples were kept cool (4 °C) and in the dark until analysis. Field temperature and specific (@ 25 °C) conductivity (sp. conductivity) were determined with a Y.S.I. Model 85 multimeter. Field blanks were collected along with ten percent of samples being collected in triplicate to test for quality control.

Catchment surface soil and slump scar soil samples were also collected June 20-21, 2011, by coring down to the frost line, which ranged from 4.0 cm below the surface to 14.5 cm below the surface. The slump scar soil samples were further sub-categorized into stable and active. Cores were then sectioned into 0.5 cm vertical sections. Lake sediments were also collected during this period by Ekman grabs from lake-centre with the upper 2 cm being collected into bulk samples. Headwall samples were collected throughout March, 2010, while frozen ranging from 30 cm to

700 cm vertically across the face of the headwall. Soil and sediment samples were then stored at -20 °C until further processing for organic carbon content and heavy metals, including Hg.

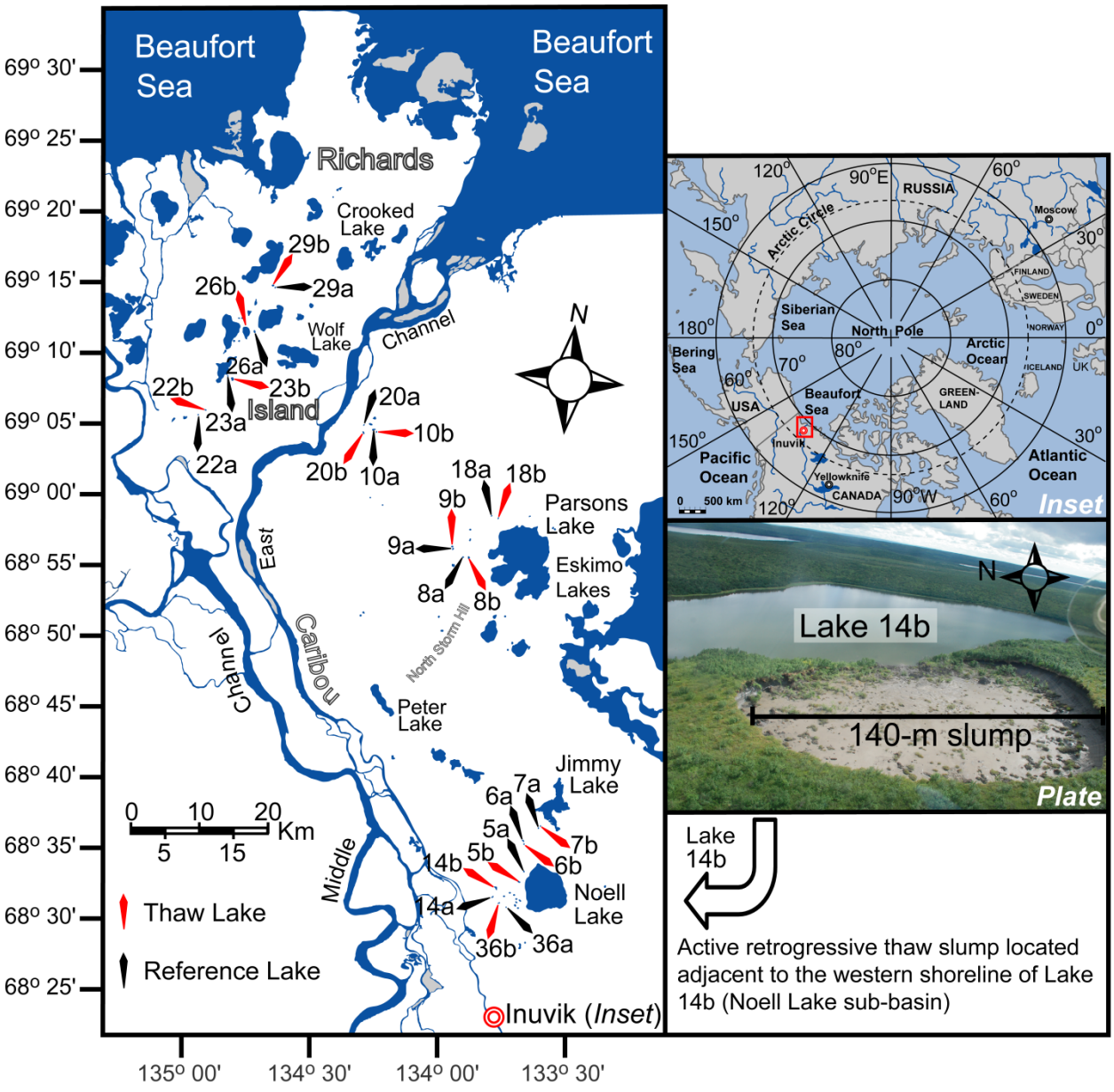

Figure 3.1: Map of the study region in the upland tundra zone northeast of Inuvik, Northwest Territories, Canada. The paired-lake study design is delineated by thaw and reference lakes. The upper right enlarged map indicates our location (red box) within the Arctic polar region. In the lower right, a representative active shoreline retrogressive thaw slump is shown.

Table 3.1: Physical characteristics of our 38 study lakes in the eastern Mackenzie River Delta uplands NWT, Canada, categorized by shoreline retrogressive thaw slump activity. Lakes were sampled June-July, 2009-11.

Lake	˚N	˚W	D to Coast (km)	Slump Activity	%CD	LA (ha)	CA (ha)	Z_{max} (m)	Surficial Geology	Burn Status
26b	69°14'45	134°38'21	30	Active	6	116.5	254.4	3.5	Moraine	Unburned
22b	69°08'44	134°47'02	41	Active	29	3.5	11.7	6.9	Moraine	Unburned
11b	69°08'09	134°10'25	48	Active	6	10.5	39.4	5.2	Moraine	Unburned
10b	69°07'14	134°10'52	49	Active	31	11.4	23.3	10.4	Moraine	Unburned
09b	68°58'14	133°53'59	67	Active	34	3.6	7.2	3	Moraine	Unburned
16b	68°56'48	133°53'48	69	Active	6	14.1	63	6.6	Colluvial	Unburned
08b	68°57'24	133°50'27	69	Active	12	6.5	32.7	4.1	Moraine	Unburned
15b	68°51'39	133°56'06	74	Active	2	10.4	229.9	7	Moraine	Unburned
07b	68°36'32	133°35'12	99	Active	3	3.1	34.7	5	Moraine	Unburned
14b	68°31'45	133°44'14	104	Active	5	9.2	45.1	10.5	Moraine	Recent
05b	68°32'14	133°39'27	104	Active	7	2.8	27.7	9	Moraine	Unburned
29b	69°18'23	134°32'30	25	Stable	21	5.7	14.3	4.5	Moraine	Unburned
23b	69°11'08	134°41'18	36	Stable	4	17.7	74.3	5.9	Moraine	Unburned
20b	69°07'01	134°12'53	49	Stable	8	4.8	17.9	3	Moraine	Unburned
18b	69°00'13	133°43'55	64	Stable	12	2.7	4.7	5.2	Moraine	Unburned
19b	68°52'58	134°12'56	67	Stable	6	6.1	28.1	7	Glaciofluvial	Unburned
06b	68°35'17	133°38'16	99	Stable	11	1.2	7.5	2	Moraine	Unburned
02b	68°30'26	133°40'08	107	Stable	6	4.9	15.9	3.4	Moraine	Recent
04b	68°30'49	133°39'08	107	Stable	14	5	17.8	9.9	Moraine	Recent
03b	68°30'40	133°39'51	107	Stable	24	4	15.3	11.3	Moraine	Recent
36b	68°30'37	133°43'34	108	Stable	20	3.9	24.4	7.4	Moraine	Recent
12b	68°31'55	133°21'13	112	Stable	8	8.7	14.2	6.5	Moraine	Unburned
29a	69°18'13	134°31'56	25	Reference	0	3	14.5	3.8	Glaciofluvial	Unburned
26a	69°14'50	134°36'37	30	Reference	0	6.5	58.2	2.8	Moraine	Unburned
22a	69°08'28	134°49'06	40	Reference	0	1.9	8.3	2.8	Moraine	Unburned
10a	69°07'05	134°10'05	49	Reference	0	2.3	26.3	3.4	Moraine	Unburned
18a	69°00'26	133°45'28	65	Reference	0	2.1	18.4	5	Moraine	Unburned
09a	68°58'05	133°53'53	67	Reference	0	3.1	29.3	2.7	Moraine	Unburned
19a	68°52'44	134°13'29	67	Reference	0	2.8	24.6	4.2	Glaciofluvial	Unburned
06a	68°35'25	133°38'33	99	Reference	0	3.6	19.7	2.3	Moraine	Unburned
07a	68°36'18	133°35'27	100	Reference	0	1.4	18.1	2.7	Moraine	Unburned
05a	68°33'04	133°38'23	103	Reference	0	2.9	20.9	10.9	Moraine	Unburned
03a	68°31'14	133°40'18	106	Reference	0	1.3	13.1	10.3	Moraine	Recent
04a	68°30'57	133°39'39	106	Reference	0	1.2	15.5	2.5	Moraine	Recent
14a	68°31'02	133°44'55	106	Reference	0	3.4	33.5	7.5	Moraine	Recent
02a	68°30'09	133°39'55	108	Reference	0	2	17.2	6.1	Moraine	Recent
36a	68°30'10	133°42'02	108	Reference	0	0.8	6.6	9.5	Moraine	Recent
12a	68°31'06	133°22'27	114	Reference	0	2.8	25	6.8	Moraine	Unburned

D to Coast: distance to Arctic marine coast; %CD: percent of catchment area disturbed by thaw slumping; LA: lake area; CA: catchment area; Z_{max}: maximum lake depth; Burn Status: catchments with fire occurrence in last 50 years

3.3.2. Chemical Analyses

Water chemistry parameters were measured as described in Houben et al (2016). All chemical analyses were performed at either Environment Canada's (EC) National Laboratory for Environmental Testing (NLET), Burlington, ON, or Taiga Environmental Laboratory, Yellowknife, NT, which both maintain Canadian Association for Laboratory Accreditation. At NLET, pH was determined with a Thermo Orion Model 106 meter. The remaining analyses at NLET were performed following EC's standard operating procedures (SOP): *i*) Cl^- and SO_4^{2-} (major anions SOP #1080); *ii*) DOC and DIC (SOP #1021).

Mercury measurements (total mercury (Hg_T) and methyl mercury (MeHg)) were determined at the University of Ottawa's LANSET (Laboratory for the Analysis of Natural and Synthetic Environmental Toxicants) which also maintains CALA accreditation for Hg_T in water. Hg_T concentrations in water were determined by cold-vapour atomic fluorescence (CVAF) spectrometry as per U.S. EPA Method 1631(E). In brief, BrCl was added to samples to oxidize Hg to Hg^{2+} which, in turn, was sequentially reduced with NH_2OH•HCl to destroy free halogens. All Hg was then completely reduced to volatile Hg^0 with $SnCl_2$; Hg^0 was collected on a gold trap while purging the sample with N_2 and then transported, following thermal desorption, to a second gold trap from which Hg^0 was transported by an N_2 stream to the CVAF spectrophotometer (Tekran Instrument Corp., Series 2600). Detection limit was 0.1 ng/L and instrument blanks averaged 0.10 +/- 0.13 ng/L (1 standard deviation), while field blanks averaged 0.12 +/- 0.17 ng/L. Recovery of Hg standards was 99% +/- 4% based on concurrent analyses of NIST-certified stock solutions, with a r^2=0.9996 for the calibration curve. Hg_T recovery was 93% based on concurrent analyses of NIST-certified stock solutions. Analyses were carried out using a Tekran 2600 analyzer (Tekran Inc.) according to EPA method 1631 revision E. Hg_T concentrations in solids, soil, sediment, and periphyton tissue, were assessed on a dry weight basis using a Nipon Hg Analyzer SP-3D (Nippon Instruments Corporation, Osaka Japan).

Determination of $MeHg_T$ was performed by capillary gas chromatography-atomic fluorescence spectrometry (GC-AFS), as per Cai et al. (1996). Sample aliquots (approximately 1 L) were passed through a sulfhydryl-cotton column, which is then treated with 6 times 1 mL mix of KBr/CuSO4 1 M (2:1). The eluate was extracted with 150 µL CH_2Cl_2 under agitation for 30

minutes, centrifuged at 5000 rpm for 10 minutes, before measurement on a Ai Cambridge Model GC 94 Gas Chromatograph (800°C pyrolysis) equipped with a CTC A200S Autosampler and PSA Merlin Detector. The detection limit of the method was estimated to be about 2 pg/L and calculated as three times the standard deviation of baseline noise, which was 0.2 pg/L. After every five analyses of MeHg in lake samples, a blank sample was analyzed followed by a MeHg standard (2 pg/L) analysis for control.

3.3.3. Periphyton collections

Periphyton samples were collected from artificial substrates after 3-4 weeks *in situ* growing period. At each lake, three clean, white polyethylene shields (60 x 12 cm) with a total combined surface area of 6443 cm^2, were deployed at 0.5 m under the water surface and left for periphytic algae to colonize for 3-4 weeks. Shields were then collected and stored in bags at -20°C until they were processed. Using 250 mL of deionized water, periphyton were scraped and rinsed from the shields into an algal slurry. For chlorophyll analysis, a 10 mL aliquot was then filtered onto a 45 mm GF/F filter and then stored at -20°C before assaying (Desrosiers et al., 2006). Chlorophyll concentrations were then measured using a dimethyl sulfoxide extraction with subsequent absorbance measured on a spectrophotometer at wavelengths of 664, 647, and 630 nm for Chl-*a*, *b*, and *c*, respectively (Burnison, 1980).

3.3.4. Statistical Treatment

The statistical design involved the pairing of a disturbed thaw slump-affected lake with a nearby reference lake. Pairings were based primarily on geographic closeness (Figure 3.1), but other factors such as morphometric similarity, and lake and catchment area were also considered (Table 3.1) as determined in Kokelj et al (2005). Because the lakes comprising a pair were located close to one another, we assumed that atmospheric Hg deposition to lake surfaces and catchments were similar on an areal basis, and that lake catchment geologies were similar.

This study first outlines potential sources of Hg to tundra lakes east of the Mackenzie Delta region, immediately north of Inuvik up to Richard's Island in the Beaufort Sea. In order to determine if environmental factors other than thaw slumping influenced Hg dynamics in lakes, we contrasted water chemistry measurements with proximity to the cooler Arctic coast, the treeline, and the recent fire zone of 1968. For this comparison, we used data collected in 2009 as the survey

incorporated the longest north-south transect ranging 25-108 km inland, beginning on Richards Island heading southward to the Noel Lake area.

Surface soil samples were categorized by undisturbed reference catchment soils and slump scar soils also compared using one-way ANOVA. To infer the effects of permafrost thawing on water chemistry, the chemistry of slump-affected lakes was compared to that of reference lakes with paired-sample *t*-tests. Linear regression was used to determine how water chemistry varied in relation to the degree of permafrost thaw (0–34% of catchment area). Hg_T BCFs from water to periphyton samples were determined for each lake by dividing concentrations in periphyton (ng/g dw) by concentrations in water (ng/L), resulting in BCF.

3.4. Results

3.4.5. Mercury Sources

A significant temperature gradient of colder coastal lakes to warmer inland lakes was observed in our 2009 North-South transect (Figure 3.2). Chloride ions within our reference lakes were also found to have a significant negative relationship (r^2=0.78, p<0.001, n=11) to distance from the coast (Figure 3.2a), ranging from almost 8 mg/L in reference lakes closest to the coast, to less than 2 mg/L in lakes over 100 km inland. Notably, this was the only major ion measured that did not relate to percent of catchment area disturbed by thaw slumping (%CD), as observed in related studies (Houben et al., 2016; Kokelj et al., 2005). A similar enrichment near the ocean coast was found with Na^+ ions (r^2=0.33, p=0.078), though not significant due to the relatively high Na^+ concentration in lake INV-14a, 106 km inland; the only reference lake in our 2009 survey to have been disturbed by the 1968 fire (Burn and Kokelj, 2009), suggesting lingering fire-related thawing effects may be the cause for elevated ion concentrations including sodium, sulfate and calcium. Once lake INV-14a is removed, the negative relationship between Na^+ and coastal proximity is significant (r^2=0.67, F=16.4, p=0.004). These relationships between chloride and sodium with coastal proximity were not significant in slump-affected lakes (Figure 3.2a). For aquatic Hg measurements we also found a significant negative relationship between the distance from the marine coast and Hg_T concentrations in reference lakes (Figure 3.2b). To contrast, slump-affected lakes exhibited no significant Hg response to coastal proximity and average Hg concentrations were lower than all reference lake Hg measurements. Additionally, we measured a positive

relationship between Hg_T and Cl^- (r^2=0.37, F=5.17, p=0.049), but no overlapping spatial trend between pH and coastal proximity.

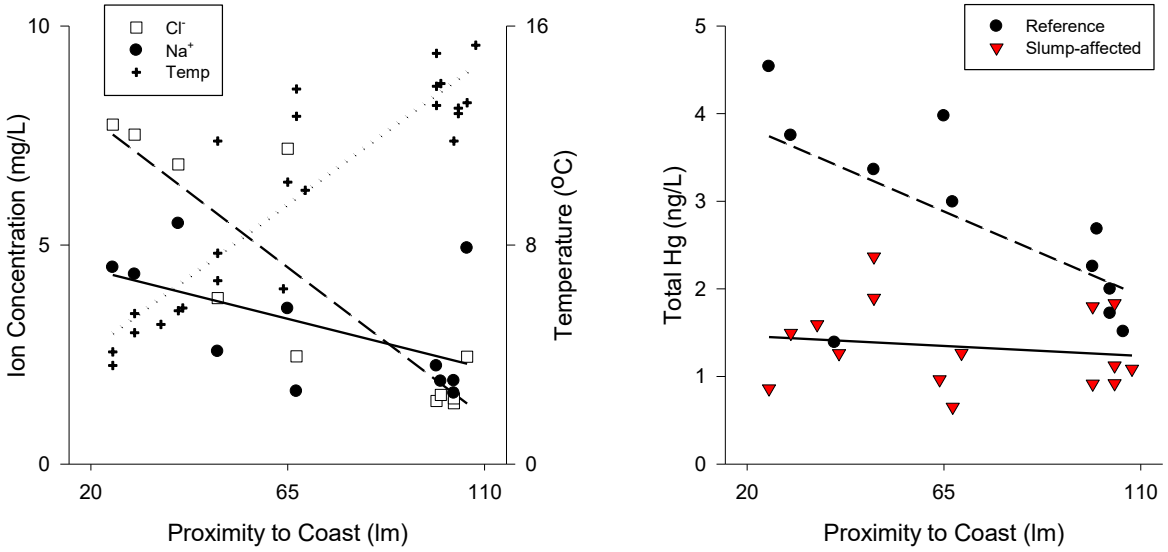

Figure 3.2: Physical-chemical properties of upland tundra lakes with respect to Arctic Ocean coast. Left: Aquatic chloride and sodium ions and lake water temperature with relation to coastal proximity as measured in reference lakes from our 2009 survey (n=11). Right: Aquatic Hg measured in relation to proximity to marine arctic coast for both reference lakes and slump-affected lakes. Study lakes were selected across a North-South gradient from 25 km inland from the Arctic coast on Richards Island to 108 km inland near Inuvik, NT. Cl^-: r^2=0.78, p<0.001; Na^+: r^2=0.31, p=0.08; Temperature: r^2=0.72, p=0.002; Reference Hg_T: r^2=0.41, p=0.03; Slump-affected Hg_T: r^2=0.03, p=0.56.

We analysed various soil categories to contrast the potential relative terrestrial loading of Hg to our lakes with or without SRTS events. Figure 3.3 illustrates that within the upper 0.0-0.5 cm of catchment soils, reference catchment soils had a median of 46.1% organic carbon (C_{org}) with a median soil Hg concentration of 212.1 ng/g dw. In contrast, measurements for organic carbon and Hg in all slump scar soil samples were much lower with median values of 3.7% C_{org} and 69.1 ngHg/g dw. When further comparing between active and stable slump scar soil measurements, stable slumps demonstrate greater variability with C_{org} ranging from 2.8-49.3% and Hg from 47.4-157.8 ng/g dw, while active slump scars have a narrower range from 1.8-4.2% C_{org} and 54.1-93.5 ngHg/g dw, respectively. Additionally, in the reference soil samples, $\%C_{org}$ and Hg concentrations became lower in deeper soil sections generally corresponding to 4-14 cm below surface, and were typically similar in Hg concentration to the slump scar soils, as soil sections also transitioned from higher organic content at the surface to clays and silts in deeper sections. In comparison, thaw

slump headwall soil samples collected vertically from 0.3-7.0 m below surface had Hg measurements of 17.9-123.0 ng Hg/g dw (median=53.8 ng/g dw). Measurements of Hg (ng/g dw) in lake sediments indicated that slump-affected lakes were significantly lower ($t=6.96$, $p<0.001$, $df=40$) with a median concentration of 94.87 ng/g dw compared to 167 ng/g dw for reference lakes. Once lake sediments were standardized for organic carbon content there was no significant difference between reference and slump-affected lakes (median=1812 ng·Hg/g·C_{org} and 1630 ng·Hg/g·C_{org}, respectively; $t=0.75$, $p=0.459$).

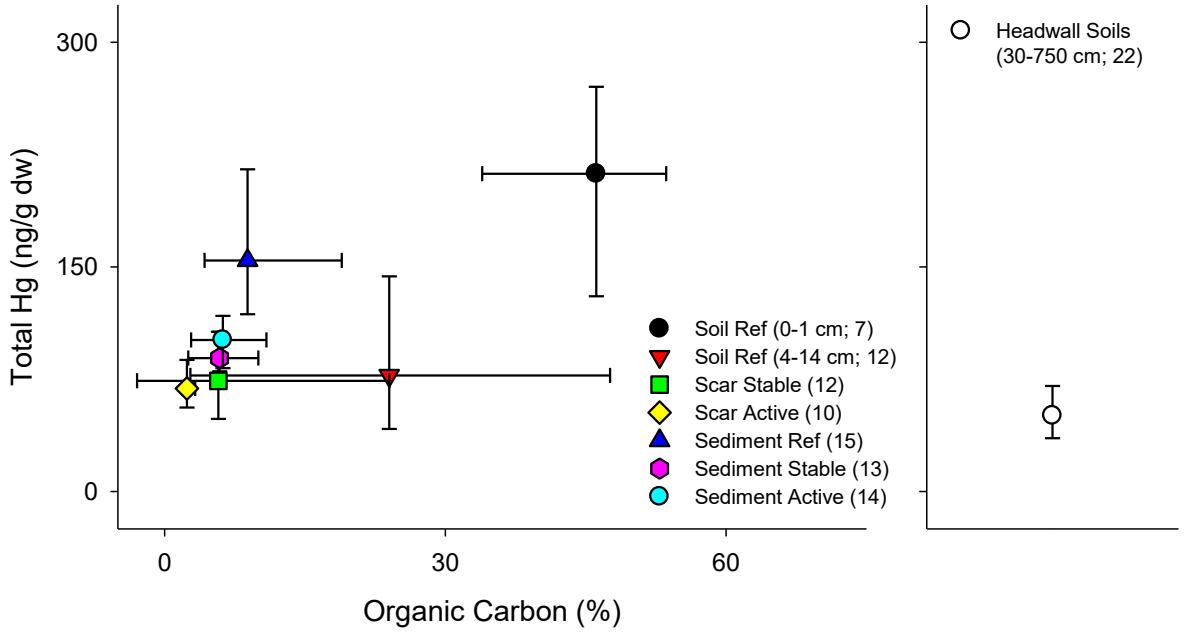

Figure 3.3: Soil analyses of organic carbon content and total Hg in undisturbed upland catchment soils, slump scar soils, headwall soils, and lake sediments, in the upland Mackenzie Delta region. For soils, the upper 0-1 cm was compared to the lower 4-14 cm, while lake sediments were the upper 0-2 cm. The deeper soil samples collected from exposed active headwall surfaces (30-750 cm), had only Hg concentrations measured. The n-value for each category is in parentheses.

3.4.6. Water chemistry in slump-affected lakes

In slump-affected lakes, aquatic total Hg (Hg_T) concentrations ranged from 0.34-3.54 ng/L with a median of 1.00 ng/L, while reference lakes ranged 1.20-4.54 ng/L with a median of 2.88 ng/L (Figure 3.4A,B). When incorporating the scale of thaw slumping, Hg_T and dissolved Hg (Hg_D) concentrations had significant ($p<0.001$) negative relationships to the percent of catchment area disturbed (%CD) by thaw slump events (Figure 3.4A), with the large majority of Hg in the

dissolved fraction. Methyl Hg (MeHg) measurements indicated significant inter-annual variation and were measured separately by annum (Figure 3.4C,D). For each individual year, there is a negative trend between MeHg concentration and %CD (Figure 3.4C), however, only the 2011 survey was significant (r^2=0.36, p=0.02, n=24). The range in MeHg concentrations for all lakes ranged from below detection to 0.26 ng/L. Calculations for MeHg:Hg_T ratios were not significantly related to %CD in any specific study year (Figure 3.4E). When comparing the mean MeHg:Hg_T ratios between slump-affected and reference lake categories for each individual year (Figure 3.4F), we generally observed greater MeHg:Hg_T ratios in slump-affected lakes, though not significant. The MeHg:Hg_T ratios ranged from 0-30% with a median of 3.9% for all lakes, 1.7% for reference lakes, and 4.8% in slump-affected lakes. The median %MeHg for each year was 0.01%, 4.44%, and 7.17%; for 2009, 2010, and 2011, respectively.

Several key water quality parameters, including DOC, pH, and sulfate, that were significantly correlated to slump disturbance (Houben et al., 2016) were also correlated to aquatic Hg concentrations (Figure 3.5). Total Hg concentrations in the surface waters were positively related to DOC concentrations in our lakes, while negatively correlated with pH and sulfate. For our slump-affected lakes the median DOC concentration was 9.4 mg/L and ranged from 2.2-17.9 mg/L, while our reference lakes ranged from 9.6-36.4 mg/L with a median of 16.3 mg/L of DOC.

Aquatic pH measurements were negatively related to Hg_T, with all of our slump-affected lakes were alkaline, ranging from pH 7.13-8.59 with a median of 7.86. Our reference lakes had a median pH of 7.08 and ranged from pH 6.04-8.96 (Figure 3.5B). Thus, median pH concentrations of slump-affected lakes were 0.78 pH units more alkaline than our reference lakes.

Aquatic sulfate concentrations were also negatively related to Hg_T (Figure 3.5C). Sulfate concentrations were ten-fold greater in slump-affected lakes, ranging from 3.9-347.0 mg/L with a median concentration of 81.0 mg/L. In contrast, our reference lakes had a much lower median value of 6.0 mg/L and ranged from 0.3-47.5 mg/L. As reported in (Houben et al., 2016; Kokelj et al., 2005), most major ions reflected similar large increases in concentration in our slump-affected lakes, with the exception of Cl^-.

Due to significant inter-annual variation, we report MeHg relationships with DOC, pH, and sulfate, for each survey year from 2009-11, separately. Notably, 2011 was again the only year where MeHg concentrations were significantly related to DOC and sulfate; MeHg was positively correlated with DOC concentrations (Figure 3.5D) and negatively with sulfate (Figure 3.5F).

Regardless of year, we observed the highest MeHg concentrations when sulfate concentrations were less than 50 mg/L.

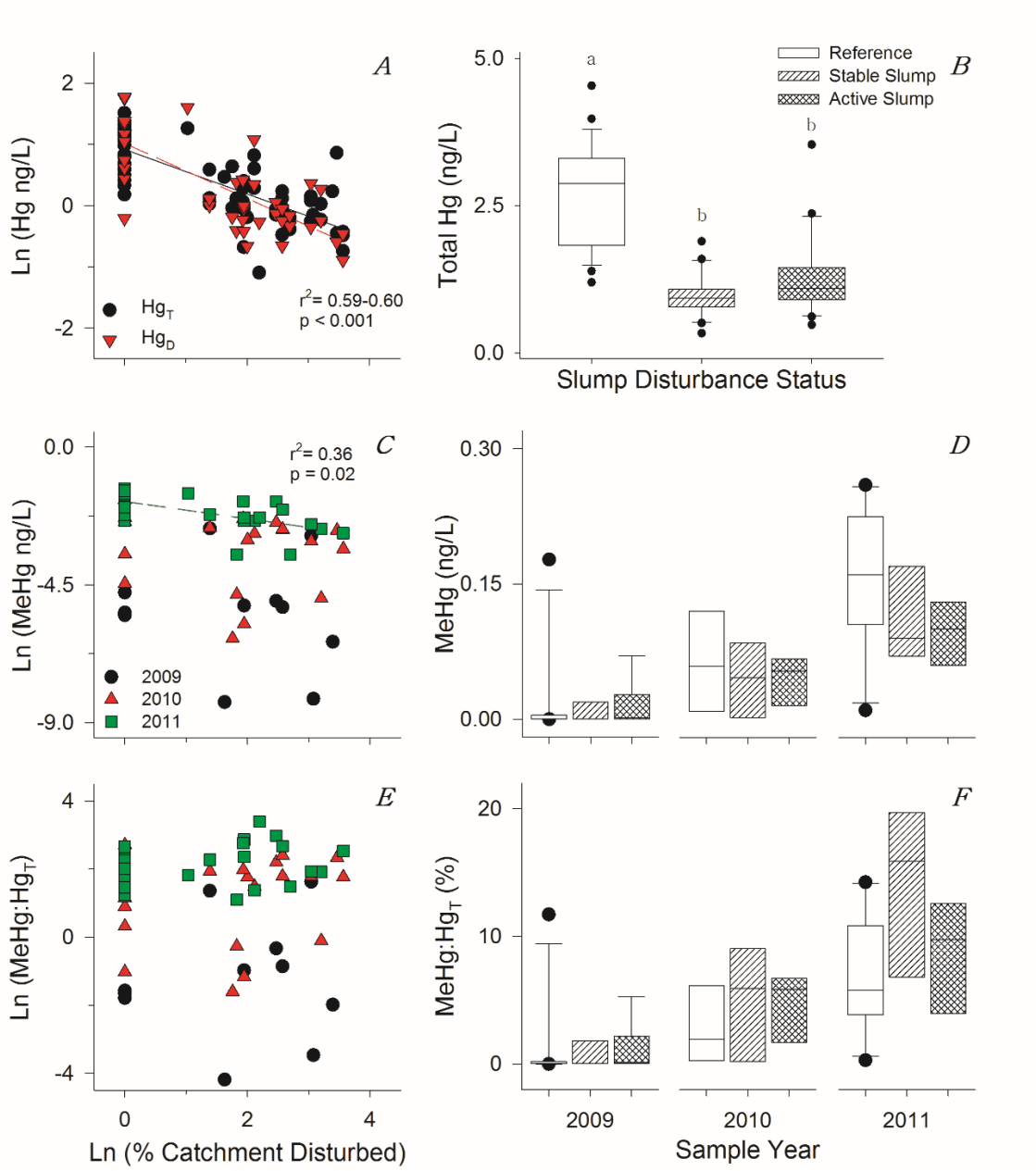

Figure 3.4: Aquatic mercury measurements in relation to the percent catchment area disturbed (Ln %CD+1) by thaw slumping (A,C,E) and by thaw slump status categories (B,D,F) in small, upland tundra lakes east of the Mackenzie River delta. In A, both total Hg (HgT: black circle, r2 = 0.59, p<0.001, n=71) and total dissolved Hg (HgD: red triangle, r2 = 0.60, p<0.001, n=71) are plotted. In C-F, individual years are plotted separately due to interannual variation. For organic methyl Hg (MeHg), plotted in C, only a significant negative relationship with %CD was measured (2009, n=25; 2010, n=22; 2011, r2=0.36, p=0.02, n=24). E indicates the proportion of total Hg in the organic methyl Hg form. For B, total Hg is depicted for all sample years, 2009-11, by disturbance status category, whereby reference lakes were significantly higher than the stable and active slump categories (F=45, p<0.001). Meanwhile, in D and F, individual years were plotted.

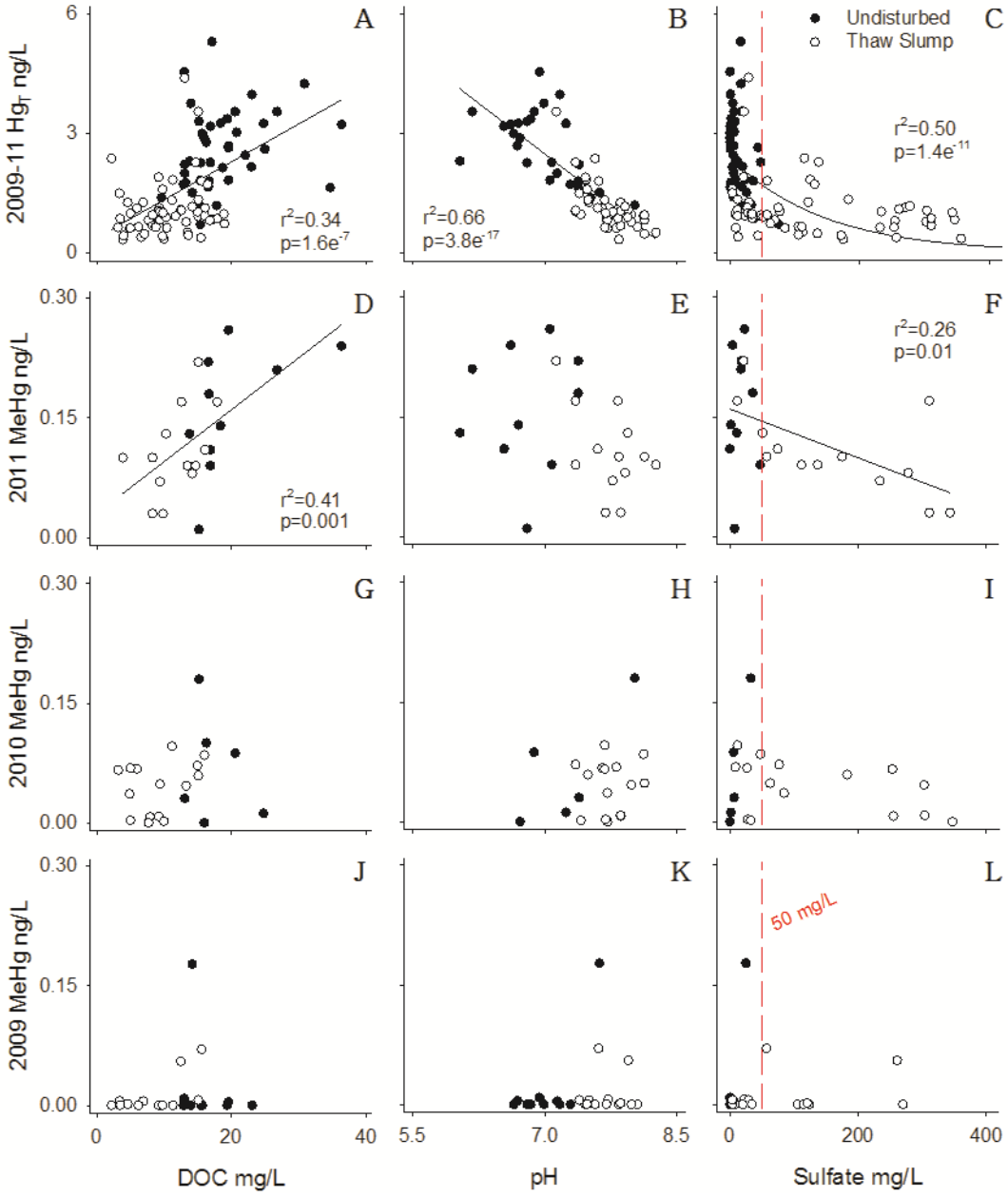

Figure 3.5: Aquatic total Hg and methyl Hg concentrations plotted against DOC, pH, and sulfate, while grouped by reference lakes (black) and slump-affected lakes (white). Samples were collected from 2009-11 for a total of 70 samples. MeHg results are presented by individual year due to significant inter-annual variation. Within the sulfate plots the red, dashed line indicates 50 mg/L of sulfate, demarcating a known threshold for Hg methylation.

3.4.7. Algal mercury bioconcentration

Periphyton tissue Hg_T concentrations ranged from 25.7-218.4 ng·Hg/g·dw, median of 101.3 ng·Hg/g·dw, and were not significantly related to %CD or DOC concentration in lakes (Figure 3.6A-B). This is in contrast to the positive relationship between aquatic Hg_T concentrations and %CD (Figure 3.4A) and negative relationship with DOC concentrations (Figure 3.5A). Periphyton tissue MeHg concentrations ranged from 0.78-35.81 ng·MeHg/g dw, median of 5.76 ng/g dw. Further, within our periphyton tissue we measured the percent of Hg_T in the MeHg form to range from 1%-40%, with a median value of 9%. and were comparable in Hg_T and MeHg concentrations to other periphyton studies (Desrosiers et al., 2006; Walters et al., 2015). Bioconcentration factors (BCF) for Hg_T in periphyton tissue, ranged from 14-230 for all lakes, with median values of 42 for reference lakes and 89 for slump-affected lakes ($F=4.6$, $p=0.037$). Further, periphyton Hg_T BCF was positively and significantly related to %CD (Figure 3.6C). Due to the non-linear nature of the Hg-BCF to DOC relationship, we plotted periphyton Hg_T BCF with aquatic DOC concentrations using a three-factor Lorenztian model (Figure 3.6D). A threshold concentration of 5.8 mg DOC/L, indicated a positive relationship between periphyton Hg_T BCF when DOC was less than 5.81 mg/L and a negative relationship at DOC concentrations greater than 5.8 mg/L. Similar tests for periphyton tissue MeHg BCFs did not demonstrate significant positive or negative relationships with %CD or aquatic DOC.

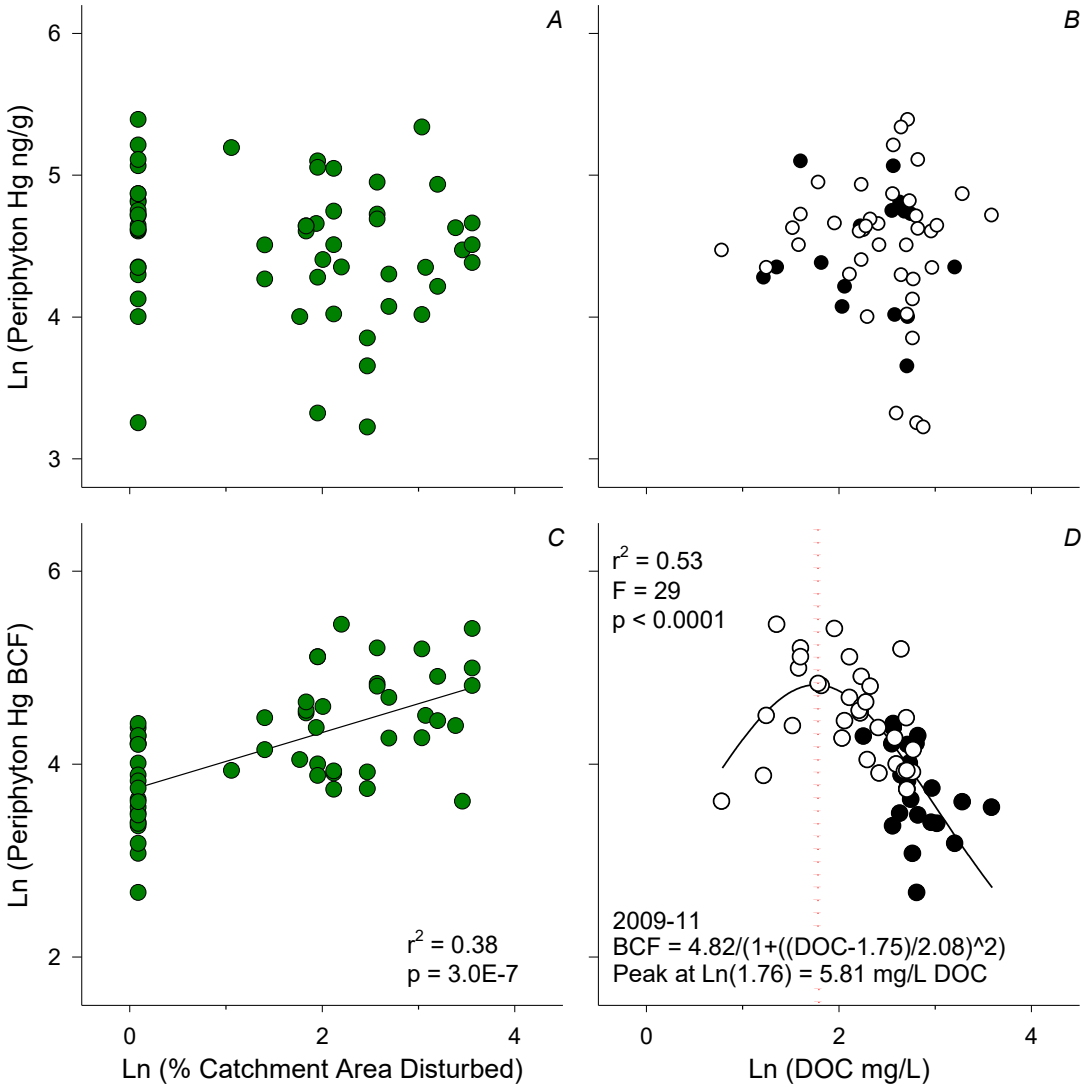

Figure 3.6: Periphyton Hg concentrations and bioaccumulation factors (BCF) in small upland tundra lakes east of the Mackenzie River delta. From 2009-11, 58 samples were collected. Linear regression was performed for the first three plots, while a three-factor Lorentzian model was utilized in creating the final plot. Further, in the fourth plot reference lakes are in black and slump-affected lakes are in white.

3.5. Discussion

We observed a significant positive relationship between periphyton Hg bioconcentration factors (BCF) and the percent of catchment area disturbed (%CD) by thaw slumping (Figure 3.6C), which suggests that the Hg in the slump-affected lakes may be more available for bioaccumulation (Figure 3.4). Further, we also observe a threshold relationship between Hg_T BCFs in periphyton tissue samples and aquatic DOC concentrations peaking at 5.81 mg DOC/L (Figure 3.6D). At DOC

concentrations lower than 5.81 mg/L we observe a positive relationship with Hg_T BCF, indicating greater Hg uptake in periphyton at low DOC concentrations that are only established in our slump-affected lakes. At DOC concentrations above 5.81 mg/L we note that this relationship reverses and DOC may actually reduce Hg-uptake by periphyton. This parallels French et al (2012), where they measured a similar threshold relationship in amphipods, with a noted DOC threshold concentration of 8.5 mg/L across the same study region. This threshold dynamic may be due to competitive binding between DOC and aquatic Hg under nonequilibrium conditions, as proposed by Chiasson-Gould et al (2014); at low DOC concentrations below 10 mg/L and within 24 hours of Hg delivery, DOC may enhance Hg bioaccumulation by acting as a transport shuttle to bacterial cells. Given the large pulse of catchment run-off during the spring freshet as well as polar spring AMDEs at our study site, this may provide sufficient new Hg to these aquatic systems to enhance Hg bioaccumulation in periphyton within our slump-affected, low-DOC lakes. The above studies combined illustrate similar patterns in how DOC affects Hg bioaccumulation in bacteria, primary producers, and aquatic invertebrates, at DOC concentrations below 10 mg/L.

Both total and methyl Hg concentrations in our study lakes were found to be negatively related to %CD. We highlight two potential mechanisms that may lead to the lower total mercury concentrations within the water column of slump-affected lakes (Figure 3.4): i) the reduced retention and transport of DOC-bound Hg from the catchment to adjacent lakes following a thaw slump; and ii) the burial of DOC-bound Hg in lake sediments during a thaw slump event.

For the former, we note that the bulk of organic carbon, and subsequently, Hg content, is predominantly located within the upper 0-4 cm of catchment soil (Figure 3.3). Within our slump scar soils, the lack of organic material is likely the cause for lower Hg, as any Hg being deposited atmospherically on slump scars will be less likely to form complexes with organic matter functional groups such as Cl- and S- (Barkay et al., 1997; Bengtsson and Picado, 2008) and thus will be more readily available for subsequent revolatilization (Selin, 2009). Due to this Hg-C_{org} complexation in catchment soils, C_{org}-bound Hg is likely the main source of overland run-off of Hg to adjacent lakes (O'Driscoll et al., 2005; Semkin et al., 2005) once the active layer thaws. Additionally, the much lower organic carbon content within slump scar soils following a slump event may lead to less capture of atmospherically deposited Hg. Hintelman et al (2002) estimated that 5-60% of atmospherically deposited Hg is promptly recycled back to the atmosphere with highly organic soils and snow being at the opposite ends of the range, respectively. Given that up

to one third of the catchment area was affected by thaw slumping in our study (Table 3.1), this leads to a large proportion of the catchment area that is much less capable of binding and subsequently delivering Hg to adjacent lakes. Our reference upland catchment soils had a median of 46.1% organic carbon, leading to a median soil Hg concentration of 212.1 ng/g dw. To compare, our slump scar soil samples, with the exception of two slump scars, had a median $\%C_{org}$ of 3.1% with a maximum value of 8.0%, and median 67.7 ng Hg/g dw and maximum 94.2 ng Hg/g dw. The two slump scars that were well above this range were at lakes INV-02b and -03b, with 24.4% and 49.3% C_{org}, and 83.5 and 157.8 ng Hg/g dw, respectively. Both of these thaw slumps have been stabilized for several years, as there is a large amount of re-vegetation including thick woody stands of willows 1-2 m in height and a greater accumulation of organic topsoil. These two thaw slumps highlight the broad range of conditions observed within our stable thaw slump category, and the return towards natural pre-disturbance conditions (Kokelj et al., 2009a). Further, the Hg_T concentrations measured within our headwalls from much deeper depths ranging 0.3 to 7.0 m were also less than or equal to our slump scar soil measurements, indicating that the surficial geology within the permafrost is not a relatively high source for Hg during a thaw slump event.

For the burial of DOC-bound Hg to the lake sediments, Deison et al (2012) showed that Hg is higher in the sediments of slump-affected lakes versus reference lakes once standardized for organic carbon content; additionally, slump-affected lake sediments are diluted by the incoming inorganic slump material when measured on a dry weight basis. Additionally, lower DOC (Kokelj et al., 2009b) and nutrients (Houben et al., 2016; Thompson et al., 2012) were observed in similar slump-affected lakes, indicating the dramatic influence of thaw slump material on removing large quantities of organic and particulate material to the sediments. This burial of organics and particulates suggests that Hg bound to incoming organic matter during a slump event is more likely to be deposited in lake sediments. These results suggest that any remaining Hg within the water column is less likely to be bound to organic carbon and related complexing sulfur groups, and to be much more labile and available for biotic methylation and/or uptake as discussed above.

We also see a consistent negative relationship between aquatic MeHg concentrations and %CD (Figure 3.4C). This trend may be related to the overall supply of Hg(II) for methylation, and ultimately the lower total Hg being transported to our slump-affected lakes (Figure 3.4A). Additionally, MeHg production is largely driven by sulfate reducing bacteria (SRB) and a steady supply of sulfate (Compeau and Bartha, 1985; Gilmour et al., 1992). However, it has been observed

that when sulfate concentrations exceeds 50 mg/L in sediment pore water, MeHg production may be hindered (Gilmour et al., 1992). We observed that all of our reference lakes were below 47.50 mg·SO_4^{2-}/L (Figure 3.5), while our slump-affected lakes had a median sulfate concentration of 81.0 mg/L, ranging from 3.9-347.0 mg/L. Thus, half of our stable lakes and over three quarters of our active thaw slump lakes are above 50 mg/L, potentially leading to sulfate-inhibited Hg methylation.

The background Hg_T concentrations in our reference lakes indicate an increasing gradient towards the Arctic marine coast. These higher Hg concentrations closer to the marine coast (Figure 3.2b) suggest that the more northern lakes may be experiencing relatively lower volatility of the gaseous elemental mercury (GEM) due to the much cooler temperatures and shorter ice-free season. This may lead to relatively greater retention of GEM within lakes nearer to the coast, as would be predicted by a local grasshopper effect (Wania and Mackay, 1996) across such a relatively large temperature gradient over a short geographical distance of up to 120 km inland from the much cooler Arctic Ocean. Concurrently, a marine aerosol influence may be transporting Hg inland via AMDEs (Steffen et al., 2008). The corresponding Cl^- and potential Na^+ ion concentrations act as proxies for marine aerosols, correlating with coastal proximity (Figure 3.2a). This coastal relationship with chloride was also observed by Pienitz et al. (1997). The significant correlation between Hg_T and Cl^-, also support this coastal influence assumption. After polar sunrise, GEM is oxidized by reactive halogens (Lindberg et al., 2002) yielding reactive gaseous mercury (RGM), Hg(II), which subsequently experiences relatively rapid wet and dry deposition (Steffen et al., 2008). To date, it is acknowledged that the basic UV-induced atmospheric chemical reactions occur over open marine waters experiencing refreezing sea ice, during the polar spring. Indeed, during this period of rapid chemical change for GEM to RGM, marine aerosols containing RGM have been suggested to travel inland at least 75 km and possibly up to 200 km (Carignan and Sonke, 2010), and are largely dependent on prevailing winds (Douglas and Sturm, 2004). Hg deposition from AMDEs is generally expected to revolatilize back to the atmosphere relatively quickly, however we show here that the reference lakes may be experiencing such lingering effects of AMDEs inland up to 100-120 km into at least early July, and are in the downstream location of our study site's predominant winds originating from the NNE over the Arctic Ocean (Environment Canada, 2009, *http://climate.weather.gc.ca/*). Measurement of Hg within snow-pack before and after polar sunrise and prior to the spring freshet could help define the extent of AMDE influence

within our study site and the greater Mackenzie River delta region separate from a Hg revolatilization gradient in relation to a strong coastal temperature gradient. Though there is a large gradient in aquatic Hg_T in our reference lakes, regardless of the potential source, we see no such relationship in our slump-affected lakes (Figure 3.2B). Indeed, Hg_T in slump-affected lakes is actually much lower on average than the most inland reference lake concentrations, further indicating the dramatic influence of thaw slump events on Hg_T in slump-affected lakes.

3.6. Conclusion

In this study, we highlight the significant influence of thaw slump events on Hg cycling in adjacent lake systems, and how through several inter-related chemical responses, slump-affected lakes with relatively low DOC concentrations may be more prone to greater Hg bioconcentration in primary producers. This is potentially counterintuitive to the negative linear correlation between the scale of thaw slumping and aquatic Hg concentrations, but further corroborates several recent studies (Chiasson-Gould et al., 2014; French et al., 2014) that demonstrated the potential for non-equilibrium dynamics in Hg accumulation in various biota. Further, this is in contrast to other thermokarst studies (Carrie et al., 2010; MacMillan et al., 2015; Vonk et al., 2015) in how higher DOC and nutrients are a common result of thawing, thus understanding regional geology and catchment processes is critical in identifying resultant Hg dynamics. With continued warming across the Arctic, thaw slump events will continue to increase in frequency in a variety of landscapes. In catchments with similar glaciolacustrine tills as within our study site, warming will lead to an increasing number of affected lakes with a relatively higher capacity for Hg bioconcentration.

3.7. Acknowledgements

We thank Michael Pisaric (Carleton University), Joshua Thienpont (Queen's University), and Peter deMontigny (Carleton University) for field, project-design, and technical support. We are especially grateful to William Hurst of Aurora Research Institute (Aurora College, Inuvik) for logistical support, his warm welcome to Inuvik (including a tour), and for setting us up with well-equipped laboratory space. Financial and logistical support for this research was provided by NSERC Discovery and Strategic grants to J.M.B. and J.P.S., Northern Contaminants Program,

Polar Continental Shelf Program, Northern Scientific Training Program, Indian and Northern Affairs Canada, Environment Canada, and Aurora College.

3.8. References

ACIA (2005) *Arctic Climate Impact Assessment*. Cambridge, United Kingdom: Cambridge University Press.

AMAP (2011) *AMAP Assessment 2011: Mercury in the Arctic*. Arctic Monitoring and Assessment Programme (AMAP),Oslo, Norway. Xiv + 193 pp.

Barkay T, Gillman M and Turner RR (1997) Effects of dissolved organic carbon and salinity on bioavailability of mercury. *Applied and Environmental Microbiology* 63(11): 4267–71.

Bengtsson G and Picado F (2008) Mercury sorption to sediments: dependence on grain size, dissolved organic carbon, and suspended bacteria. *Chemosphere* 73(4): 526–31. doi:10.1016/j.chemosphere.2008.06.017.

Braune BM, Outridge PM, Fisk AT, Muir DCG, Helm PA, Hobbs K, et al. (2005) Persistent organic pollutants and mercury in marine biota of the Canadian Arctic: an overview of spatial and temporal trends. *Science of the Total Environment* 351–352: 4–56. doi:10.1016/j.scitotenv.2004.10.034.

Burn CR and Kokelj S V (2009) The environment and permafrost of the Mackenzie Delta Area. *Permafrost and Periglacial Processes* 20: 83–105: doi:10.1002/ppp.

Burnison BK (1980) Modified dimethyl sulfoxide (DMSO) extraction for chlorophyll analysis of phytoplankton. *Canadian Journal of Fisheries and Aquatic Sciences* 37: 729–733.

Cai Y, Jaffe R, Alli A and Jones RD (1996) Determination of organomercury compounds in aqueous samples by capillary gas chromatography-atomic fluorescence spectrometry following solid-phase extraction. *Analytica Chimica Acta* 334(3): 251–259. doi:10.1016/S0003-2670(96)00309-1.

Carey SK (2003) Dissolved organic carbon fluxes in a discontinuous permafrost subarctic alpine catchment. *Permafrost and Periglacial Processes* 14(2): 161–171. doi:10.1002/ppp.444.

Carignan J and Sonke J (2010) The effect of atmospheric mercury depletion events on the net deposition flux around Hudson Bay, Canada. *Atmospheric Environment*. 44(35): 4372–4379. doi:10.1016/j.atmosenv.2010.07.052.

Carrie J, Wang F, Sanei H, Macdonald RW, Outridge PM and Stern GA (2010) Increasing contaminant burdens in an Arctic fish, burbot (*Lota lota*), in a warming climate. *Environmental Science & Technology* 44(1): 316–322.

Chiasson-Gould SA, Blais JM and Poulain AJ (2014) Dissolved Organic Matter Kinetically Controls Mercury Bioavailability. *Environmental Science & Technology* 48(6): 3153–3161.

Cole AS and Steffen A (2010) Trends in long-term gaseous mercury observations in the Arctic and effects of temperature and other atmospheric conditions. *Atmospheric Chemistry and Physics* 10(10): 4661–4672. doi:10.5194/acp-10-4661-2010.

Cole AS, Steffen A, Eckley CS, Narayan J, Pilote M, Tordon R, et al. (2014) A Survey of Mercury in Air and Precipitation across Canada: Patterns and Trends. *Atmosphere* 5(3): 635–668. doi:10.3390/atmos5030635.

Compeau GC and Bartha R (1985) Sulfate-reducing bacteria: principal methylators of mercury in anoxic estuarine sediment. *Applied and Environmental Microbiology* 50(2): 498–502.

Desrosiers M, Planas D and Mucci A (2006) Total mercury and methylmercury accumulation in periphyton of Boreal Shield lakes: influence of watershed physiographic characteristics. *Science of the Total Environment* 355(1–3): 247–58. doi:10.1016/j.scitotenv.2005.02.036.

Douglas TA and Sturm M (2004) Arctic haze, mercury and the chemical composition of snow across northwestern Alaska. *Atmospheric Environment* 38: 805–820: doi:10.1016/j.atmosenv.2003.10.042.

French TD, Houben AJ, Desforges J-PW, Kimpe LE, Kokelj S V, Poulain AJ, et al. (2014) Dissolved organic carbon thresholds affect mercury bioaccumulation in Arctic lakes. *Environmental Science & Technology* 48: 3162–3168. doi:10.1021/es403849d.

Friedlingstein P, Cox PM, Betts R, Bopp L, von Bloh W, Brovkin V, et al. (2006) Climate–carbon cycle feedback analysis: results from the C4MIP Model Intercomparison. *Journal of Climate* 19: 33373353.

Gilmour CC, Henry EA and Mitchell R (1992) Sulfate stimulation of mercury methylation in freshwater sediments. *Environmental Science & Technology* 26(11): 2281–2287.

Hammerschmidt CR, Fitzgerald WF, Lamborg CH, Balcom PH and Tseng CM (2006) Biogeochemical cycling of methylmercury in lakes and tundra watersheds of Arctic Alaska. *Environmental Science & Technology* 40(4): 1204–11.

Hintelmann H, Harris R, Heyes A, Hurley JP, Kelly C a., Krabbenhoft DP, et al. (2002) Reactivity and mobility of new and old mercury deposition in a boreal forest ecosystem during the first year of the METAALICUS study. *Environmental Science & Technology* 36(23): 5034–5040: doi:10.1021/es025572t.

Houben AJ, French TD, Kokelj S V, Wang X, Smol JP and Blais JM (2016) The impacts of permafrost thaw slump events on limnological variables in upland tundra lakes, Mackenzie Delta region. *Fundamental and Applied Limnology* 189:11-35: doi:10.1127/fal/2016/0921.

Hylander LD and Goodsite ME (2006) Environmental costs of mercury pollution. *Science of the Total Environment* 368(1): 352–70. doi:10.1016/j.scitotenv.2005.11.029.

Kattsov VM and Källén E (2005) Future climate change: modeling and scenarios for the Arctic. In: Symon C, Arris L and Heal B (eds) *Arctic Climate Impact Assessment*. Cambridge, United Kingdom: Cambridge University Press, 99–150.

Kirk JL, Muir DCG, Antoniades D, Douglas MS V, Evans MS, Jackson T a, et al. (2011) Climate change and mercury accumulation in Canadian high and subarctic lakes. S1. *Environmental Science & Technology* 45(3): 964–70. doi:10.1021/es102840u.

Kokelj S V and Burn CR (2005) Geochemistry of the active layer and near-surface permafrost, Mackenzie Delta region, Northwest Territories, Canada. *Canadian Journal of Earth Sciences* 42: 37–48. doi:10.1139/E04-089.

Kokelj S V, Jenkins RE, Milburn D, Burn CR and Snow NB (2005) The influence of thermokarst disturbance on the water quality of small upland lakes, Mackenzie Delta region, Northwest Territories, Canada. *Permafrost and Periglacial Processes* 16(4): 343–353. doi:10.1002/ppp.536.

Kokelj S V, Lantz TC, Smith SL, Kanigan JCN and Coutts R (2009a) Origin and Polycyclic Behaviour of Tundra Thaw Slumps, Mackenzie Delta region, Northwest Territories, Canada. *Permafrost and Periglacial Processes* 20: 173–184: doi:10.1002/ppp.

Kokelj S V, Zajdlik B and Thompson MS (2009b) The impacts of thawing permafrost on the chemistry of lakes across the subarctic boreal-tundra transition, Mackenzie Delta region, Canada. *Permafrost and Periglacial Processes* 20: 185–199: doi:10.1002/ppp.

Lacelle D, Bjornson J and Lauriol B (2010) Climatic and geomorphic factors affecting contemporary (1950-2004) activity of retrogressive thaw slumps on the Aklavik Plateau, Richardson Mountains, NWT, Canada. *Permafrost and Periglacial Processes* 21(1): 1–15. doi:10.1002/ppp.666.

Lantz TC and Kokelj S V (2008) Increasing rates of retrogressive thaw slump activity in the Mackenzie Delta region, N.W.T., Canada. *Geophysical Research Letters* 35(6): 1–5. doi:10.1029/2007GL032433.

Leitch DR, Lean DRS, Carrie J, Macdonald RW, Stern GA and Wang F (2007) The delivery of mercury to the Beaufort Sea of the Arctic Ocean by the Mackenzie River. *Science of the Total Environment* 373(1): 178–195. doi:10.1016/j.scitotenv.2006.10.041.

Lindberg SE, Brooks SB, Lin CJ, Scott KJ, Landis MS, Stevens RK, et al. (2002) Dynamic oxidation of gaseous mercury in the Arctic troposphere at polar sunrise. *Environmental Science & Technology* 36(6): 1245–56.

MacMillan GA, Girard C, Chételat J, Laurion I and Amyot M (2015) High methylmercury in Arctic and subarctic ponds is related to nutrient levels in the warming eastern Canadian Arctic. *Environmental Science & Technology* 49(13): 7743–7753. doi:10.1021/acs.est.5b00763.

Muir DCG, Wang X, Yang F, Nguyen N, Jackson TA, Evans MS, et al. (2009) Spatial trends and historical deposition of mercury in eastern and northern Canada inferred from lake sediment cores. *Environmental Science & Technology* 43(13): 4802–9.

O'Driscoll NJ, Rencz A and Lean DRS (2005) The biogeochemistry and fate of mercury in the environment. In: Sigel A, Sigel H and Sigel RKO (eds) *Metal Ions in Biological Systems, Volume 43 - Biogeochemical Cycles of Elements*. CRC Press, 221–38.doi:10.1201/9780824751999.ch9.

Outridge PM, Sanei H, Stern GA, Hamilton PB and Goodarzi F (2007) Evidence for control of mercury accumulation rates in Canadian high Arctic lake sediments by variations of aquatic primary productivity. *Environmental Science & Technology* 41(15): 5259–5265.

Outridge PM, Stern GA, Hamilton PB, Percival JB, Neely RMC, Lockhart WL, et al. (2005) Trace metal profiles in the varved sediment of an Arctic lake. *Geochimica et Cosmochimica Acta* 69(20): 4881–4894. doi:10.1016/j.gca.2005.06.009.

Pienitz R, Smol JP and Lean DRS (1997) Physical and chemical limnology of 59 lakes located between the southern Yukon and the Tuktoyaktuk Peninsula, Northwest Territories (Canada). *Canadian Journal of Fisheries and Aquatic Sciences* 54(2): 330–346. doi:10.1139/cjfas-54-2-330.

Selin NE (2009) Global biogeochemical cycling of mercury: a review. *Annual Review of Environment and Resources* 34(1): 43–63. doi:10.1146/annurev.environ.051308.084314.

Semkin RG, Mierle G and Neureuther RJ (2005) Hydrochemistry and mercury cycling in a High Arctic watershed. *Science of the Total Environment* 342(1–3): 199–221. doi:10.1016/j.scitotenv.2004.12.047.

Serreze MC, Walsh JE, Chapin FSI, Osterkamp T, Dyurgerov M, Romanovsky VE, et al. (2000) Observational evidence of recent change in the northern high-latitude environment. *Climatic Change*. Springer 46(1): 159–207.

Steffen A, Bottenheim JW, Cole AS, Ebinghaus R, Lawson G and Leaitch WR (2014) Atmospheric mercury speciation and mercury in snow over time at Alert, Canada. *Atmospheric Chemistry and Physics* 14(5): 2219–2231. doi:10.5194/acp-14-2219-2014.

Steffen A, Douglas TA, Amyot M, Ariya PA, Aspmo K, Berg T, et al. (2008) A synthesis of atmospheric mercury depletion event chemistry in the atmosphere and snow. *Atmospheric Chemistry and Physics* 8(6): 1445–1482. doi:10.5194/acp-8-1445-2008.

Steffen A, Schroeder WH, Macdonald RW, Poissant L and Konoplev A (2005) Mercury in the Arctic atmosphere: an analysis of eight years of measurements of GEM at Alert (Canada) and a comparison with observations at Amderma (Russia) and Kuujjuarapik (Canada). *Science of the Total Environment* 342(1–3): 185–98. doi:10.1016/j.scitotenv.2004.12.048.

Stern GA, Sanei H, Roach P, DeLaronde J and Outridge PM (2009) Historical interrelated variations of mercury and aquatic organic matter in lake sediment cores from a subarctic lake in Yukon, Canada: further evidence toward the algal-mercury scavenging hypothesis. *Environmental Science & Technology* 43(20): 7684–7690.

Thompson MS, Wrona FJ and Prowse TD (2012) Shifts in plankton, nutrient and light relationships in small tundra lakes caused by localized permafrost thaw. *Arctic* 65(4): 367–376.

Vonk JE, Tank SE, Bowden WB, Laurion I, Vincent WF, Alekseychik P, et al. (2015) Reviews and syntheses: effects of permafrost thaw on arctic aquatic ecosystems. *Biogeosciences Discussions* 12(13): 10719–10815. doi:10.5194/bgd-12-10719-2015.

Walters DM, Raikow DF, Hammerschmidt CR, Mehling MG, Kovach A and Oris JT (2015) Methylmercury bioaccumulation in stream food webs declines with increasing primary production. *Environ. Sci. Technol.* 49(13): 7762–7769. doi:10.1021/acs.est.5b00911.

Wania FI and Mackay DH (1996) Tracking the Distribution of Persistent Organic Pollutants. *Environmental Science & Technology* 30(9): 390A–396A.

4. Factors Affecting Elevated Arsenic and Methyl Mercury Concentrations in Small Shield Lakes surrounding Gold Mines near the Yellowknife, NT, (Canada) Region.

Adam James Houben,*[1] Rebecca D'Onofrio[1], Steven V Kokelj[2], Jules M Blais[1]

[1] University of Ottawa - Program for Chemical and Environmental Toxicology, Department of Biology, University of Ottawa, Ottawa, ON, Canada K1N 6N5,
[2] NWT Geoscience Office, Government of the Northwest Territories, Yellowknife, NWT, Canada X1A 2R3,

This article has been published as *Houben et al. 2015. PLOS One. 11:4* with minor modifications for this thesis.

Statement of author contributions:
Conceived and designed the experiments: AH SK JB. Performed the experiments: AH RD. Analyzed the data: AH. Contributed reagents/materials/analysis tools: SK JB. Wrote the paper: AH SK JB

4.1. Abstract

Gold mines in the Yellowknife, NT, region - in particular, the Giant Mine - operated from 1949-99, releasing 237,000 tonnes of waste arsenic trioxide (As_2O_3) dust, among other compounds, from gold ore extraction and roasting processes. For the first time, we show the geospatial distribution of roaster-derived emissions of several chemical species beyond the mine property on otherwise undisturbed taiga shield lakes within a 25 km radius of the mine, 11 years after its closing. Additionally, we demonstrate that underlying bedrock is not a significant source for the elevated concentrations in overlying surface waters. Aquatic arsenic (As) concentrations are well above guidelines for drinking water (10 µg/L) and protection for aquatic life (5 µg/L), ranging up to 136 µg/L in lakes within 4 km from the mine, to 2.0 µg/L in lakes 24 km away. High conversion ratios of methyl mercury were shown in lakes near the roaster stack as well, with MeHg concentrations reaching 44% of total mercury. The risk of elevated exposures by these metals is significant, as many lakes used for recreation and fishing near the City of Yellowknife are within this radius of elevated As and methyl Hg concentrations.

Keywords: arsenic; methyl mercury; atmospheric deposition; Giant Gold Mine: taiga shield lake; Yellowknife, NT

4.2. Introduction

Resource extraction has the potential to result in severe contamination of surface waters. Giant Mine near Yellowknife, NT, is one of the world's most prolific examples of local contamination from historical mining activities. Here, gold was found in ore bodies of arsenopyrite (FeAsS), where subsequent roasting was required, converting As and S to As2O3 and sulfur dioxide (SO2) before being vented to the atmosphere (Hocking et al., 1978), along with other notable metals within the ore, such as antimony (Sb) (Hutchinson et al., 1982). During the roasting process, As is oxidized to arsenite and precipitated from the vapours as As2O3 (Lloyd and Oremland, 2006; Sharma and Sohn, 2009) containing both As(III) and As(V) (Walker et al., 2005). Most forms of As are toxic to organisms and inorganic arsenicals are carcinogenic (Ng, 2005; Smith et al., 1992). The level of As toxicity is highly dependent on chemical speciation, where inorganic forms utilizing the trivalent As(III) ion are typically at the more toxic end of the scale (Rahman et al., 2012; Sharma and Sohn, 2009). Additionally, inorganic substances such as sulfide can complex strongly with As(III) species enhancing toxicity; while due to competitive binding, phosphate inhibits As adsorption to, or increases As leaching from mineral surfaces, enhancing inorganic As mobility (Raab et al., 2007; Sharma and Sohn, 2009). Further, phosphate can also drive the biological processing of As-complexes (Hellweger and Lall, 2004) potentially leading to more toxic As compounds.

Beyond the mine property, the primary source of As pollution to landscapes is atmospheric deposition due to mining combustion processes being released from the roaster stacks. Estimates for roaster stack emissions of As to the atmosphere from 1947 to 1974, for Giant Mine and Con. Mine were 16,467 and 2,484 tons, respectively (Hocking et al., 1978). Atmospheric emissions consisted of both particulate and gaseous As, most likely as As_2O_3, though installation of scrubbers and filters reduced some of the particulate load over time. A wet scrubber was added in 1949. In 1951 and 1955 two electro-static precipitators were installed, and in 1958 a baghouse dust collector was added to reduce particulate emissions from the roaster stack, though increased roasting activity also occurred. These technologies reduced atmospheric emissions from 20,000 kg As_2O_3 per day to 454 kg/day, and then to 136-227 kg/day after the final baghouse installation (Hutchinson et al., 1982). Indeed, particulate removal was somewhat successful, though gaseous emissions continued.

Several studies of the landscape outside of the mine property have noted elevated concentrations of As and other related mining combustion by-products, such as higher sulfate and other trace metal concentrations in lake sediments (Andrade et al., 2010; Galloway et al., 2015) and soils and vegetation (Hutchinson et al., 1982; Koch et al., 2000a, 2000b; St-Onge, 2007), as well as bird species (Koch et al., 2005). These studies have attributed high As and S concentrations in both soils and vegetation up to 25 km away from the mine to emissions from the roaster stack (Hocking et al., 1978; Hutchinson et al., 1982). The steep decline in As concentration with distance from source suggested relatively immediate atmospheric fallout as opposed to gaseous dispersion, likely due to rapid condensation of As_2O_3 vapour (Hocking et al., 1978). Wagemann et al. (Wagemann et al., 1978) noted that the surrounding soils and rock of the Yellowknife region, as a whole, are not abnormally high in arsenic, ranging from 2 to 10 ppm, though higher As concentrations do occur up to 140 ppm, mainly in pyrite and pyrrhotite. However, mine tailings at both Giant and Con. Mine are exceptionally high in As, ranging from 600-700 ppm (Wagemann et al., 1978). Wagemann et al. (1978) was also one of the few studies to measure As in surface waters of lakes outside of these mine properties, though only five lakes were measured in total. Two of these lakes were directly connected to Con. Mine tailings ponds and had exceptional total As concentrations (up to 5.5 ppm), while three undisturbed lakes 10-26 km away from the mines were all lower than 0.01 ppm.

Hg is also often a by-product of smelters, and released to the atmosphere followed by wet/dry deposition to nearby catchment soils and water-ways, though due to the longer atmospheric residence time of Hg(0) we do not expect total Hg to demonstrate a local response within our study range of 25 km from the roaster stack. However, elevated sulfate associated with roasting at Giant Mine may enhance Hg methylation (Jeremiason et al., 2006) in lakes closer to the smelters as any increase in sulfate concentrations up to 50 mg/L can stimulate sulfate reducing bacteria (SRB) activity (Gilmour et al., 1992). Mercury is a naturally occurring metal and neurotoxin that is readily bioaccumulated by organisms once in the organic methylated form. Understanding Hg sources, methylation (and demethylation) processes, and where elevated Hg methylation may be occurring is important to environmental management and human health. To the best of our knowledge, elevated methyl Hg has not been reported in lakes or catchments around the Yellowknife mines, and has not been typically reported as a problem near mining roaster stacks.

Most Giant Mine pollution studies have detailed elevated As and other metal concentrations within the directly disturbed tailings ponds and in mine ground water interacting with underground stopes and chambers containing stored As. Of the studies measuring mining pollution relating to atmospheric deposition around the Giant Mine, most have focused on terrestrial soils and vegetation. Within the Yellowknife region, there have been few regional studies on the numerous small, shallow lakes exposed to atmospheric deposition from the mining and roasting processes of gold ore that occurred from 1949-1999 at the Giant Mine and to a lesser extent at the nearby Consolidated Mining and Smelting Company of Canada Ltd. (Con. Mine). This study investigates the extent of As contamination in freshwater lakes outside the mine boundaries, which are not connected to any downstream flow from tailings ponds or As waste storage-related groundwater. We also examine methyl Hg concentrations in lakes near Yellowknife to assess whether the spatial extent of mining-related atmospheric deposition influences aquatic Hg dynamics in local lakes. Specifically, we report water chemistry for 25 small lakes within a 25 km radius of the Giant Mine roaster stack to evaluate potential relationships between emission products (As, Sb, S) and related chemical constituents as a function of distance to the stack. Giant Mine was chosen as the study centre due to its long-term stack emissions, while Con. Mine was a smaller operation, producing less emissions, and ceased smelting altogether by 1971 (Hocking et al., 1978). Due to the relatively rapid atmospheric deposition of emitted roaster stack combustion by-products, we hypothesize elevated concentrations of arsenic, sulfate, and other related compounds in lakes closer to the stack and an exponential decline in concentrations with increasing distance from Giant Mine. We also hypothesize elevated methyl Hg is associated with elevated sulphate concentration proximal to the roaster stack. In addition, we hypothesize that the underlying bedrock (in particular the volcanic, arsenopyrite-rich bedrock) will not be a significant factor for elevated As, and other related metals.

4.3. Methods

4.3.1. Study Area

The 25 study lakes (Table 4.1) are small (0.4-17.8 ha; median of 2.9 ha), shallow (less than 4.3 m, with one exception at 11.5 m; median of 1.2 m) lakes within a 25 km radius of the Giant Mine roaster stack, which is located 5 km north of the city of Yellowknife, NT, (Fig 4.1). The gold ore zones mined are within the volcanic Yellowknife Bay Formation (YBF) within the Kam Group

(Isachsen and Bowring, 1997). This volcanic formation is made up of mafic and felsic volcanic rocks, including basalts and andesites (Kerr and Wilson, 2000) containing high proportions of sulfides, including pyrite, arsenopyrite, sphalerite, chalcopyrite, stibnite, and Sb-bearing sulfosalts (Coleman, 1957). These minerals are the likely sources for the oxidized species of arsenic, antimony, and sulfur dust collected within roaster stack precipitators and baghouse filters, as well as the source for similar atmospheric particulate and gaseous emissions (Clark and Raven, 2004). Five of the study lakes have catchments within this belt of volcanic bedrock. Metasedimentary rocks underlie study lakes along Detah Road to the southeast of the mine, while widespread intrusions of younger granodiorite underlie the catchments of many study lakes to the east (Burwash set) and west (Defeat Suite) of Yellowknife (Kerr and Wilson, 2000). All 25 lakes are within the Level III Taiga Shield High Boreal (HB) ecoregion, with 14 lakes in the Level IV Great Slave Lowland HB. The remaining 11 lakes are in the Great Slave Upland HB (Ecosystem Classification Group, 2008), where much of the landscape has exposed outcrops of the Slave structural province of the Canadian Shield. The upland systems are generally bedrock dominated landscapes, with black spruce and jack pine forests growing in rock fractures and on discontinuous till and lacustrine deposits between bedrock exposures. The lowland systems are low-elevation granitic bedrock plains with discontinuous till and lacustrine deposits from glacial Lake McConnell between outcrops. Abundant bedrock and presence of permafrost in the unconsolidated sediments limit groundwater contributions and interaction between surface water and deeper, underlying soils. Mixed conifer and conifer-deciduous forests on and between rock outcrops are the main treed areas, while shore and floating fens and peat plateaus in wet depressions are present throughout. Prevailing winds are from the east, though during summer predominant wind energy is from the south (Bromstad and Jamieson, 2011; Indian and Northern Affairs Canada and Government of the Northwest Territories, 2010; St-Onge, 2007).

Table 4.1: Physical characteristics of the 25 study lakes (2010) ordered by distance to the Giant Mine roaster stack, Yellowknife, NT, Canada. *dd* is decimal degree units. *D-Stack* is the lake distance to the mine roaster stack. YBF is Yellowknife Bay Formation, Z_{max} is maximum lake depth. LA and CA are lake and catchment area, respectively.

Lake	Latitude (dd)	Longitude (dd)	Elevation (m)	D-Stack (Km)	Eco-Type	Bedrock	Secondary Class	Z_{max} (m)	CA (ha)	LA (ha)	CA:LA Ratio
01	62.530297	-114.351650	192	2.5	Lowland	Volcanic	YBF	1.00	12.93	0.89	14.53
02	62.543164	-114.352419	193	3.9	Lowland	Volcanic	YBF	0.50	3.55	0.43	8.26
03	62.542683	-114.349253	194	3.9	Lowland	Volcanic	YBF	1.30	1.55	0.64	2.42
04	62.543200	-114.377928	198	4.2	Lowland	Volcanic	YBF	1.22	15.73	13.07	1.20
05	62.475245	-114.293533	191	4.5	Lowland	Sedimentary	Metaturbidites	0.86	17.07	1.55	11.01
06	62.472445	-114.293622	195	4.8	Lowland	Sedimentary	Metaturbidites	2.00	29.08	2.49	11.68
07	62.571433	-114.367528	204	7.1	Upland	Volcanic	YBF	2.20	52.99	2.70	19.63
08	62.440636	-114.299393	166	7.9	Lowland	Sedimentary	Metaturbidites	1.15	21.21	5.56	3.81
09	62.435292	-114.293284	163	8.5	Lowland	Sedimentary	Metaturbidites	1.92	15.35	1.35	11.37
10	62.535330	-114.142851	171	10.9	Upland	Sedimentary	Metaturbidites	0.67	39.44	2.88	13.69
11	62.455219	-114.531467	194	11.2	Lowland	Granodiorite	Defeat Suite	4.30	15.05	1.03	14.61
12	62.461200	-114.558220	191	12.1	Lowland	Granodiorite	Defeat Suite	0.90	45.75	2.55	17.94
13	62.456072	-114.595051	186	14.0	Lowland	Granodiorite	Defeat Suite	1.15	47.44	3.82	12.42
14	62.457357	-114.604978	185	14.5	Lowland	Granodiorite	Defeat Suite	1.05	33.82	8.81	3.84
15	62.603725	-114.113978	169	16.0	Upland	Granodiorite	Burwash	4.30	32.18	2.67	12.05
16	62.614448	-114.136894	176	16.0	Upland	Granodiorite	Burwash	0.97	23.90	3.58	6.68
17	62.617269	-114.133060	176	16.4	Upland	Granodiorite	Burwash	3.50	136.62	2.98	45.85
18	62.615192	-114.122138	192	16.6	Upland	Granodiorite	Burwash	1.48	18.82	1.11	16.95
19	62.588500	-114.057050	173	17.3	Upland	Granodiorite	Burwash	1.10	41.69	8.52	4.89
20	62.564500	-114.013818	228	18.3	Upland	Granodiorite	Burwash	11.50	32.05	11.53	2.78
21	62.561215	-114.005324	227	18.5	Upland	Granodiorite	Burwash	2.10	40.44	17.83	2.27
22	62.558277	-113.986598	231	19.4	Upland	Granodiorite	Burwash	1.00	22.16	4.37	5.07
23	62.558581	-113.975771	234	19.9	Upland	Granodiorite	Burwash	1.05	29.67	5.55	5.35
24	62.482972	-114.734067	179	20.2	Lowland	Granodiorite	Defeat Suite	4.25	54.73	1.28	42.76
25	62.507736	-114.815690	179	24.2	Lowland	Granodiorite	Defeat Suite	1.20	19.66	3.50	5.62

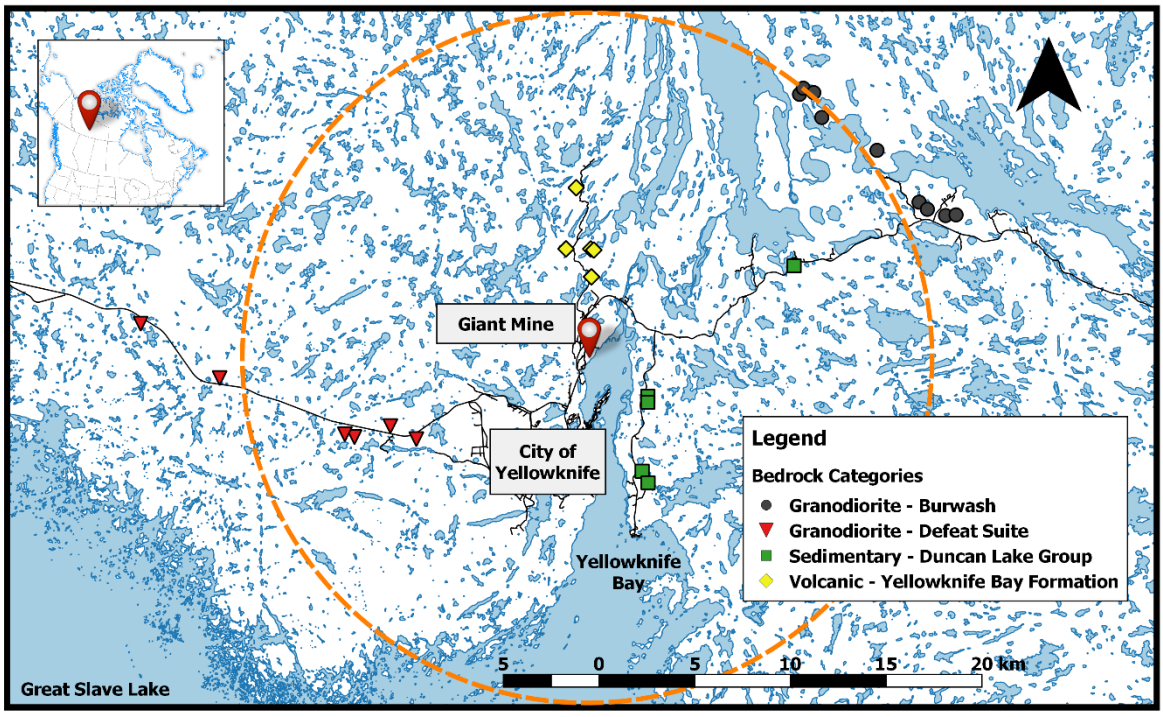

Figure 4.1: Location of 25 study lakes in the Yellowknife, NT, region categorized by underlying bedrock, centred on the Giant Mine roaster (red pin). The dashed ring indicates a 17 km radius from the roaster stack, a surface area of 921 km^2, demarcating the regressed distance from the roaster for lakes that are above the CWQG for protection of aquatic life from As, set at 5 µg/L (CCME 1997). Inset indicates the location of Yellowknife, Northwest Territories, Canada, along Yellowknife Bay of Great Slave Lake. Map produced in QGIS using Canvec+, NRCan.

4.3.2. Field Sampling

The 25 study lakes were selected for nearby road access while still being removed from any direct anthropogenic influence, such as roads bisecting catchments. Study locations did not require specific permission, while the overall research permit was approved by the Aurora Research Institute, Inuvik, NT; application number 1427. Surface water grab samples (0.5m) were collected July 21-28, 2010, from lake-centre by boat, using gloves; 10% of lake samples for all parameters were performed in triplicate for quality control. Prior to sampling, bottles (polyethylene) and caps were cleaned with dilute HCl (3-d soak), followed by triple rinsing with distilled deionized water, (10% HNO_3 was used for trace metal collection bottles). Bottles were triple rinsed with lake water

and filled to the rim to void the sample of air. Samples for trace metal (e.g. As, Sb) analyses were preserved with concentrated HNO_3 to 2% of sample volume (dissolved fractions preserved after filtration). Water samples were kept cool (4 °C) and in the dark until analysis. Field temperature and specific (@ 25 °C) conductivity (SpC) were determined with a YSI Model 85 multimeter.

4.3.3. Water Analyses

Trace metals (EPA Method 208-1) were analyzed at Taiga Environmental Laboratory, Yellowknife, NT, a Canadian Association for Laboratory Accreditation Inc. (CALA) institute. Analyses were also performed at Environment Canada's National Laboratory for Environmental Testing (NLET) (CALA accredited), Burlington, ON, using Environment Canada standard operating procedures (SOP): nitrogen (N) (SOP#1170) phosphorus (P) (SOP#1190); pH was determined with a Thermo Orion Model 106 meter; Chloride (Cl^-) and sulfate (SO_4^{2-}) major anions (SOP #1080); Calcium (Ca^{2+}), magnesium (Mg^{2+}), sodium (Na^+) and potassium (K^+) major cations (SOP #1061); Dissolved organic carbon (DOC) and dissolved inorganic carbon (DIC) (SOP #1021).

Mercury measurements were performed at the CALA accredited Laboratory for the Analysis of Natural and Synthetic Environmental Toxicants (LANSET), University of Ottawa. Total mercury (Hg_T) concentrations were determined by cold-vapour atomic fluorescence (CVAF) spectrometry (DL = 0.2 ng L^{-1}) as adapted to U.S. EPA Method 1631(E) using Tekran 2600 Analyzer manufacture suggestions, using fluorinated HDPE bottles (Fischer Scientific Cat. 03-312-15) sealed in plastic bags to prevent contamination (Avramescu et al., 2011; French et al., 2014) in lieu of glass. In brief, BrCl was added to samples to oxidize Hg to Hg^{2+} which was sequentially reduced with NH_2OH•HCl to destroy free halogens. Hg was then completely reduced to volatile Hg^0 with $SnCl_2$; Hg^0 was collected on a gold trap while purging the sample with N_2 and then transported, following thermal desorption, to a second gold trap from which Hg^0 was transported by an N_2 stream to the CVAF spectrophotometer (Tekran Instrument Corp., Series 2600). Two Initial Precision Recovery (IPR) samples along with both field and lab blanks were analyzed prior to field samples. Ongoing Precision Recovery (OPR) samples were then analyzed after every ten field samples. Recovery (IPR + OPR) was 98.28% ± 0.72% based on concurrent analyses of NIST-certified stock solutions, with a r^2=0.9996 for the calibration curve. Tekran 2600

analyzer (Tekran Inc.) detection limit was 0.1 ng/L. Instrument blanks averaged 0.01 ± 0.13 ng/L (1 standard deviation), while field blanks averaged 0.12 ± 0.17 ng/L.

$MeHg_T$ was determined by capillary gas chromatography-atomic fluorescence spectrometry (GC-AFS), as per Cai et al. (Cai et al., 1996). In brief, 1 L samples were passed through a sulfhydryl-cotton column. The column is then treated 6 times with a 1 mL mix of KBr/$CuSO_4$ 1 M (2:1). The solution was extracted with 150 µL of methylene chloride under agitation for 30 minutes, and then centrifuged at 5000 rpm for 10 minutes. Final $MeHg_T$ concentrations determined on an Ai Cambridge Model GC 94 Gas Chromatograph (800 °C pyrolysis) equipped with a CTC A200S Autosampler and PSA Merlin Detector. The detection limit of the method was calculated as three times the standard deviation of baseline noise, which was 0.2 pg/L. After every five analyses of MeHg in lake samples, a blank sample was analyzed followed by a MeHg standard (2 pg/L) analysis for control.

4.3.4. Statistical Treatment

Data were Ln-transformed prior to statistical analyses to meet assumptions of normality for parametric tests. A correlation matrix (Table 4.2) was created in order to determine key water chemistry parameters to test with the distance to the Giant Mine roaster stack. For the most affected and key chemical parameters, linear regression was then used to predict relevant distances to the roaster stack for toxicity thresholds. To test any confounding influence by the underlying bedrock, ANCOVA was used to compare lakes by bedrock, while controlling for distance to the roaster stack. Multiple linear regression using distance to the roaster stack and bedrock category as predictive variables was also used to test if either variable alone or in combination was the best predictor of analyte concentration in our study lakes. All statistical analyses were completed using SPSS 16.0 (2007).

Table 4.2: Pearson correlation coefficients for 25 study lakes, July 2010, located within a 25 km radius of the Giant Mine, Yellowknife, NT. Note, all variables were Ln-transformed. Bold type indicates $p < 0.05$

	D-Mine	CA:LA	Z_{max}	pH	TN	TP	SO_4	As_T	Sb_T	Al_T	Fe_T	Mn_T	Hg_T	MeHg	%MeHg
D-Mine	1	0.09	0.33	0.01	**-0.67**	**-0.62**	**-0.74**	**-0.77**	**-0.87**	0.36	0.06	-0.24	-0.19	**-0.52**	**-0.55**
CA:LA	0.09	1	0.16	**-0.48**	0.27	0.01	-0.27	-0.07	-0.05	**0.40**	**0.47**	-0.32	**0.42**	0.18	-0.08
Z_{max}	0.33	0.16	1	-0.22	**-0.53***	**-0.52***	-0.18	-0.31	-0.22	-0.02	-0.23	-0.26	-0.08	-0.26	-0.28
pH	0.01	**-0.48**	-0.22	1	-0.16	0.03	0.29	0.15	0.14	-0.34	**-0.71**	-0.01	-0.19	0.02	0.12
TN	**-0.67**	0.27	**-0.53***	-0.16	1	**0.65**	**0.43**	**0.53**	**0.62**	-0.06	0.33	0.28	**0.42**	**0.43**	0.33
TP	**-0.62**	0.01	**-0.52***	0.03	**0.65**	1	**0.45**	**0.76**	**0.68**	0.06	0.18	**0.47**	0.36	**0.59**	**0.43**
SO_4	**-0.74**	-0.27	-0.18	0.29	**0.43**	**0.45**	1	**0.57**	**0.71**	**-0.48**	**-0.42**	-0.01	0.00	0.33	**0.57**
As_T	**-0.77**	-0.07	-0.31	0.15	**0.53**	**0.76**	**0.57**	1	**0.93**	-0.29	-0.11	0.26	0.10	**0.50**	**0.44**
Sb_T	**-0.87**	-0.05	-0.22	0.14	**0.62**	**0.68**	**0.71**	**0.93**	1	-0.33	-0.14	0.16	0.17	**0.56**	**0.50**
Al_T	0.36	**0.40**	-0.02	-0.34	-0.06	0.06	**-0.48**	-0.29	-0.33	1	**0.47**	-0.02	0.52	-0.09	-0.42
Fe_T	0.06	**0.47**	-0.23	**-0.71**	0.33	0.18	**-0.42**	-0.11	-0.14	**0.47**	1	0.15	0.20	0.19	-0.07
Mn_T	-0.24	-0.32	-0.26	-0.01	0.28	**0.47**	-0.01	0.26	0.16	-0.02	0.15	1	0.02	0.02	-0.14
Hg_T	-0.19	**0.42**	-0.08	-0.19	**0.42**	0.36	0.00	0.10	0.17	0.52	0.20	0.02	1	0.38	-0.03
MeHg	**-0.52**	0.18	-0.26	0.02	**0.43**	**0.59**	0.33	0.50	**0.56**	-0.09	0.19	0.02	0.38	1	**0.74**
%MeHg	**-0.55**	-0.08	-0.28	0.12	0.33	**0.43**	**0.57**	0.44	**0.50**	-0.42	-0.07	-0.14	-0.03	**0.74**	1

* - significance due to one deep outlier lake; not significant once removed

4.4. Results

We found the highest As and MeHg concentrations in lake water in sites closest to the Giant Mine roaster stack, strongly suggesting the influence of atmospheric deposition from the roaster on surface waters. Log-transformed total As concentrations demonstrated a significant negative relationship with distance to the Giant Mine roaster stack (Fig 4.2). These ranged from 27–136 µg/L at small lakes less than 4 kmfrom the roaster stack to as low as 2.0 µg/L in lakes ranging 18–24 km from the roaster stack. When separated by underlying bedrock categories, average (standard deviation) AsT was 70.3 (48.9), 21.2 (17.4), 19.5 (19.5), and 3.1 (1.3), µg/L for YBF, western granodiorite sedimentary, and eastern granodiorite, respectively. Of these 25 study lakes, 16 were found to be above the 5 µg/L threshold for the protection of aquatic life (CCME 1997). Using the calculated regression, we estimate that within a radius of 17 km to the Giant Mine roaster stack, lakes are predicted to be above this 5 µg As/L threshold. Within this predicted 17 km radius "hot zone" from the Giant Mine roaster stack, only 5 lakes were below this threshold and were located as a cluster in the Burwash geological formation 16.0–16.6 km east of the roaster stack (Fig 4.1). Outside of this 17 km radius, several lakes found 20.2–24.2 km to the west of the roaster stack were above the threshold.

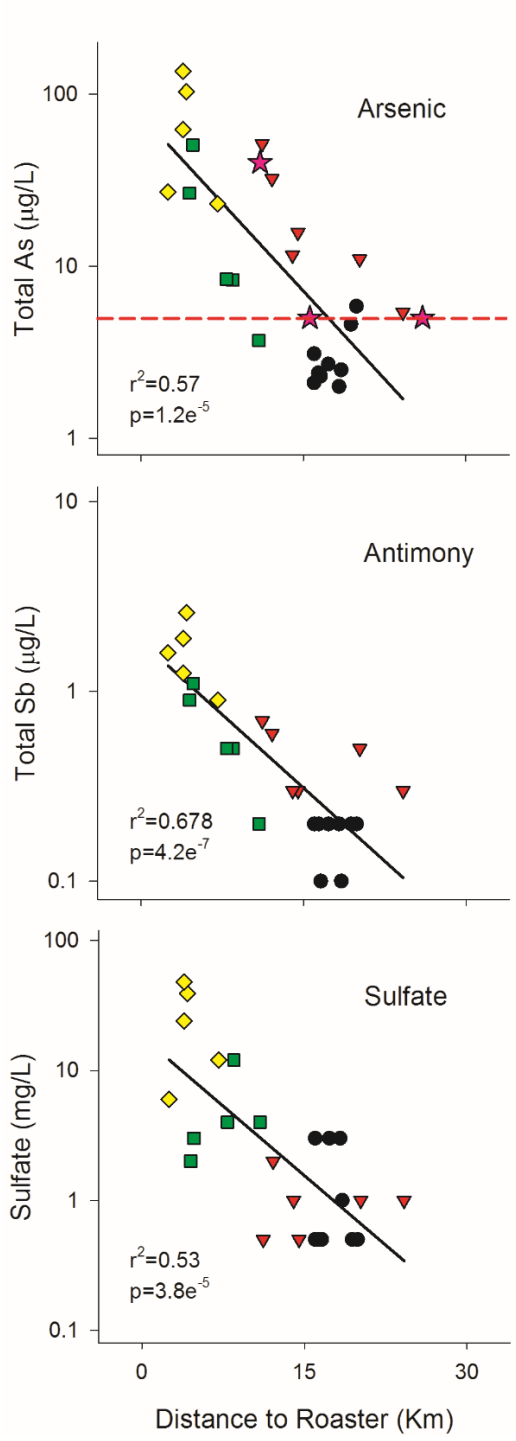

Figure 4.2: Ln-transformed lake water concentrations of total arsenic, total antimony, and sulfate in 25 lakes within the Yellowknife, NT, region. Lakes are plotted by underlying bedrock - Yellow diamond: Volcanic Yellowknife Bay Formation; green square: sedimentary Metaturbidites; red triangle: Granodiorite west; black circle: Granodiorite east; purple star: 3 undisturbed lakes from Wagemann et al 1978. The red dashed line indicates the 5 µg/L arsenic water quality guideline for the protection of aquatic life (CCME 1997), intersecting with the regression line at 17 km from the roaster.

Total antimony (Sb_T) concentrations ranged from 0.10-2.60 µg/L, with median of 0.30 µg/L, while sulfate was 0.50-48.00 µg/L, median of 2.00 µg/L. Both Sb_T and sulfate were negatively correlated to distance from the Giant Mine roaster stack (Fig 4.2), with lakes nearest to the stack having concentrations 10 times greater than the most distant lakes surveyed. Again, the lowest concentrations of both Sb_T and sulfate were measured in the most northeastern lakes located at distances greater than 16.0 km from the stack. Additionally, all three suspected mine-related water chemistry variables, (As, Sb, SO_4), were highly correlated to each other (Table 4.2), in particular As and Sb (r=0.93). To contrast, several metals (total Al, Fe, and Mn) had aquatic concentrations that were not significantly correlated with the distance to the roaster stack ($p>0.05$), while Al and Fe were both positively correlated to CA:LA ratios (Table 4.2). Although not reported in figures or summary table, Ca^{2+} ion concentrations were also found to be negatively correlated (r=-0.55, p=0.005) to the distance from the roaster stack.

Total mercury (Hg_T) concentrations ranged from 0.49 to 2.41 ng/L; methyl mercury (MeHg) concentrations from 0.01 to 0.55 ng/L; resulting in MeHg:Hg_T ratios ranging from 1% to 46%; median of 10%. Most natural lakes correspond to a less than 1% MeHg conversion ratio (Ullrich et al., 2001). Further, within a review of 6 studies surveying 74 lakes across Canada's Arctic, average %MeHg ranged from 2.9% to 8.0% (Chételat et al., 2014). Total Hg was unrelated to roaster stack distance (r=-0.19), but was positively correlated with catchment to lake area ratios (CA:LA) (r=0.42) and DOC (r=0.38) (Table 4.2). MeHg concentrations were indeed higher nearer to the roaster stack (Fig 4.3), though not correlated with CA:LA nor above the 4 ng MeHg/L guideline for the protection of aquatic life (CCME, 1987). The MeHg:Hg_T ratio was also negatively related to distance from the roaster stack (r=-0.55, Table 4.2; r^2=0.24, Fig 4.3) and though significant, some of the remaining variation may be due to seasonal and annual variation of complex whole lake systems. Further, the MeHg:Hg_T ratio was positively related to sulfate (r=0.57), though it was not correlated to DOC (r=0.06) or CA:LA (r=0.09) (Table 4.2).

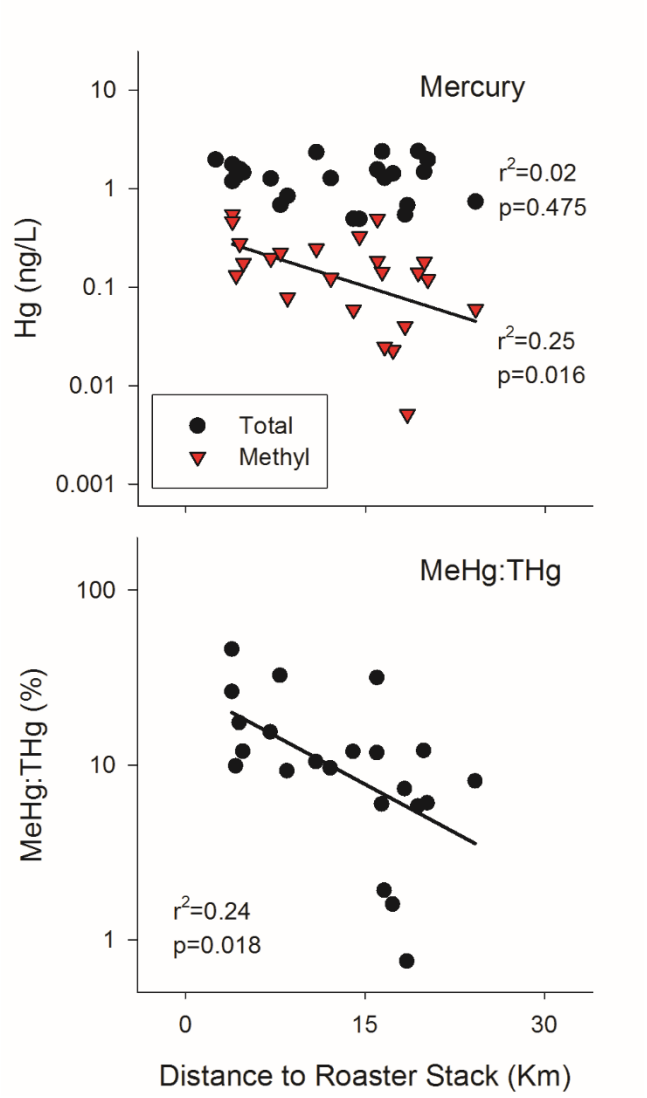

Figure 4.3: top: Ln-transformed lake water concentrations of total (black circle) and methyl mercury (red triangle); bottom: proportion of THg that is MeHg, in 25 lakes within the Yellowknife, NT, region.

Minimum concentrations for total phosphorus (TP), total dissolved (TDP), and soluble reactive (SRP) were 3.90, 2.00, and 0.20 µg/L, while maxima were 77.4, 74.9, and 69.1 µg/L, with regression coefficients of r^2=0.39, 0.51, and 0.57, respectively (Fig 4.4). Concentrations for total nitrogen (TN) ranged from 365-1870 µg/L and total Kjeldahl nitrogen (TKN) from 347-2410 µg/L, with r^2=0.45 and 0.22, respectively (Fig 4.4). The proportion of TDP and SRP was inversely related to distance from Giant Mine, ranging from over 90% for both TDP and SRP in our nearest lakes less than 4 km from the roaster stack; to as low as 6% TDP and 5% SRP at our distant lakes

more than 20 km from the stack. To note, N and P measurements were also inversely correlated to lake depth (Table 4.2), however this is likely due to one lake (lake 20) being nearly three-fold deeper than the next deepest lake in our study, and once lake 20 was removed any relationship between depth and total N and total P was not significant, except SRP. SRP was still found to have a significant inverse relationship with lake depth with or without lake 20 included. No other water chemistry variables, including As and MeHg, were observed to correlate with lake depth. Additionally, percent dissolved oxygen ranged from 47% to 135% (median of 94%, SD = 19%).

Controlling for distance to the roaster stack using ANCOVA, resulted in significant differences between underlying bedrock categories for each of As, Sb, and SO_4 (S1 Table). However, the estimated marginal means, (the adjusted means after controlling for the covariate of distance), indicated that the western granodiorite lakes had the highest As concentrations, more than doubling the volcanic Yellowknife Bay Formation that contains arsenopyrite. For Sb, both the Yellowknife Bay Formation and western granodiorite categories were similar, having the highest estimated marginal mean concentrations. For sulfate, estimated marginal means suggested that the Yellowknife Bay Formation had by far the highest concentrations once distance was considered. Methyl Hg ANCOVA results demonstrated no significant relationship to bedrock categories, regardless of controlling for distance to the roaster stack (S1 Table).

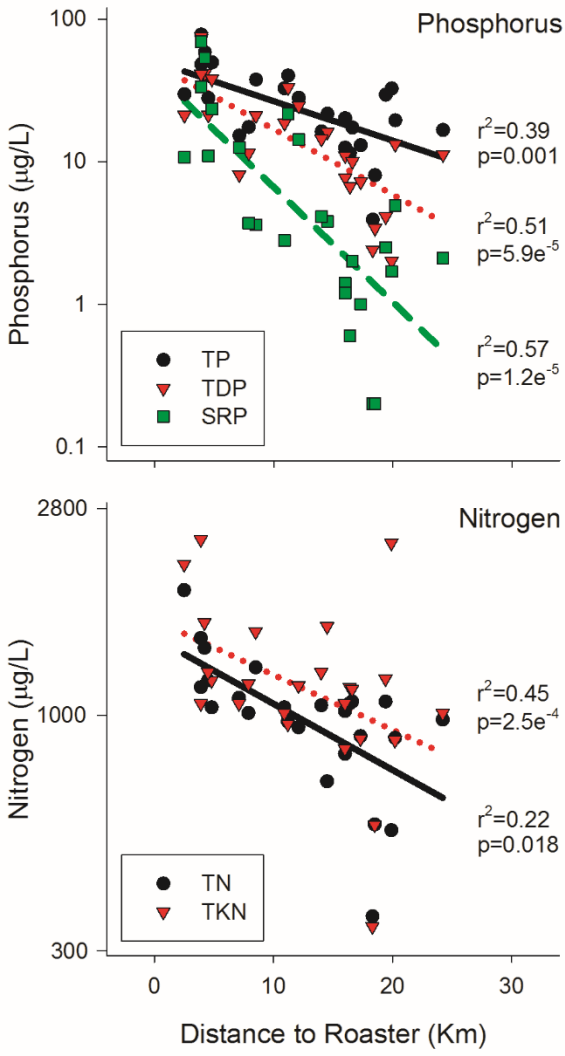

Figure 4.4: Aquatic phosphorus and nitrogen concentrations in study lakes as relating to distance to the Giant Mine roaster stack. n=25. Total (TP), total dissolved (TDP), and soluble reactive (SRP) phosphorus, as well as total (TN), total Kjedhal (TKN) nitrogen concentrations were measured.

Using both distance to the roaster stack and bedrock category as predictive variables in backward stepwise multiple linear regression, we observed a variable response from our dependent variables (As, Sb, SO_4, and MeHg) to either predictor (S2 Table). Both As and Sb suggested that both distance and bedrock together produced the strongest models (adjusted r^2=0.69 and 0.76, $p<0.001$, respectively), though both models indicate that distance was the greater contributor via p-partial statistics. For sulfate, bedrock category was a marginally stronger predictor alone (adjusted r^2=0.65, $p<0.001$) than it was when paired with distance (adjusted r^2=0.65 $p<0.001$).

Methyl Hg was most strongly predicted by distance alone (adjusted r^2=0.27, $p<0.001$) over any model that also included bedrock category, whereas Hg_T demonstrated no significant relationship to either distance to roaster stack or underlying bedrock. The regression coefficient may also be affected by seasonal and inter-annual variation within each catchment.

4.5. Discussion

Our analysis shows a clear point source distribution of arsenic in surface waters surrounding the gold mines near Yellowknife, NT, and that the concentrations of arsenic are well above drinking water quality guidelines (10 µg/L) and protection for aquatic life (5 µg/L) for lakes within 17 km of the Giant Mine roaster stack (Fig 4.2). This relationship is not surprising when considering that approximately two thirds of baghouse dust from the roaster stack is composed of As_2O_3 (Clark and Raven, 2004). Antimony was also highly correlated with arsenic (r = 0.93, Table 5.2) and was also shown to be the third largest oxide concentration in the baghouse dust collections. Similar trends for both antimony and sulfur radiating from the roaster stack were also observed (Fig 4.2), indicating a depositional influence for these two elements on our lakes for at least the 25 km limit of our study set. As well, MeHg concentrations are higher nearer to the roaster stack (Fig 4.3) and MeHg/Hg_T ratios are exceptionally higher when contrasting with typical natural waters; neither have been reported in any prior analyses of Giant Mine pollution.

We demonstrate statistically that the relationship of aquatic As concentrations to the roaster stack is unlikely related to any influence from the underlying volcanic arsenopyrite-rich YBF bedrock, from which the gold is mined. ANCOVA analysis using distance to roaster stack as a covariate showed that the volcanic YBF bedrock is not associated with the highest aquatic As concentrations (S1 Table). Further, the western Granodiorite lakes demonstrated the highest estimated marginal means, even though they are 11-24 km West of the roaster stack, and not the lakes with catchments underlain by the arsenopyrite-rich volcanic rocks. The importance of distance to the stack was also reflected in the stepwise multiple regression as both bedrock category and distance to roaster stack are included in the optimal model (S2 Table). Though the YBF lakes have the highest average As_T concentrations as a bedrock category, the more distant western Granodiorite lakes likely demonstrate the highest estimated marginal means for As_T concentrations in our ANCOVA due to downwind effects from the predominantly easterly winds in the region

(Bromstad and Jamieson, 2011; Indian and Northern Affairs Canada and Government of the Northwest Territories, 2010; St-Onge, 2007), as opposed to underlying geology.

ANCOVA results for MeHg showed that bedrock category had no significant influence on MeHg concentrations (S1 Table), which was also reflected in multiple regression results where only distance to the mine was selected as the stronger model (S2 Table). Sulfate concentrations in lake water decreased significantly with distance to the roaster stack (Fig 4.2), however, both ANCOVA and multiple regression results suggested a potential bedrock source relating to the YBF. However, it is difficult to delineate if this is related to underlying bedrock influences or to more rapid atmospheric fall-out once emitted from the stack.

It is noteworthy that both Fe and Al total metal concentrations were not related to distance from the roaster stack (Table 4.2), as they are the second and fourth most dominant oxides in baghouse dust collections, respectively (Clark and Raven, 2004). Sb was the third most abundant oxide in the baghouse collections and was significantly correlated to distance to roaster stack. All three of these metal oxides (Fe_3O_3, SbO, Al_2O_3) were less than 1.6% of the baghouse dust concentrations, while As_2O_3 was approximately 65%. This highlights that the Sb signal was observed due to its relatively low environmental background abundance, while any Al and Fe deposition was negligible to environmental background concentrations. Also, using environmentally abundant metals that were not present in baghouse dust collections (e.g. Mn), we further demonstrate that no discernible regional patterns are potentially responsible for any similar trends that were observed for our metals of concern: As, Sb, Hg. In several other studies, for comparison, atmospheric deposition of mining-related metals (e.g. Cu and Ni) into nearby lakes were measured 50 km downwind prior to emissions reductions, and still 20-30 km from smelters post-reductions (Keller et al., 2004).

Arsenic speciation is of concern as this will ultimately determine bioavailability and the degree of toxicity to organisms. Within our study lakes, arsenic speciation is expected to be predominantly in the oxidized inorganic As(V) form as gaseous and particulate As_2O_3 is emitted from the roaster stack (Clark and Raven, 2004). The atmospheric residence time is expected to be relatively short, depositing on the landscape as condensate (Hocking et al., 1978). Due to these lakes also being relatively shallow and oxygen-rich (average max depth of 2.1 m, median DO of 91%), the As(V) will likely remain as the dominant inorganic arsenic ion in surface waters. However, phytoplankton activity may also drive toxic As speciation depending on nutrient

concentrations. Using phosphorus as an index of trophic status, our study lakes range from oligotrophic to highly eutrophic (Fig 4.4), and suggest that greater proportions of As(V) may be reduced by phytoplankton to the more toxic As(III) in higher phosphorus lakes (Hellweger et al., 2003; Hellweger and Lall, 2004; Rahman et al., 2012). Further investigation into the As speciation and bioaccumulation in biota is required to resolve the potentially compounded toxic effects in eutrophic lakes closer to the roaster stack.

Waste ponds on the Giant Mine site have measured total As concentrations up to 8 mg/L in tailings ponds and surface waters to over 4000 mg/L in underground mine seepages (Clark and Raven, 2004), however few studies have looked beyond the mine's boundaries for surface water pollution. Wagemann et al (Wagemann et al., 1978) looked at 5 larger lakes in 1972-75, finding two of the lakes 10 and 12 km south of the Giant Mine roaster stack with elevated As concentrations between 0.7-5.5 mg/L. These two lakes were located immediately adjacent to the Con. Mine at the south of Yellowknife receiving both sewage waters and As-containing seepages from Pud Lake; a tailings pond. A third lake 10 km from Giant Mine and 4 km from Con. Mine was not directly connected to Con. Mine, which had just recently ceased roasting operations in 1971, and had much lower As concentrations of 0.01-0.07 mg/L. The remaining two undisturbed lakes were more distant, 16 and 26 km northeast of the Giant Mine roaster stack, and were both <0.01 mg/L. Excluding the directly disturbed tailings pond-contaminated lakes, the results for the three undisturbed lakes from the early 1970s fit within the 95% prediction interval of our current As model (Fig 4.2), indicating the lasting legacy effects of the Giant Mine roaster stack emissions on local lake systems over 10 years after mining activity has ceased, or much longer if considering the effectiveness of scrubbers and precipitators installed between 1949-1955.

Greater MeHg concentrations in lakes nearer to the roaster stack may be an indirect response to the significant increase in sulfate emissions and subsequent deposition into the nearby catchments from roaster emissions. In our study lakes, the range of $\%Hg_T$ as MeHg is 1-46%, with a median of 10%, which is notably higher than the expected 1% MeHg in most natural lakes (Ullrich et al., 2001) or even the 2.9% to 8.0% MeHg range observed in several more geographically relevant Arctic studies in Canada (Chételat et al., 2014). To contrast, within a site along the St. Lawrence River, near a pulp mill in Cornwall, Ontario, direct inputs of Hg pollution led to %MeHg in sediment pore water as high as 64% (Canario et al., 2007). As indicated by our Hg_T relationship with CA:LA (Table 4.2), overland catchment run-off of Hg can be responsible

for up to 94% of total Hg inputs to adjacent wetlands and lakes (O'Driscoll et al., 2005; Semkin et al., 2005), and due to the strong affinity of Hg to sulfhydryl groups on DOC (Barkay et al., 1997) it is not surprising to see a similar correlation. However, the increase in %MeHg may be due to enhanced MeHg production within catchments nearer to the roaster stack (Fig 4.3). Hg emissions from gold mining activities are well known (Engstrom et al., 2014), however due to the very long atmospheric residence time (0.5-1.0 years) of Hg it is not surprising that a point-source influence of Hg_T is not observed within our 25 km radius from the roaster stack. This result suggests that within-catchment processing of available Hg to MeHg may be elevated in lakes nearer to the roaster stack and the significant correlation between sulfate and %MeHg (Table 4.2) may corroborate this process.

Sulfur is likely emitted from the roaster stack as SO_2, before being converted to sulfuric acid within the atmosphere and lake waters. This increase in atmospheric sulfate loading may ultimately lead to enhanced Hg methylation by sulfate reducing bacteria (Compeau and Bartha, 1985; Gilmour et al., 1992). Further, our maximum sulfate concentration is 48 mg/L, thus below a generally accepted threshold of 50 mg/L where sulfate can begin limiting Hg methylation (Gilmour et al., 1992). Also, it is not uncommon for sulfate and MeHg concentrations to be uncorrelated during high methylation periods, as sulfate is being consumed during the process. We also note that experiments by Dageune et al (Daguené et al., 2012) demonstrated that greater base cation concentrations, in particular Ca^{2+} and Mg^{2+}, inhibit Hg(II) uptake and subsequent methylation. In our study we observed significantly higher Ca^{2+} concentrations nearer to the roaster stack, which would suggest greater cation inhibition of Hg(II) and thus lower MeHg concentrations, however we observed greater MeHg, further pointing to sulfate as an influence on MeHg formation.

These increases in both As compounds and organic methyl Hg in surface waters due to direct and indirect influences from Giant Mine emissions are cause for concern of bioaccumulation in aquatic food-webs. Additionally, due to the ephemeral drainage of many of these small lakes, it is possible that transfer of materials from the affected catchments could continue for several years after the mine ceased roaster stack operations. Our results and the related hydrology imply that these lakes are sinks, not only for water but also for materials deposited on the catchments, suggesting greater implications for aquatic ecosystems. Considering that roaster stack emission-controls were installed at Giant Mine before 1960, the legacy contamination we measured 55 years later demonstrates a high persistence of arsenic and other stack emission products in these lakes.

Drinking water for the town of Yellowknife is sourced from the Yellowknife River, less than 5 km from the roaster stack. However, as the relationship between contaminants and distance declines exponentially from the mine, concentrations for both contaminants of concern are likely lower in the river due to its large watershed of over 10,000 km^2, and have been monitored by the City of Yellowknife. To contrast, however, there are still numerous small lakes even closer to the mine than our survey sampled for, with likely equal or higher concentrations of As. The elevated total As and MeHg concentrations in lake waters within approximately 20 km of the Giant Mine roaster stack, will potentially be of concern for enhanced bioaccumulation of these persistent pollutants in aquatic food webs.

4.6. Acknowledgements

Additional support for this study was thanks to the Cumulative Impact Monitoring Program through Environment and Natural Resources, Government of Northwest Territories, (formerly through Indigenous and Northern Affairs Canada), and the NSERC Northern Research Internship program.

4.7. References

Andrade CF, Jamieson HE, Kyser TK, Praharaj T and Fortin D (2010) Biogeochemical redox cycling of arsenic in mine-impacted lake sediments and co-existing pore waters near Giant Mine, Yellowknife Bay, Canada. *Applied Geochemistry*. 25(2): 199–211. doi:10.1016/j.apgeochem.2009.11.005.

Avramescu M-L, Yumvihoze E, Hintelmann H, Ridal J, Fortin D and Lean DRS (2011) Biogeochemical factors influencing net mercury methylation in contaminated freshwater sediments from the St. Lawrence River in Cornwall, Ontario, Canada. *Science of the Total Environment*. 409(5): 968–78. doi:10.1016/j.scitotenv.2010.11.016.

Barkay T, Gillman M and Turner RR (1997) Effects of dissolved organic carbon and salinity on bioavailability of mercury. *Applied and Environmental Microbiology* 63(11): 4267–71.

Bromstad M and Jamieson HE (2011) Giant Mine, Yellowknife, Canada: Arsenite waste as the legacy of gold mining and processing. In: Santini JA and Ward SA (eds) *The Metabolism of Arsenite*. CRC Press, 25–42.

Cai Y, Jaffe R, Alli A and Jones RD (1996) Determination of organomercury compounds in aqueous samples by capillary gas chromatography-atomic fluorescence spectrometry following solid-phase extraction. *Analytica Chimica Acta* 334(3): 251–259. doi:10.1016/S0003-2670(96)00309-1.

Canario J, Poissant L, O'Driscoll NJ, Ridal J, Delongchamp TM, Pilote M, et al. (2007) Mercury partitioning in surface sediments of the Upper St. Lawrence River (Canada): evidence of the importance of the sulphur chemistry. *Water, Air, and Soil Pollution* 187(1-4): 219–231. doi:10.1007/s11270-007-9510-1.

Chételat J, Amyot M, Arp P, Blais JM, Depew D, Emmerton CA, et al. (2014) Mercury in freshwater ecosystems of the Canadian Arctic: Recent advances on its cycling and fate. *Science of the Total Environment*. Elsevier B.V. 509-510: 41–66. doi:10.1016/j.scitotenv.2014.05.151.

Clark ID and Raven KG (2004) Sources and circulation of water and arsenic in the Giant Mine, Yellowknife, NWT, Canada. *Isotopes in Environmental and Health Studies* 40(2): 115–28. doi:10.1080/10256010410001671014.

Coleman LC (1957) Mineralogy of the Giant Yellowknife gold mine, Yellowknife, NWT. *Economic Geology* 52(4): 400–425.

Compeau GC and Bartha R (1985) Sulfate-reducing bacteria: principal methylators of mercury in anoxic estuarine sediment. *Applied and Environmental Microbiology* 50(2): 498–502.

Daguené V, McFall E, Yumvihoze E, Xiang S, Amyot M and Poulain AJ (2012) Divalent base cations hamper Hg II uptake. *Environmental Science and Technology* 46(12): 6645–6653: doi:10.1021/es300760e.

Ecosystem Classification Group (2008) *Ecological Regions of the Northwest Territories - Taiga Shield.* Yellowknife, NT, Canada.

Engstrom DR, Fitzgerald WF, Cooke CA, Lamborg CH, Drevnick PE, Swain EB, et al. (2014) Atmospheric Hg emissions from preindustrial gold and silver extraction in the Americas: a reevaluation from lake-sediment archives. *Environmental Science and Technology* 48(12): 6533–43. doi:10.1021/es405558e.

French TD, Houben AJ, Desforges J-PW, Kimpe LE, Kokelj S V, Poulain AJ, et al. (2014) Dissolved organic carbon thresholds affect mercury bioaccumulation in Arctic lakes. *Environmental Science and Technology* 48: 3162–3168. doi:10.1021/es403849d.

Galloway JM, Palmer M, Jamieson HE, Patterson RT, Nasser N, Falck H, et al. (2015) *Geochemistry of lakes across ecozones in the Northwest Territories and implications for the distribution of arsenic in the Yellowknife region. Part 1: Sediments*. doi:10.4095/296954.

Gilmour CC, Henry EA and Mitchell R (1992) Sulfate stimulation of mercury methylation in freshwater sediments. *Environmental Science and Technology* 26(11): 2281–2287.

Hellweger FL, Farley KJ, Lall U and Di Toro DM (2003) Greedy algae reduce arsenate. *Limnology and Oceanography* 48(6): 2275–2288.

Hellweger FL and Lall U (2004) Modeling the effect of algal dynamics on arsenic speciation in Lake Biwa. *Environmental Science and Technology* 38(24): 6716–6723.

Hocking D, Kuchar P, Plambeck JA and Smith RA (1978) The impact of gold smelter emissions on vegetation and soils of a sub-Arctic forest-tundra transition ecosystem. *Journal of the Air Pollution Control Association* 28(2): 133–137. doi:10.1080/00022470.1978.10470580.

Hutchinson TC, Aufreiter S and Hancock RG V (1982) Arsenic pollution in the Yellowknife area from gold smelter activities. *Journal of Radioanalytical Chemistry* 71(1-2): 59–73. doi:10.1007/BF02516141.

Indian and Northern Affairs Canada, Government of the Northwest Territories (2010) Giant Mine remediation project: developer's assessment report. Environmental Assessment EA0809-001.

Isachsen CE and Bowring SA (1997) The Bell Lake group and Anton Complex: a basement-cover sequence beneath the Archean Yellowknife greenstone belt revealed and implicated in greenstone belt formation. *Canadian Journal of Earth Sciences* 34: 169–189.

Jeremiason JD, Engstrom DR, Swain EB, Nater EA, Johnson BM, Almendinger JE, et al. (2006) Sulfate addition increases methylmercury production in an experimental wetland. *Environmental Science and Technology* 40(12): 3800–6.

Keller W, Heneberry J, Gunn JM, Snucins E, Morgan G and Leduc J (2004) *Recovery of acid and metal-damaged lakes near Sudbury, Ontario: trends and status*. Cooperative Freshwater Ecology Unit, Department of Biology, Laurentian University, Sudbury, Ontario.

Kerr DE and Wilson P (2000) Preliminary surficial geology studies and mineral exploration considerations in the Yellowknife area, Northwest Territories. *Geological Survey of Canada* C3: 1–8.

Koch I, Mace J V and Reimer KJ (2005) Arsenic speciation in terrestrial birds from Yellowknife, Northwest Territories, Canada: the unexpected finding of arsenobetaine. *Environmental Toxicology and Chemistry* 24(6): 1468–1474: doi:10.1897/04-155R.1.

Koch I, Wang L, Ollson C a., Cullen WR and Reimer KJ (2000a) The predominance of inorganic arsenic species in plants from Yellowknife, Northwest Territories, Canada. *Environmental Science & Technology* 34(1): 22–26. doi:10.1021/es9906756.

Koch I, Wang L, Reimer KJ and Cullen WR (2000b) Arsenic species in terrestrial fungi and lichens from Yellowknife, NWT, Canada. *Applied Organometallic Chemistry* 14(5): 245–252. doi:10.1002/(SICI)1099-0739(200005)14:5<245::AID-AOC986>3.0.CO;2-K.

Lloyd JR and Oremland RS (2006) Microbial transformations of arsenic in the environment: from soda lakes to aquifers. *Elements* 2: 85–90.

Ng JC (2005) Environmental contamination of arsenic and its toxicological impact on humans. *Environmental Chemistry* 2: 146–60.

O'Driscoll NJ, Rencz A and Lean DRS (2005) The biogeochemistry and fate of mercury in the environment. *In:* Sigel A, Sigel H and Sigel RKO (eds) *Metal Ions in Biological Systems,*

Volume 43 - Biogeochemical Cycles of Elements. CRC Press, 221–38. doi:doi:10.1201/9780824751999.ch9.

Raab A, Wright SH, Jaspars M, Meharg AA and Feldmann J (2007) Pentavalent arsenic can bind to biomolecules. *Angewandte Chemie - International Edition* 46(15): 2594–2597: doi:10.1002/anie.200604805.

Rahman MA, Hasegawa H and Lim RP (2012) Bioaccumulation, biotransformation, and trophic transfer of arsenic in the aquatic food chain. *Environmental Research* 116: 118–135. doi:10.1016/j.envres.2012.03.014.

Semkin RG, Mierle G and Neureuther RJ (2005) Hydrochemistry and mercury cycling in a High Arctic watershed. *Science of the Total Environment* 342(1-3): 199–221. doi:10.1016/j.scitotenv.2004.12.047.

Sharma VK and Sohn M (2009) Aquatic arsenic: toxicity, speciation, transformations, and remediation. *Environment International* 35(4): 743–59. doi:10.1016/j.envint.2009.01.005.

Smith AH, Hopenhayn-Rich C, Bates MN, Goeden HM, Hertz-Picciotto I, Duggan HM, et al. (1992) Cancer risks from arsenic in drinking water. *Environmental Health Perspectives* 97: 259–267.

St-Onge SM (2007) Impacts of arsenic and sulphur dioxide contamination from mining activities on forest health near Yellowknife, NWT. MSc Thesis, Carleton University, Ottawa, Canada.

Ullrich S, Tanton T and Abdrashitova S (2001) Mercury in the aquatic environment: a review of factors affecting methylation. *Critical Reviews in Environmental Science and Technology* 31(3): 241–293. doi:10.1080/20016491089226.

Wagemann R, Snow NB, Rosenberg DM and Lutz A (1978) Arsenic in sediments, water and aquatic biota from lakes in the vicinity of Yellowknife, Northwest Territories, Canada. *Archives of Environmental Contamination and Toxicology* 7(2): 169–91.

Walker SR, Jamieson HE, Lanzirotti A, Andrade CF and Hall GEM (2005) The speciation of arsenic in iron oxides in mine wastes from the Giant Gold Mine, N.W.T.: application of synchrotron micro-XRD and micro-Xanes at the grain scale. *The Canadian Mineralogist* 43(4): 1205–1224. doi:10.2113/gscanmin.43.4.1205.

4.8. Supporting Information

Table 4.S1: ANCOVA results for select water chemistry variables in Yellowknife lakes contrasting bedrock categories with distance to roaster stack as covariant. Bolded p-values indicate significant p<0.01. Bedrock categories: YBF=Yellowknife Bay Formation; SED=sedimentary metaturbidite; Gran=granodiorite east (E) and west (W)

Dependent Variable	Bedrock summary statistics		Estimated marginal mean concentration, calculated at distance = 2.4 km, grouped by bedrock category				
	F	p	YBF	SED	GranE	GranW	Units
As	9.39	$4.4x10^{-4}$	12.18	6.55	6.49	29.67	µg/L
Sb	6.92	$2.2x10^{-3}$	0.63	0.37	0.28	0.61	µg/L
SO4	6.06	$4.2x10^{-3}$	34.22	5.20	0.74	0.72	mg/L
MeHg	0.19	$9.0x10^{-1}$	0.15	0.13	0.10	0.16	ng/L
THg	0.46	$4.6x10^{-1}$	1.25	1.17	1.47	0.97	ng/L

Table 4.S2: Multiple linear regression results of several metals in lake water from the Giant Mine, Yellowknife, NT, region, and the independent variables Bedrock Category and Distance to Roaster Stack (Ln transformed).

Dependent Variable	Adj. r^2	SE_{EST}	F	p	Predictor variables	Coefficient ± SE	$p_{(partial)}$
Ln As	0.69	0.74	27.4	$1.1x10^{-6}$[a]	Distance	-2.6 ± 0.4	$2.4x10^{-6}$[a]
					Bedrock	0.7 ± 0.2	$6.6x10^{-3}$[a]
					Constant	6.4 ± 0.6	$1.6x10^{-10}$[a]
Ln Sb	0.76	0.44	39.9	$4.8x10^{-8}$[a]	Distance	-1.6 ± 0.2	$1.7x10^{-6}$[a]
					Bedrock	0.3 ± 0.1	$8.2x10^{-2}$
					Constant	2.1 ± 0.3	$3.7x10^{-6}$[a]
Ln SO_4^{2-}	0.65	0.85	45.5	$7.0x10^{-7}$[a]	Distance	-[b]	-[b]
					Bedrock	-1.1 ± 0.2	$7.0x10^{-7}$[a]
					Constant	3.7 ± 0.5	$3.3x10^{-8}$[a]
Ln MeHg	0.27	0.94	10.0	$4.3x10^{-3}$[a]	Distance	-0.9 ± 0.3	$4.3x10^{-3}$[a]
					Bedrock	-[b]	-[b]
					Constant	0.1 ± 0.7	$8.4x10^{-1}$
Ln THg	0.00	0.48	-	-	Distance	-[b]	-[b]
					Bedrock	-[b]	-[b]
					Constant	0.2 ± 0.1	$4.2x10^{-2}$[a]

[a] statistically significant ($p<0.05$)
[b] removed in stepwise regression

Table 4.S3: Key water chemistry measurements for 25 small lakes within 25 km of the Giant Mine roaster stack, Yellowknife, NT, sampled July 21-28, 2010. Unless specified, concentrations are for total analyte analysis. (SpC: specific conductivity)

Lake	pH	DIC	DOC	N	P	SpC	SO4	Ca	Al	As	Fe	Li	Mn	Sb	Sr	U	Total Hg	Methyl Hg
#	-	mg/L	mg/L	µg/L	µg/L	µS/cm	mg/L	mg/L	µg/L	µg/L	µg/L	µg/L	µg/L	µg/L	µg/L	µg/L	ng/L	ng/L
1	7.25	14.9	29.8	1870	29.6	137	6.0	24.4	24.0	26.9	338.0	3.5	37.6	1.6	50.4	0.1	1.98	
2	8.51	31.0	25.2	1470	77.4	376	48.0	45.8	16.0	136.0	20.0	9.6	7.6	1.9	162.0	0.6	1.20	0.55
3	7.51	35.4	23.2	1150	47.9	343	24.0	47.9	6.0	62.4	46.0	6.8	16.1	1.3	118.0	0.3	1.77	0.47
4	8.85	18.8	25.2	1400	58.2	265	39.0	30.1	28.0	103.0	22.0	3.8	82.7	2.6	136.0	0.2	1.33	0.13
5	7.36	9.9	33.4	1190	27.8	105	2.0	11.2	39.0	26.6	574.0	5.1	12.9	0.9	50.2	0.1	1.59	0.28
6	6.87	7.1	30.4	1040	49.5	75	3.0	7.7	159.0	50.7	594.0	3.8	29.7	1.1	32.0	0.1	1.47	0.18
7	8.54	19.4	22.0	1090	15.2	192	12.0	33.0	6.0	23.1	10.0	1.6	9.5	0.9	36.4	0.1	1.27	0.20
8	8.00	16.8	27.8	1010	17.4	195	4.0	17.2	8.0	8.4	311.0	7.4	15.0	0.5	86.0	0.1	0.69	0.22
9	7.45	18.4	33.5	1270	37.5	205	12.0	20.4	14.0	8.3	192.0	11.5	33.1	0.5	81.6	0.1	0.85	0.08
10	8.01	5.1	30.6	1040	32.6	73	4.0	6.5	169.0	3.7	550.0	4.8	12.3	0.2	27.7	0.2	2.35	0.25
11	7.29	4.5	34.8	969	40.0	62	0.5	6.9	35.0	51.4	308.0	4.2	38.3	0.7	22.2	0.1		
12	7.41	5.9	29.9	941	28.0	71	2.0	8.5	97.0	32.3	287.0	3.6	13.3	0.6	32.7	0.1	1.28	0.12
13	7.67	16.7	25.8	1050	16.2	259	1.0	22.7	19.0	11.6	361.0	4.5	31.6	0.3	80.3	0.1	0.49	0.06
14	8.08	21.8	30.0	718	21.6	298	0.5	23.9	10.0	15.7	301.0	7.3	33.4	0.3	100.0	0.1	0.49	0.33
15	7.56	8.0	31.4	1020	12.5	87	0.5	9.9	88.0	3.1	308.0	5.4	7.8	0.2	46.5	1.2	1.57	0.19
16	7.04	12.4	22.8	824	20.1	131	3.0	13.8	52.0	2.1	374.0	5.5	16.0	0.2	71.8	0.8	1.56	0.49
17	7.64	7.4	31.2	1060	11.4	82	0.5	9.2	60.0	2.4	150.0	5.9	7.3	0.2	38.7	1.2	2.39	0.14
18	6.41	6.2	31.2	1070	17.3	71	0.5	7.1	99.0	2.3	793.0	4.6	31.5	0.1	33.1	0.2	1.29	0.02
19	7.90	8.5	23.0	900	13.0	91	3.0	10.0	38.0	2.7	153.0	7.6	11.0	0.2	47.2	1.7	1.43	0.02
20	7.94	6.6	8.6	365	3.9	67	3.0	9.0	20.0	2.0	8.0	5.5	5.4	0.2	18.8	1.2	0.55	0.04
21	8.23	7.8	12.6	578	8.0	176	1.0	10.1	20.0	2.5	13.0	5.7	17.0	0.1	20.5	0.5	0.68	0.01
22	8.14	7.0	31.6	1070	29.4	95	0.5	14.7	85.0	4.6	99.0	5.1	78.4	0.2	26.3	0.9	2.41	0.14
23	8.61	3.0	45.2	562	32.5	61	0.5	9.2	87.0	5.9	47.5	4.4	28.2	0.2	16.7	0.9	1.49	0.18
24	7.61	5.8	29.5	892	19.4	66	1.0	6.5	112.0	11.0	222.0	2.4	3.7	0.5	22.4	0.1	1.98	0.12
25	7.80	19.7	28.0	978	16.6	248	1.0	19.1	39.0	5.4	281.0	7.7	9.1	0.3	103.0	0.2	0.74	0.06

5. General Discussion

5.1. Summary

Objective 1. To identify basic limnological responses to shoreline retrogressive thaw slump events in a tundra highland landscape in Canada's western Arctic continuous permafrost zone, and to estimate this response relative to other Arctic and non-Arctic studies in the context of primary production.

This research demonstrates that across our relatively homogenous tundra upland landscape underlain with glaciolacustrine till, shoreline retrogressive thaw slump events were the principal factor in dramatically altering the physico-chemical regime of affected lakes. As demonstrated in prior studies (Kokelj et al., 2005) major ions, pH, and water clarity were greatly increased while organic carbon and particulates were found to be much lower in slump-affected lakes compared to reference lakes. By extending this analysis across a gradient of slump disturbance (measured as the percent of catchment area disturbed by thaw slumping), ranging from 0-34% of catchment area, we were able to demonstrate several significant relationships between limnological variables and the scale of the thaw slump disturbance. Shoreline thaw slumps were the dominant factor in controlling key nutrients (e.g. N & P), and in turn biomass (as measured by phytoplankton and periphyton Chl-*a* concentrations). Using regression analysis, we estimated that Chl-*a* concentrations may be up to two-thirds lower in our most affected lakes, i.e in lakes with 34% of their catchment disturbed by thaw slumping.

After establishing the extent of change and which key nutrients were driving primary production in our lakes, we contrasted these results to several other studies across the Canadian Arctic, as well as alpine and temperate studies to estimate how great an influence thaw slumps were on reducing primary production. When compared to other low Arctic studies, it was demonstrated through an ANCOVA where P was used a covariate, our active thaw slump lakes were significantly lower in Chl-*a* concentrations than other landscape categories. Notably, the observations measured within our slump-affected lakes are in stark contrast to other studies that often report lakes exposed to thawing permafrost having experienced elevated organic material and nutrients.

Objective 2. To identify changes in Hg cycling in lakes affected by shoreline retrogressive thaw slump events in tundra lakes.

Shoreline thaw slumps demonstrated a clear impact on both aquatic Hg availability and bioconcentration in periphyton. This was demonstrated in the loss of organic carbon in catchment surface soils, encompassing up to one-third of the catchment area. Atmospherically deposited Hg is less likely to bind to organic carbon compounds and their associated functional groups. Subsequent overland run-off to adjacent lakes is also likely lower in organically bound Hg. Further, much of the organic carbon and related Hg within slump-affected lakes is additionally deposited into the sediments, whereby we identified significantly lower total and methyl Hg within the overlying water column. Though there is a lower absolute concentration in Hg in slump-affected lakes, this counter-intuitively results in greater Hg bioavailability and thus, higher Hg bioconcentration factors in periphyton tissue samples with coinciding low DOC concentrations.

Objective 3. To examine the chemical relationships between Hg, DOC, and other aquatic chemical parameters in relation to Hg uptake in invertebrates.

We identify a novel nonlinear relationship between DOC and Hg bioaccumulation in two different trophic levels of freshwater ecosystems influenced by thawing permafrost and thus exhibiting a large gradient of DOC concentrations over an otherwise relatively homogenous landscape. Using equilibrium modelling we delineate the positive influence of fulvic acids on Hg bioaccumulation up until a relatively environmentally low concentration, whereby a threshold concentration is reached and any further increases in organic carbon leads to a negative relationship with Hg bioaccumulation. This is notable as only our slump-affected lakes achieved such low DOC concentrations to enhance Hg bioaccumulation, i.e. less than 8.5 mg DOC/L for invertebrates and less than 5.8 mg DOC/L for periphyton samples. With increased warming expected throughout the Arctic over coming decades, Hg bioaccumulation will likely become of increasing importance.

Objective 4. To determine the extent that the Giant Gold Mine is a significant influence on lake chemistry within the same Yellowknife, NT, region experiencing significant warming and shoreline subsidence.

The Giant Gold Mine was in operation from 1949-1999, with the majority of atmospheric emissions (~85%) occurring before the mid-1960s. Emissions were over 60% As_2O_3, and have led to legacy pollution in most lakes study lakes up to 25 km radius from the roaster stack. Notably, through our regression analysis, lakes within 17 km of the stack are expected to be above arsenic

water quality guidelines. Additionally, the unexpected increase in methyl mercury concentrations in lakes nearer to the roaster stack are likely an indirect consequence of elevated sulfur emissions from the gold roasting process.

5.2. Principal Findings

The principal findings of this thesis are as follows:

1. Shoreline retrogressive thaw slump events are the principal factor driving physical-chemical change; in particular, lower nutrients (e.g. N&P), organic carbon, and relevant trace metals (e.g. Fe & Al), are the likely cause for significantly lower phytoplankton and periphyton Chl-*a* concentrations.
2. Using phosphorus as a covariate in ANCOVA, we demonstrate that our Active thaw slump lakes are significantly lower in phytoplankton Chl-*a*, not only within our study, but across most other landscapes in Canada's low Arctic.
3. Along with lower nutrients and primary production in slump-affected lakes, both total and methyl mercury concentrations are significantly lower in these same lakes.
4. Causes for this lower Hg is likely a combination to surficial landscape changes (i.e. less organic matter), and sediment burial within lakes adjacent to thaw slumps.
5. However, even with the lower total Hg in slump-affected lakes, there is a significant positive relationship between Hg bioconcentration (factors) in periphyton and %CD.
6. This result is likely a result of non-equilibrium dynamics in slump-affected lakes that are also experiencing exceptionally (relatively low DOC concentrations. A threshold relationship between Hg BCF and DOC was observed, peaking at 5.8 mg DOC/L. This supports similar studies in invertebrates (French et al., 2014) in this same study site, and experiments with bacteria (Chiasson-Gould et al., 2014). This may present a human health concern for fish consumption in slump-affected lakes, though future study of higher trophic levels is recommended.
7. Shoreline subsidence in the Yellowknife region, taiga shield landscape within the discontinuous permafrost zone, demonstrates findings more in-line with most other thermokarst studies that demonstrate increased organic carbon and nutrients. Again this is likely a factor of the underlying surficial geology being the dominant driver of how thermokarst will impact adjacent aquatic systems.

8. Within the Yellowknife region, overlapping confounding influences from the Giant Mine gold ore roasting process has demonstrated the complex interactions between local anthropogenic activities and broader climate warming. Within a 17 km radius of the roaster stack aquatic total arsenic concentrations are above water quality guidelines for drinking water and the protection for aquatic life. Similarly, this is also demonstrated in related compounds such as sulfate and antimony.
9. Further, unexpected cumulative impacts of the Giant Mine activities have led to elevated methyl Hg concentrations in lakes nearer to the roaster stack, and are likely a response to the elevated sulfate emissions.
10. Together the Yellowknife region shoreline subsidence and mining activity demonstrate complex interactions between climate and industry.

The work presented in this thesis is an important step in delineating the limnological and ecotoxicological responses of freshwater systems to shoreline retrogressive thaw slump events, natural resource development, and the potential for compounding affects in Canada's warming Arctic environs. The changes to tundra lakes in Canada's western Arctic following a slump event, indicate significant reductions in nutrients and organic matter, leading to lower phytoplankton biomass. With expected increases in atmospheric warming these changes are likely to increase in scale and number of lakes affected. We also observed elevated Hg bioaccumulation in slump-affected lakes and higher MeHg concentrations in lakes near the Giant Mine roaster stack. Additionally, higher As concentrations were noted in slump-affected lake sediments and were above soil quality guidelines, while As was significantly above water quality guidelines in lakes nearer to the roaster stack. The potential for compounding effects from climate warming and resource development are apparent, and mitigation and adaptation plans which consider multiple stressors will need to be developed in order to safeguard community health and ensure sustainable northern development.

6. Appendix: Dissolved Organic Carbon Thresholds Affect Mercury Bioaccumulation in Arctic Lakes

Todd D. French[1], Adam J. Houben[1], Jean-Pierre W. Desforges[1 †], Linda E. Kimpe[1], Steven V. Kokelj[2], Alexandre J. Poulain[1], John P. Smol[3], Xiaowa Wang[4] and Jules M. Blais[1]*

[1]Department of Biology, University of Ottawa, Ottawa, Ontario, K1N 6N5, Canada

[2]Northwest Territories Geoscience Office, Government of the Northwest Territories, Yellowknife, NT, Canada, X1A 2R3, Canada

[3]Paleoecological Environmental Assessment and Research Lab, Department of Biology, Queen's University, Kingston, Ontario, K7L 3N6, Canada

[4]Environment Canada, 867 Lakeshore Road, Burlington, Ontario, L7R 4A6, Canada

This article has been published as *French et al. 2014. ES&T. 48:3162-3168.* with minor modifications for this thesis.

Statement of author contributions:

Conceived and designed the experiments: TF AH JB. Performed the experiments: AH TF JD LK. Analyzed the data: AH JD. Performed equilibrium modelling: TF AP. Contributed reagents/materials/analysis tools: LK SK JS XW JB. Wrote the paper: TF AH JB

6.1. Abstract:

Dissolved organic carbon (DOC) is known to affect the Hg cycle in aquatic environments due to its overriding influence on complexation, photochemical, and microbial processes, but its role as a mediating factor in the bioaccumulation of Hg in aquatic biota has remained enigmatic. Here we examined 26 tundra lakes in Canada's western Arctic that span a large gradient of DOC concentrations to show that total Hg (Hg_T) and methyl mercury (MeHg) accumulation by aquatic invertebrates is defined by a threshold response to Hg-DOC binding. Our results showed that DOC promotes Hg_T and MeHg bioaccumulation in tundra lakes having low DOC (<8.6 – 8.8 mg C L^{-1}; DOC threshold concentration, T_C) whereas DOC inhibits Hg_T and MeHg bioaccumulation in lakes having high DOC (>DOC T_C), consistent with bioaccumulation results in a companion paper (this issue) using a microbial bioreporter. Chemical equilibrium modeling showed that Hg bioaccumulation factors were elevated when Hg was associated mainly to fulvic acids, but became dramatically reduced when DOC was > 8.5 mg C L^{-1}, at which point Hg was associated primarily with strong binding sites on larger, less bioaccessible humic acids. This study demonstrates that the biological uptake of Hg in lakes is determined by binding thresholds on DOC, a water quality variable predicted to change markedly with future environmental change.

6.1. Introduction:

Global anthropogenic mercury (Hg) emissions have increased since pre-industrial times, with the global emission in 2008 being 2,000 t and the present-day tropospheric burden (5,200 t) being about three-fold higher than that before the Industrial Revolution (Lamborg et al., 2002; Streets et al., 2011). Atmospheric Hg transport from industrialized regions to the Arctic is also increasing and this, acting in tandem with climate-related changes, has resulted in a net increase in Hg deposition to land and water surfaces in several Arctic regions (Cole and Steffen, 2010). Presently, the contribution of anthropogenic Hg to the total body burdens of predatory birds and mammals, including humans, ranges from 74% to 94% across the Arctic (Dietz et al., 2009) and evidence of chronic sub-lethal Hg toxicity has been shown in Arctic wildlife populations and in indigenous peoples who rely primarily on traditional country foods.

In addition to the stresses caused by Hg and other pollutants, Arctic ecosystems are being markedly affected by rapid climate change. Ground temperatures and thermokarst activity in

Canada's western Arctic have increased with warming temperatures since the 1970s, such that up to 15% of the water bodies in the region have shoreline retrogressive thaw slumps (Fig 6.1). Spatial variability in the distribution and magnitude of permafrost thaw slumps has resulted in extremely wide pH (6.6 – 8.1) and DOC (6.8 – 30.0 mg C L^{-1}) gradients amongst tundra lakes in the western Arctic (Kokelj et al., 2005). Given that these key variables regulate Hg bioaccumulation and affect the post-depositional processing of Hg (Barkay et al., 1997; Jeremiason et al., 2006; Watras and Morrison, 2008), we hypothesized that permafrost thawing is affecting Hg bioaccumulation in western Arctic lakes. Here, we use the wide gradients in lake water DOC amongst tundra lakes to determine its effect on Hg bioaccumulation patterns in Arctic lakes.

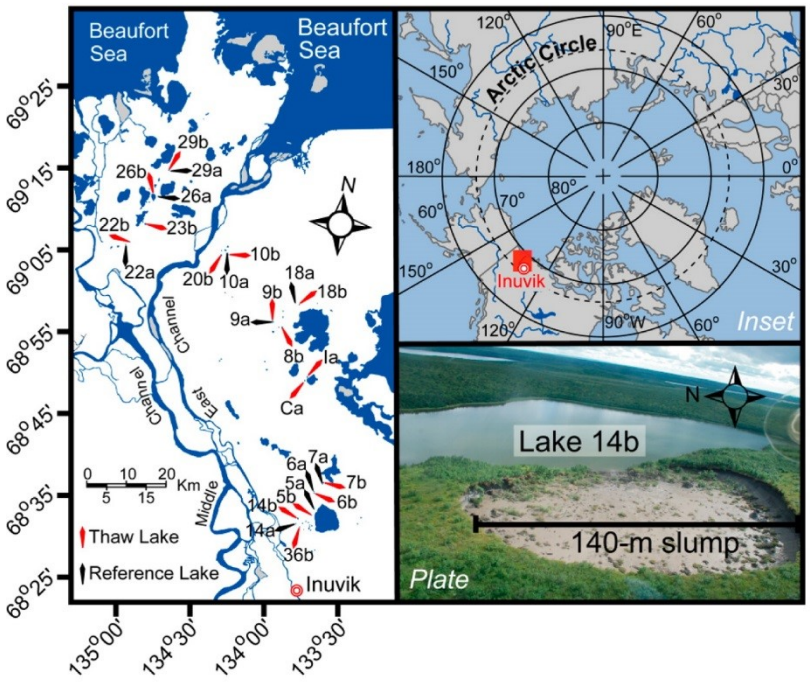

Lake	A_o (ha)†	C (ha)‡	C Slumped (%)§	Z_m (m)⊥
I. Reference Lakes				
5a	2.9	20.9	0.0	10.9
6a	3.6	19.7	0.0	2.3
7a	1.4	18.1	0.0	2.7
9a	3.1	29.3	0.0	2.7
10a	2.3	26.3	0.0	3.4
14a	3.4	33.5	0.0	7.5
18a	2.1	18.4	0.0	5.0
22a	1.9	8.3	0.0	2.8
26a	6.5	58.2	0.0	2.8
29a	3.0	14.5	0.0	3.8
Ia	7.2	28.3	0.0	n.d.
Ca	1.6	19.8	0.0	n.d.
II. Thaw Lakes				
5b	2.8	27.7	7.3	9.0
6b	1.2	7.5	10.8	2.0
7b	3.1	34.7	3.0	5.0
8b	6.5	32.7	12.1	4.1
9b	3.6	7.2	34.3	3.0
10b	11.4	23.3	30.9	10.4
14b	9.2	45.1	5.2	10.5
18b	2.7	4.7	12.1	5.2
20b	4.8	17.9	4.8	3.0
22b	3.5	11.7	28.7	6.9
23b	17.7	74.3	4.1	5.9
26b	116.5	254.4	6.0	3.5
29b	5.7	14.3	20.7	4.5
36b	3.9	24.4	19.9	7.4

†A_o is lake surface area. ‡C is catchment area. §C slumped is the area of the retrogressive thaw slump in relation to C. ⊥Z_m is maximum depth. n.d. is not determined.

Figure 6.1: Study lakes in the tundra uplands east of the Mackenzie River Delta (Middle and East channels shown), Northwest Territories, Canada. Reference Lakes (without shoreline permafrost thaw slumps) and Thaw Lakes (with shoreline permafrost thaw slumps) are denoted "a" and "b", respectively. *Inset* shows the study area (red box) in relation to Inuvik (population 3,000) and the Beaufort Sea (Arctic Ocean). *Plate* shows a 140-m wide thaw slump on the western shoreline of Lake 14b. *Table* provides the general morphometry of the study lakes and the thaw slump area as percentage of catchment area.

6.2. Materials and Methods

6.2.1. Water and Amphipod Sampling.

Our study was undertaken in the tundra uplands east of the Mackenzie River delta, Northwest Territories, Canada (Fig 6.1). Twenty-six lakes were sampled in summer 2009, which consisted of "Reference Lakes" without shoreline thaw slumps (n=12) and "Thaw Lakes" with shoreline thaw slumps (n=14, Fig 6.1). Water for the analysis of total mercury (Hg_T), total methylmercury ($MeHg_T$), DOC, total dissolved Fe (Fe_D) and Al (Al_D), major ions (DIC [$\sum CO_3^{2-}$, HCO_3^-, CO_2], Mg^{2+}, Ca^{2+}, Na^+, K^+, SO_4^{2-}, Cl^-), NH_3 and NO_3^- concentrations and pH was collected from the littoral zone (0.5-m depth) of each lake in pre-cleaned/acid-washed polyethylene bottles. Bottles and caps were triple rinsed with lake water before sample collection, and bottles were filled to rim to void the sample of air. Bottles and samples for Hg analyses were maintained in sealed bags to prevent contamination (e.g., from helicopter exhaust vapors). Water samples for Hg_T and $MeHg_T$ analysis were preserved in the field with 0.5% HCl, and those for Fe_D and Al_D analyses were preserved, immediately after filtration, with conc. HNO_3 to 2% of sample volume. Littoral amphipods were collected with a D-net (63-µm). Amphipods were separated into large (>2000-µm) and small (250 – 2000 µm) size classes, and whole-body Hg_T and $MeHg_T$ dry-weight (dw) concentrations in each class were determined. Analytical procedures for the chemical analyses of water and amphipod samples are described in Methods. We used a three-factor Lorentzian model to examine Hg bioaccumulation factor (BAF) to amphipods across the broad water Hg_T and DOC gradients. Visual MINTEQ Version 3.0 (MINTEQ) was used to model Hg complexation to DOC across the water chemistry gradient.

6.2.2. Chemical analyses.

Water pH was determined with a Thermo Orion Model 106 meter. Water Hg_T and $MeHg_T$ concentrations were determined by cold-vapour atomic fluorescence spectrometry (CV-AFS, Tekran Instrument Corp. Series 2600 spectrophotometer) and capillary gas chromatography-atom fluorescence spectrometry (GC-AFS, Ai Cambridge Model 94 GC with a CTC Autosampler and PSA Merlin Detector), respectively according to EPA method 1631 revision E, with a detection limit of 0.1 ng/L. Instrument blanks averaged 0.01 ± 0.13 ng/L (1 standard deviation), while field blanks averaged 0.12 ± 0.17 ng/L. Hg recovery of standards was 99% ± 4% based on concurrent

analyses of NIST-certified stock solutions, with a r^2=0.9996 for the calibration curve. Mercury$_T$ and MeHg$_T$ concentrations in amphipod composites were determined by solid-phase thermal desorption followed by CV-AFS and GC-AFS, respectively. Water samples for DIC, DOC, Fe$_D$ and Al$_D$ determinations were hand pumped, within hours of collection, through 47-mm diam./0.45-μm Sartorius filters (supported AcetatePlus, plain) and the filtrate analyzed. Dissolved inorganic carbon and DOC concentrations were determined by infrared CO_2 detection (Phoenix 8000 TOC analyzer with gas/liquid separator, mist trap, Cl^- and CO_2-air scrubbers, and NDIR CO_2 detector) following sequential conversions, by acidification, of DIC and DOC to CO_2. Water Fe$_D$ and Al$_D$ concentrations were determined by inductively coupled plasma-sector field mass spectrometry (ICP-SFMS, Thermo-Finnigan Mass Spectrometer Element II) with direct sample aspiration. Chloride and SO_4^{2-} concentrations were determined by ion chromatography (Dionex DX500 ion chromatograph with ASRS-ULTRA-II ion/conductivity suppressor); Cl^- and SO_4^{2-} were separated from other anions on the basis of retention time. Water Ca^{2+}, Mg^{2+}, Na^+ and K^+ concentrations were determined by atomic absorption spectroscopy in an air-acetylene flame at 11 p.s.i. (Varian SpectAA22 with SPS-5 autosampler). Water NO_3^{-2} concentrations were determined photometrically (Bran+Luebbe Continuous-Flow Technicon Autoanalyzer III set at 520 nm) following sample acidification to pH 5.5 and sequential reactions with sulphanilamide and then N-1(-naphthyl)-ethylenediamine dichloride; these reactions form a reddish-purple azo dye in proportion to the concentration of NO_3^- + NO_2 in sample (sample NO_3^- converted to NO_2 in acidification step) . Water NH_3 concentrations were determined photometrically (Bran+Luebbe Continuous-Flow Technicon Autoanalyzer III set at 630 nm) following sample treatment with the Berthelot Reaction which forms indophenol blue in proportion to the concentration of NH_3 in sample.

6.2.3. Mercury bioaccumulation trends.

Hg$_T$ and MeHg$_T$ BAFs from water to amphipods were determined for each lake by dividing concentrations in amphipods (ng kg^{-1} dw) by concentrations in water (ng L^{-1}). A three-factor Lorentzian model was used to assess Hg bioaccumulation across the water Hg$_T$ and DOC concentration gradients:

$$Y = \frac{a}{1+\left(\frac{X - X_o}{b}\right)^2}$$

Where Y is the Hg concentration or BAF in amphipod composite, *a* is the height of the Lorentzian curve at the inflection point, *b* is a measure of the spread (standard deviation) of the curve, and X_o (or T_C, threshold concentration) is the inflection point along the gradient axis (*x*-axis).

6.2.4. Modeling of Hg speciation.

Equilibrium speciation calculations were undertaken with Visual MINTEQ Version 3 (Gustafsson, 2012) to model Hg interactions with inorganic ligands and DOC. Lake chemistry data (*above*) were entered into MINTEQ; pH was fixed at the value measured at sampling. The extent of Hg binding to DOC was predicted by a NICA-Donnan model (Milne et al., 2003). This model enables simulation of cation complexation to constituents that are highly heterogeneous with respect to binding affinity, such as humic (HA) and fulvic (FA) acids. The ratio of dissolved organic matter (DOM) to DOC was set by default at 1.65, which is an average based on results for lakes and streams from the Swedish Environmental Monitoring Network (Sjostedt et al., 2010). We ran the model assuming that the active DOM was comprised of 75% HA and 25% FA, which approximates the HA:FA ratio observed in lakes with watershed vegetation similar to that in the Inuvik area (Reinikainen and Hyvärinen, 1997). As modeled, each FA and HA fraction had two types of binding sites: one with a weak affinity (FA1 and HA1) for Hg and one with a strong affinity (FA2 and HA2) for Hg (Drexel et al., 2002). The weak binding sites are representative of interaction with carboxyl groups while the strong binding sites are representative of binding with organic thiol functional groups (Drexel et al., 2002; Haitzer et al., 2003; Ravichandran, 2004). The generic NICA-Donnan model parameters for Hg were based those recommended by Milne *et al*. (2003). The estimated binding affinities for Hg are described by the equations below:

$Hg^{2+} + 2H_2O \Rightarrow Hg(OH)_2 + 2H^+$ log K = 6.2

$H\text{-}FA1 + Hg(OH)_2 + H^+ \Rightarrow [FA1\text{-}Hg]^+ + 2H_2O$ log K = 14

$H\text{-}FA2 + Hg(OH)_2 + H^+ \Rightarrow [FA2\text{-}Hg]^+ + 2H_2O$ log K = 30

$H\text{-}HA1 + Hg(OH)_2 + H^+ \Rightarrow [HA1\text{-}Hg]^+ + 2H_2O$ log K = 14

$H\text{-}HA2 + Hg(OH)_2 + H^+ \Rightarrow [HA2\text{-}Hg]^+ + 2H_2O \qquad \log K = 30$

We also ran simulations for which the binding constants for Hg to the strong binding sites onto fulvic and humic acids (FA2 and HA2) varied from logK = 25 to logK = 30 to reflect variability observed in conditional constant estimates (Dong et al., 2011; Haitzer et al., 2003).

Two-segment piecewise regression was used to analyze the MINTEQ output; the model was:

$$f = \begin{cases} \dfrac{m_1(T_C - c) + m_2(c - c_1)}{T_C - c_1}, \text{for } c_1 \le c \le T_C \\ \dfrac{m_2(c_2 - c) + m_2(c - T_C)}{c_2 - T_C}, \text{for } T_C \le c \le c_2 \end{cases}$$

where f is the percentage of water Hg bound to the FA and HA fractions, c is the water DOC concentration, c_1 is the lowest DOC concentration in the series (start point), c_2 is the highest DOC concentration in the series (end point), T_C (iterative quasi-Newton method) is the DOC threshold concentration, m_1 is the regression slope across DOC concentrations $<T_C$ (regression segment 1), and m_2 is the slope across DOC concentrations $>T_C$ (segment 2).

Outlier data for all trend and modeling analyses were identified with Grubbs test (Coucke et al., 2012); statistical analyses were performed with STATISTICA 9 (Stat Soft Inc.). All outliers are identified on figures.

6.3. Results and Discussion

In contrast to some field studies with limited ranges in DOC concentrations that have shown Hg concentrations in biota at lower trophic levels increasing in parallel with water Hg concentration (Adams et al., 2009; Moore et al., 2003), we observed in our tundra lakes Hg_T and $MeHg_T$ concentrations in amphipods with distinct bell-shaped patterns when analyzed against the water Hg_T gradient (0.7 – 4.7 ng L^{-1}). The threshold water Hg_T concentration (T_C, Lorentzian model inflection point) was determined to be 1.6 – 2.3 ng L^{-1} (Fig 6.2a). Mercury concentrations in amphipods increased with increasing water Hg_T concentration across lakes having water Hg_T concentrations < T_C, but Hg concentrations in amphipods decreased with increasing water Hg_T

concentration when the Hg_T T_C was exceeded (Fig 6.2a). In general, Hg_T BAFs decreased with increasing water Hg_T concentration. For large amphipods, there was some evidence that Hg bioavailability also followed a bell-shaped pattern (T_C = 1.5 ng L^{-1}; Fig 6.2b). Mercury concentrations in the tundra lakes were less than toxic levels; thus, the trajectory shifts in Hg bioaccumulation at the Hg_T T_C (Fig 6.2) cannot be explained by toxicological impairment. We suggest that the trajectory shifts were caused by changes in critical limnetic conditions that occurred in conjunction with the Hg_T T_C.

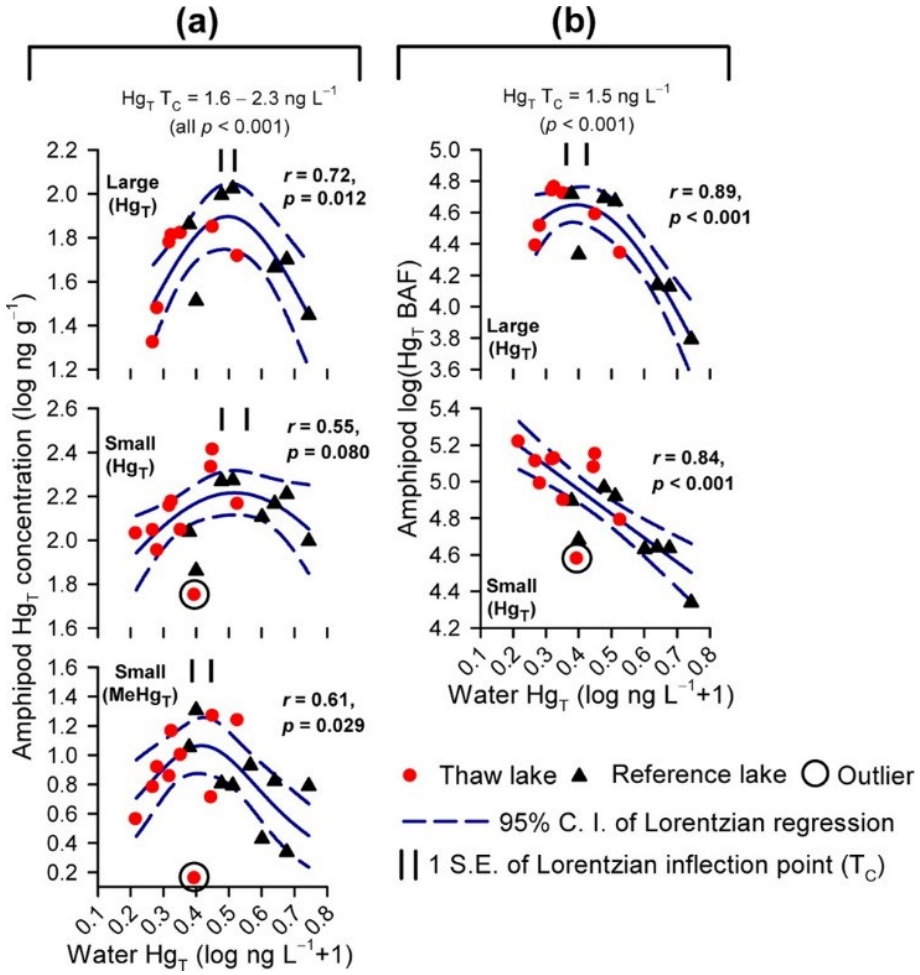

Figure 6.2: Mercury bioaccumulation in large and small amphipods in relation to lake water Hg_T concentration. **a,** Hg concentrations in amphipods versus water Hg_T concentration; $MeHg_T$ trends in large amphipods were not determined (insufficient sample size). **b,** Hg_T BAFs to amphipods versus water Hg_T concentration. Model parameter statistics (three-parameter Lorentzian functions): p_a all <0.001 and p_b = <0.001 – 0.009 (p_{Xo} shown as T_C above panels). Model parameter statistics (linear function): $p_{intercept}$ <0.001, p_{slope} <0.001. Model parameters remain significant (p<0.05) when outliers are maintained in analysis. Model parameters are defined in Methods.

Further examination of the bell-shaped relationship between Hg concentrations in amphipods and water Hg_T concentration (Fig 6.2a) revealed that lake water pH shifted from alkaline to slightly acidic at the Hg_T T_C. While Hg concentrations in amphipods were not directly correlated with pH, the alkaline lakes (mostly Thaw Lakes) comprised the upslope (Hg_T concentration $<T_C$) of the response curve, whereas the near-neutral to acidic lakes (mostly Reference Lakes) comprised the downslope (Hg_T concentration $>T_C$) of the response curve (Fig 6.2a). Mercury BAFs in amphipods also showed a distinct bell-shaped pattern when analyzed against the water DOC gradient (2.2 – 23.1 mg C L^{-1}), with the DOC T_C being 8.5 – 8.6 mg C L^{-1} (Fig 6.3a). As observed across the water Hg_T gradient (Fig 6.2a), the alkaline lakes (mostly Thaw Lakes) comprised the upslope (DOC concentration $<T_C$) of the response curve with the near-neutral to acidic lakes (mostly Reference Lakes) comprising the downslope (DOC concentration $>T_C$; Fig 6.3a). Hg bioavailability in bacteria (Kelly et al., 2003) and zooplankton (Chetelat et al., 2011) is typically related inversely to pH when DOC is not a covariate of pH. Our results show, however, that bioaccumulation cannot be predicted solely by pH in this data set, suggesting other mediating factors, which we elaborate below. $MeHg_T$ BAFs also plummeted when the DOC T_C was exceeded (Fig 6.3a). The Hg bioaccumulation patterns observed across the water Hg_T and DOC gradients were similar among large and small amphipods (Figs 6.2a and 6.3a); reasons for this pattern may include: i) Hg and DOC are co-transported to the tundra lakes (Hill et al., 2009; Moore et al., 2003); and ii) DOC complexes Hg (Haitzer et al., 2003; O'Driscoll et al., 2006) and therefore regulates Hg bioavailability (Barkay et al., 1997).

Our results indicate that DOC may both promote and inhibit Hg bioavailability in these Arctic tundra lakes, such that: *i*) DOC at low concentrations ($<T_C$) promoted Hg bioavailability; and *ii*) DOC at high concentration ($>T_C$) inhibited Hg bioavailability (Fig 6.3a). As Hg is transported to the tundra lakes with DOC (Haitzer et al., 2003; Hill et al., 2009; Moore et al., 2003; O'Driscoll et al., 2006), DOC at low concentrations may promote Hg bioaccumulation by increasing the supply of Hg to the lakes, and by stimulating microbial heterotrophic activity responsible for DOC degradation, thereby releasing bound Hg (Porcal et al., 2009). We hypothesize that the bioavailability of Hg in the high-DOC (>DOC T_C) lakes (mostly Reference Lakes) was likely reduced due to the formation of strong Hg-DOC complexes, such that DOC-bound Hg is not readily available for direct biological uptake from water, which is the primary mode of Hg uptake at low and intermediate trophic levels (Barkay et al., 1997).

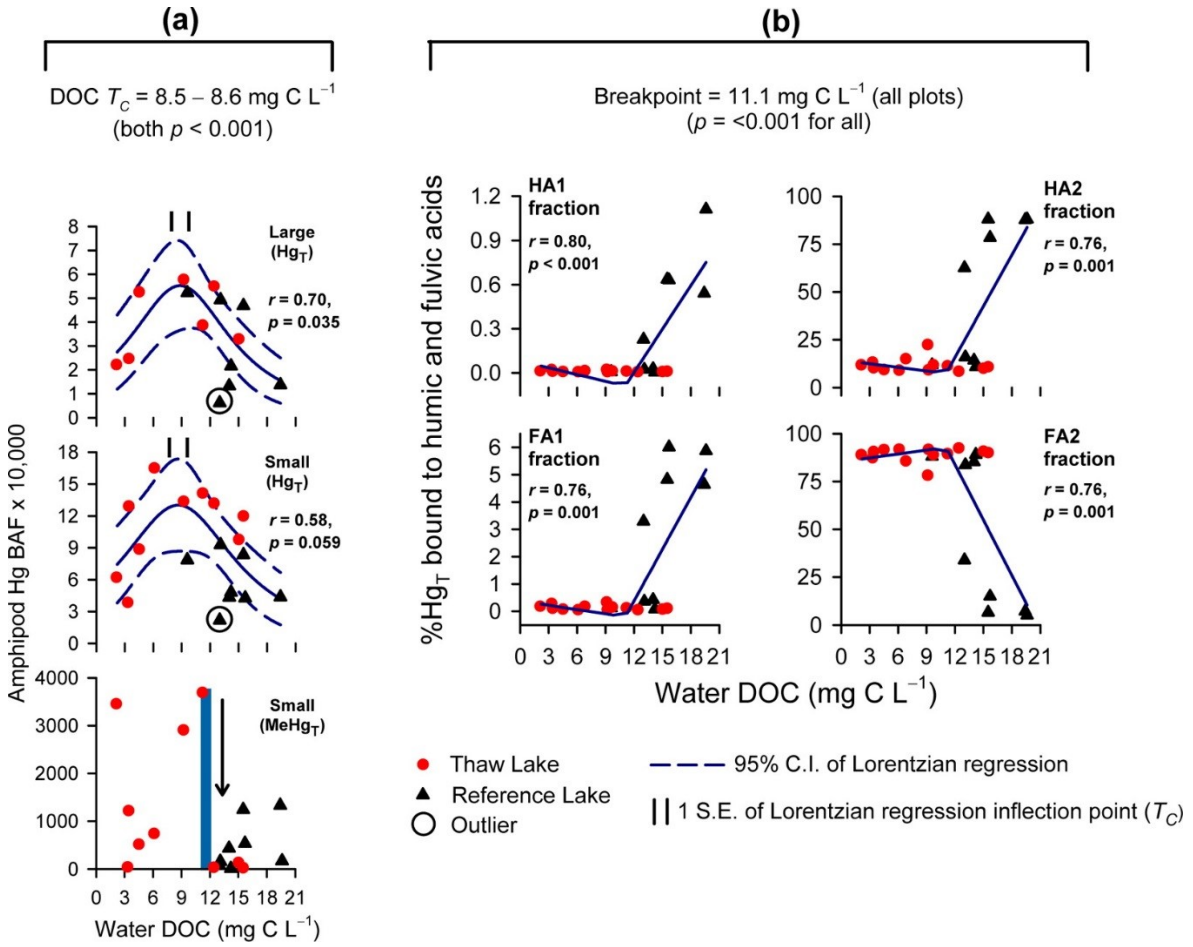

Figure 6.3: Threshold analyses of Hg BAFs in large and small amphipods in relation to lake water DOC concentration and percentage of water HgT bound to fulvic (FA) and Humic (HA) fractions in relation to DOC concentration. **a,** Top two panels show Lorentzian fit of Hg_T BAFs in large and small amphipods in relation to DOC concentration. Model parameter statistics (three-parameter Lorentzian functions): p_a all <0.001 and p_b both = 0.003 (p_{Xo} shown as T_C above panels). Blue vertical line on bottom panel illustrates that $MeHg_T$ BAFs plummeted when DOC concentrations exceeded about 11 mg C L^{-1}. Trends for $MeHg_T$ BAFs in large amphipods were not quantified (insufficient sample size). **b**, Piecewise fit of %Hg_T bound to fulvic (FA1 and FA2, weak and strong binding sites, respectively) and Humic (HA1 and HA2) fractions versus water DOC concentration MINTEQ (see Methods). Model parameters are defined in Methods.

In support of our proposed mechanism, we used a thermodynamic equilibrium model (MINTEQ) that predicted a pronounced increase in Hg adsorption to strong binding sites on humic acids (HA2, *see* Methods) and reduced adsorption to strong binding sites on fulvic acids (FA2) when the critical DOC concentration (11.7 mg C L^{-1}) was exceeded (Fig 6.3b). Interestingly, sensitivity analyses showed that the shift from fulvic to humic acids strong binding sites was most apparent when $\log K_{Hg\text{-}FA}$ was $\geq$ $\log K_{Hg\text{-}HA}$. The resulting shift in Hg binding from fulvic acids to

humic acids may result in reduced Hg bioaccumulation in aquatic biota due to greater Hg bioavailability in the presence of low molecular weight (fulvic) organic acids (Golding et al., 2002) such as those associated with the pool of fulvic acids (Remucal et al., 2012). Alternatively, shifts in Hg bioaccumulation may be linked to the complex mechanisms that drive Hg-DOC photoredox chemistry (and therefore speciation), for which threshold-type relationships have been observed over DOC gradients (Garcia et al., 2005).

Analysis of the chemical modeling data identified a breakpoint at ca. 11.1 mg C L^{-1} (Fig 6.3b). This critical DOC concentration corresponds well with the DOC T_C (8.6 – 8.8 mg C L^{-1}) estimated for the Hg BAF versus DOC relationship (Fig 6.3a). In further support of our proposed mechanism, $MeHg_T$ was not detected in the water column of high-DOC lakes; MINTEQ predicted that all of the water column Hg in these lakes would be bound to DOC, and therefore much of the Hg in lakes with high DOC levels may not be readily available to bacteria for methylation.

The results of earlier studies have led some researchers to speculate that there might be a threshold-type relationship between Hg bioaccumulation/bioavailability and DOC in freshwater ecosystems (Driscoll et al., 1994; Moore et al., 2003). Our study quantitatively demonstrates these thresholds and shows that DOC both promotes (when concentration is <DOC T_C) and inhibits (when concentration is >DOC T_C) Hg bioavailability in natural waters. One of the most widely cited papers speculating about the possibility of a DOC threshold is that by Driscoll *et al.* (1994), who studied Hg bioaccumulation in perch (*Perca flavescens*) from Adirondack Park (USA) lakes. They showed a positive linear relationship between Hg concentration in perch and DOC concentration across lakes having DOC concentrations <~10 mg C L^{-1}, but that Hg concentrations in perch from Rock Pond Lake (~27 mg C L^{-1}) deviated far below that expected from the linear trajectory. Driscoll *et al.* (1994), while suggesting the possibility of a DOC threshold, excluded the Rock Pond Lake datum as an outlier because they had insufficient data to statistically confirm the downslope of a threshold-type response trajectory. Data presented by Belger and Forsberg (2006) also showed that Hg bioaccumulation in Amazonian wolf fish (*Hoplias malabaricus*) increased linearly with increasing DOC concentration but, like Driscoll *et al.* (1994), they excluded a high-DOC system from their statistical analysis which suggested a threshold-type relationship was also present in their Amazonian study system. In contrast to previous studies, the environmental data offered by the western Arctic lake system provided us with an exceptional

DOC gradient to assess the relationship between Hg bioaccumulation and DOC (Figs 6.2a and 6.3a).

In a companion paper (Chiasson-Gould et al., 2014), we assessed the role of DOC on Hg(II) bioavailability to a whole cell biosensor using defined media and field samples from Canada's western Arctic spanning a wide range of DOC levels. The results obtained with the biosensor are consistent with what was observed here for aquatic invertebrates. The biosensor data also further support the kinetically important and complex nature of Hg (II) interaction with DOM that cannot solely be predicted by interaction at equilibrium. Together these two studies demonstrate how the biological uptake of Hg in lakes is determined by both complexation kinetics and binding thresholds on DOC, a water quality variable predicted to change markedly with future environmental change.

These results have implications for Hg bioaccumulation in many north-of-treeline lakes characterized by low DOC (< 8 mg L^{-1}, (Lim et al., 2001; Pienitz et al., 1997a, 1997b), that have rising DOC expected due to humification (Macdonald et al., 2005). Our results suggest a 2-3 fold increase in Hg bioaccumulation as these lakes approach the threshold DOC T_C of 8 mg L^{-1}, adding to the existing high Hg burdens in some northern environments.

The importance of threshold-type responses linking mercury toxicity to DOC concentrations have hitherto received little attention. Given that DOC levels mediate numerous ecosystem functions in lakes and relate closely to rapidly changing climate factors such as temperature and precipitation (Drexel et al., 2002), our results emphasize the critical role of DOC on determining the fate and bioavailability of mercury in a rapidly changing climate.

6.4. References

Adams RM, Twiss MR and Driscoll CT (2009) Patterns of mercury accumulation among seston in lakes of the Adirondack Mountains, New York. *Environmental Science & Technology* 43(13): 4836–42.

Barkay T, Gillman M and Turner RR (1997) Effects of dissolved organic carbon and salinity on bioavailability of mercury. *Applied and Environmental Microbiology* 63(11): 4267–71.

Belger L and Forsberg BR (2006) Factors controlling Hg levels in two predatory fish species in the Negro river basin, Brazilian Amazon. *Science of the Total Environment* 367(1): 451–9. doi:10.1016/j.scitotenv.2006.03.033.

Chetelat J, Amyot M and Garcia E (2011) Habitat-specific bioaccumulation of methylmercury in invertebrates of small mid-latitude lakes in North America. *Environmental Pollution* 159(1): 10–17.

Chiasson-Gould SA, Blais JM and Poulain AJ (2014) Dissolved organic matter kinetically controls mercury bioavailability. *Environmental Science & Technology* 48(6): 3153–3161.

Cole AS and Steffen A (2010) Trends in long-term gaseous mercury observations in the Arctic and effects of temperature and other atmospheric conditions. *Atmospheric Chemistry and Physics* 10(10): 4661–4672. doi:10.5194/acp-10-4661-2010.

Coucke W, China B, Delattre I, Lenga Y, Van Blerk M, Van Campenhout C, et al. (2012) Comparison of different approaches to evaluate external quality assessment data. *Clinica Chimica Acta* 413: 582–586.

Dietz R, Outridge PM and Hobson KA (2009) Anthropogenic contributions to mercury levels in present-day Arctic animals. *Science of the Total Environment* 407(6120–6131).

Dong W, Bian Y, Liang L and Gu G (2011) Binding constants of mercury and dissolved organic matter determined by a modified ion exchange technique. *Environmental Science & Technology* 45: 3576–3583.

Drexel RT, Haitzer M, Ryan JN, Aiken GR and Nagy KL (2002) Mercury(II) sorption to two Florida Everglades peats: Evidence for strong and weak binding and competition by dissolved organic matter released from the peat. *Environmental Science & Technology* 36(19): 4058–4064.

Driscoll CT, Yan C, Schofield CL, Munson R and Holsapple J (1994) The mercury cycle and fish in the Adirondack Lakes. *Environmental Science & Technology* 28(3): 136–143.

Garcia E, Amyot M and Ariya PA (2005) The relationship between DOC photochemistry and mercury redox transformations in temper- ate lakes and wetlands. *Geochimica et Cosmochimica Acta* 69: 1917–1924.

Golding GR, Kelly CA, Sparling R, Loewen PC, Rudd JWM and Barkay T (2002) Evidence for facilitated uptake of Hg(II) by Vibrio anguillarum and Escherichia coli under anaerobic and aerobic conditions. *Limnology and Oceanography* 47: 967–973.

Gustafsson JP (2012) Visual MINTEQ, a free equilibrium speciation model. *KTH, Department of Land and Water Resources Engineering*.

Haitzer M, Aiken GR and Ryan JN (2003) Binding of mercury (II) to aquatic humic substances: influence of pH and source of humic substances. *Environmental Science & Technology* 37(11): 2436–2441.

Hill JR, O'Driscoll NJ and Lean DRS (2009) Size distribution of methylmercury associated with particulate and dissolved organic matter in freshwaters. *Science of the Total Environment*. Elsevier B.V. 408(2): 408–414. doi:10.1016/j.scitotenv.2009.09.030.

Jeremiason JD, Engstrom DR, Swain EB, Nater EA, Johnson BM, Almendinger JE, et al. (2006) Sulfate addition increases methylmercury production in an experimental wetland. *Environmental Science & Technology* 40(12): 3800–6.

Kelly CA, Rudd JWM and Holoka MH (2003) Effect of pH on mercury uptake by an aquatic bacterium: implications for Hg cycling. *Environmental Science & Technology* 37(13): 2941–2946: doi:10.1021/es026366o.

Kokelj S V, Jenkins RE, Milburn D, Burn CR and Snow NB (2005) The influence of thermokarst disturbance on the water quality of small upland lakes, Mackenzie Delta region, Northwest Territories, Canada. *Permafrost and Periglacial Processes* 16(4): 343–353. doi:10.1002/ppp.536.

Lamborg CH, Fitzgerald WF, O'Donnell J and Torgersen T (2002) A non-steady-state compartmental model of global-scale mercury biogeochemistry with interhemispheric atmospheric gradients. *Geochimica et Cosmochimica Acta* 66: 1105–1118.

Lim DSS, Douglas MS V, Smol JP and Lean DRS (2001) Physical and chemical limnological characteristics of 38 lakes and ponds on Bathurst Island, Nunavut, Canadian High Arctic. *International Review of Hydrobiology* 86(1): 1–22.

Macdonald RW, Harner T and Fyfe J (2005) Recent climate change in the Arctic and its impact on contaminant pathways and interpretation of temporal trend data. *Science of the Total Environment* 342(1–3): 5–86. doi:10.1016/j.scitotenv.2004.12.059.

Milne CJ, Kinniburgh DG, Van Riemsdijk WH and Tipping E (2003) Generic NICA-Donnan model parameters for metal-ion binding by humic substances. *Environmental Science & Technology* 37: 958–971.

Moore DRJ, Pawlisz A and Teed RS (2003) Developing ambient water quality criteria for mercury: a probabilistic site-specific approach. *Water Environment Research Foundation: Alexandria, VA*. p. 184.

O'Driscoll NJ, Siciliano SD, Peak D, Carignan R and Lean DRS (2006) The influence of forestry activity on the structure of dissolved organic matter in lakes: Implications for mercury photoreactions. *Science of the Total Environment* 366(2–3): 880–893. doi:10.1016/j.scitotenv.2005.09.067.

Pienitz R, Smol JP and Lean DRS (1997a) Physical and chemical limnology of 59 lakes located between the southern Yukon and the Tuktoyaktuk Peninsula, Northwest Territories (Canada). *Canadian Journal of Fisheries and Aquatic Sciences* 54(2): 330–346. doi:10.1139/cjfas-54-2-330.

Pienitz R, Smol JP and Lean DRS (1997b) Physical and chemical limnology of 24 lakes located between Yellowknife and Contwoyto Lake, Northwest Territories (Canada). *Canadian Journal of Fisheries and Aquatic Sciences* 54(2): 347–358. doi:10.1139/cjfas-54-2-347.

Porcal P, Koprivnjak JF, Molot LA and Dillon PJ (2009) Humic substances-part 7: the biogeochemistry of dissolved organic carbon and its interactions with climate change. *Environmental Science and Pollution Research* 16(6): 714–726: doi:10.1007/s11356-009-0176-7.

Ravichandran M (2004) Interactions between mercury and dissolved organic matter - a review. *Chemosphere* 55(3): 319–331. doi:10.1016/j.chemosphere.2003.11.011.

Reinikainen J and Hyvärinen H (1997) Humic- and fulvic-acid stratigraphy of the Holocene sediments from a small lake in Finnish Lapland. *The Holocene* 7: 401–407.

Remucal CK, Cory RM, Sander M and McNeill K (2012) Low molecular weight components in an aquatic humic substance as characterized by membrane dialysis and orbitrap mass spectrometry. *Environmental Science & Technology* 46: 9350–9359.

Sjostedt CS, Gustafsson JP and Kohler SJ (2010) Chemical equilibrium modeling of organic acids, pH, aluminum, and iron in Swedish surface waters. *Environmental Science & Technology* 44: 8587–8593.

Streets DG, Devane MK, Lu ZF, Bond TC, Sunderland EM and Jacob DJ (2011) All-time releases of mercury to the atmosphere from human activities. *Environmental Science & Technology* 45: 10,485–10,491.

Watras CJ and Morrison KA (2008) The response of two remote, temperate lakes to changes in atmospheric mercury deposition, sulfate, and the water cycle. *Canadian Journal of Fisheries and Aquatic Sciences* 65: 100–116: doi:10.1139/F07-159.

6.5. Acknowledgements

Financial and logistical support were provided by NSERC Discovery and Strategic grants to J.M.B. and J.P.S., Northern Contaminants Program, Polar Continental Shelf Program, Northern Scientific Training Program, Cumulative Impact Monitoring Program, Indian and Northern Affairs Canada, Environment Canada, and Aurora College. Michael Pisaric, Joshua Thienpont, William Hurst, Kathleen Rühland, and Peter deMontigny provided critical field, project-design, and technical support. Emmanuel Yumvihoze provided technical assistance with Hg analyses. This article is NWT Geoscience Office Contribution #78.

6.6. Supporting Information

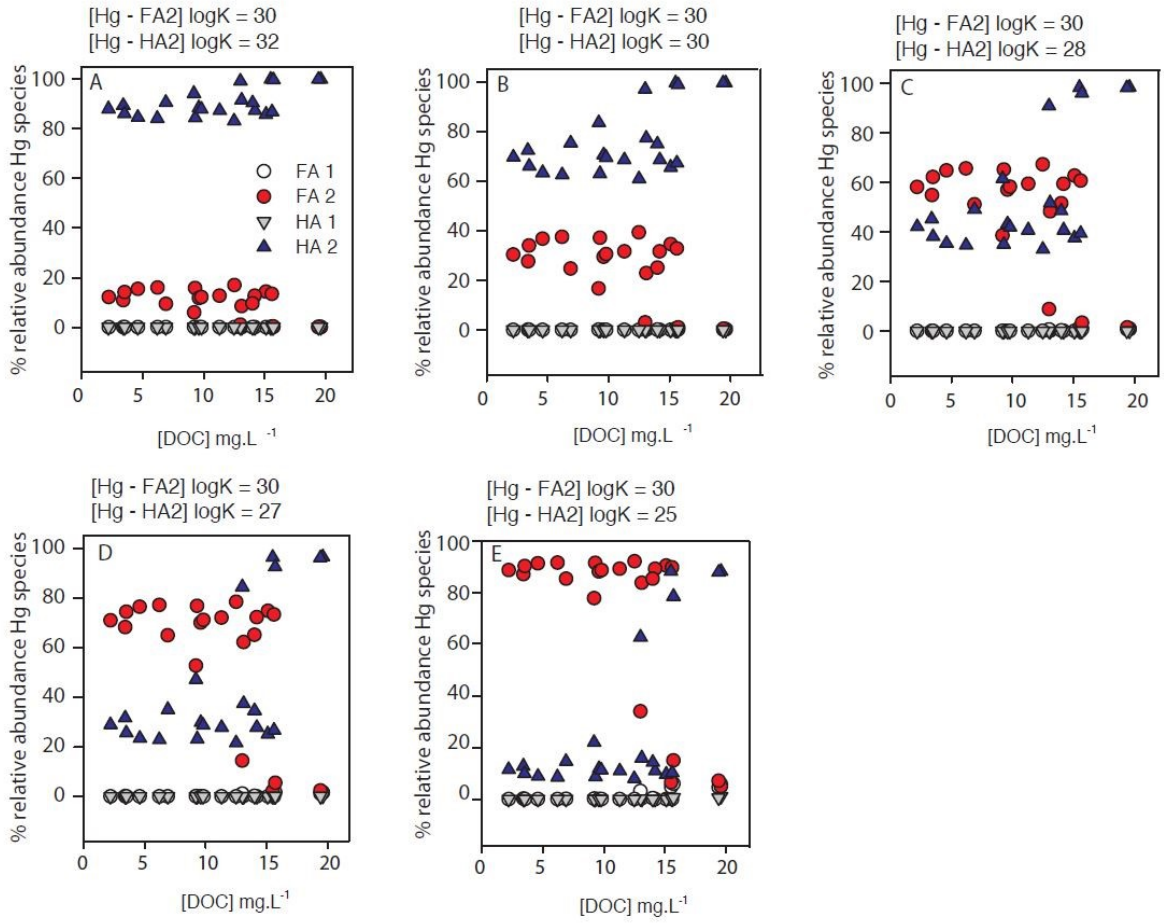

Figure 6.S1: Sensitivity analysis testing the interaction of Hg with dissolved organic matter as the binding constant for Hg to the strong binding sites of humic acids (HA2) varied from log K = 25 to log K = 32. Hg binding to strong binding sites of fulvic acids was set at log K = 30. Further details are provided in the method section of the paper.